FINAL REPORT

Understanding the Behavior of Steel Connections with Bolts and Welds in Combination

Dr. Mohamed Soliman, Ph.D., Assistant Professor
School of Civil & Environmental Engineering, Oklahoma State University
222 Engineering North, Stillwater, OK 74078,
Phone: 405-744-9777, Email: mohamed.soliman@okstate.edu,
Website: http://www.mohamedsoliman.info

Dr. Bruce W. Russell, Ph.D., P.E., F. ACI, Associate Professor
School of Civil & Environmental Engineering, Oklahoma State University

Christopher Waite, Structural Engineer, Magnusson Klemencic Associates, Seattle, WA,
Former M.Sc. Student, School of Civil & Env. Engineering, Oklahoma State University

Ligang Shen, Graduate Research Assistant, Doctoral Student
School of Civil & Environmental Engineering, Oklahoma State University

Ethan Stringer, Graduate Research Assistant, M.Sc. Student
School of Civil & Environmental Engineering, Oklahoma State University

March 1, 2021

TABLE OF CONTENTS

LIST OF FIGURES

LIST OF TABLES

EXECUTIVE SUMMARY

This report presents the results of a research investigation aiming at understanding the behavior of steel connections employing both slip-critical bolts and welds in a single load sharing system. Steel connections are typically constructed with either bolts or welds. However, there are instances where it may be desirable to use combination connections with bolts and welds sharing the load. The need to combine bolts and welds may occur most commonly during the construction phase of a project when the design load changes, when there are unforeseen difficulties in make-up or matching of bolt holes, or in retrofit of existing structures. However, due to the different load-deformation behavior of the connecting elements, bolts and welds may not reach their maximum strength simultaneously. Accordingly, the nominal strength of the connection cannot be easily predicted.

The behavior of these combination connections has been investigated in literature; however, many knowledge gaps still exist. Furthermore, the influence of several critical variables on the capacity of connections with bolts and welds sharing load is not well-understood. Examples of these critical variables include the effect of bolt grade, condition of faying surfaces, bolt pretensioning technique, load eccentricity, and connection size, among others. Therefore, this research report aims at quantifying the effect of these critical variables on the load-deformation behavior and capacity of concentrically and eccentrically loaded combination connections. The study presents and analyzes the results of experimental testing of 75 and 36 connections under concentric and eccentric loading conditions, respectively.

Based on the investigation results, it was found that when slip-critical bolts are combined with welds in a double-shear single load sharing system under concentric loading (e.g., double-shear tension splice), the resulting connection experiences an increase in the ultimate load carrying capacity compared to that of the bolted- or welded-only connection. The load-deformation behavior of the bolted- and welded-only connections can be used to characterize the behavior of the combination connection. In addition, the ultimate deformation at fracture experienced by the welds is significantly higher in the combination connections compared to welded-only connections. Furthermore, connections combining welds with slip-critical bolts installed on blast cleaned faying surface (i.e., Class B) experienced significant improvement in ductility compared to their bolted-only counterparts. These bolted-only connections under concentric loading slipped suddenly at their ultimate capacity with some losing more than 50% of their capacity at this slip event. Finally, it was found that the current AISC model for concentric loaded connections may overestimate the capacity of the connection at the slip limit of the bolts; accordingly, modifications are proposed to the current AISC equation to better predict the capacity of combination bolted and welded connections under concentric loading.

Similar improvement in the capacity was achieved in combination connections subjected to eccentric loading; however, to compute the capacity of these combination connections, it is recommended to use the instantaneous center of rotation considering all connecting elements to be in a single load sharing system with their appropriate load-deformation behavior.

ACKNOWLEDGEMENTS

1   LITERATURE REVIEW

There have been several studies in literature aiming at investigating the capacity and behavior of connecting elements (i.e., bolts or welds). Relevant studies that describe the behavior of these elements are presented in this literature survey. However, since the 1960s, fewer studies have been conducted to investigate the behavior of combination connections. These studies include both experimental and analytical research to investigate the effect of connection variables such as weld orientation, bolt bearing, bolt pretension, and the ratio between bolt strength and weld strength. The literature review covers these studies and discusses their findings.

1.1   SLIP-CRITICAL BOLT STRENGTH

An understanding of bolted connection behavior is of paramount importance in determining the capacity of combination connections. A well accepted model for describing the elastic-inelastic load-deformation behavior of mechanical fasteners was introduced by Fisher (1964). The model was developed by accounting for the deformations caused by shear, bending, and bearing. The bolt diameter, bolt grade, plate thickness, and steel grade are all important parameters that influence the load-deformation behavior. The following model in Eq. 1 highlights the load-deformation behavior of a bolted connection loaded in double shear (Fisher 1964).

$$R = R_{ult}[1 - e^{-\mu\Delta}]^{\lambda} \qquad \text{Eq. 1}$$

R_{ult} = ultimate shear strength of bolts

Δ = total deformation of bolt and bearing deformation of the connected material

μ, λ = regression coefficients

e = base of natural logarithm

The regression coefficients are computed using experimental test data of the specific connection in question partnered with the natural logarithm of Eq. 1. This expression is depicted in Eq. 2 as (Fisher 1964)

$$\log R = \log R_{ult} + \lambda \log[1 - e^{-\mu\Delta}] \qquad \text{Eq. 2}$$

The model describes the load-deformation behavior for a specific connection with known bolt and plate characteristics. Due to the need for test data, the load-deformation model developed by Fisher is not easily adaptable for connection design. Additionally, the bolted connection design strength is also a function of other failure modes that are dependent on the steel connection and bolt layout. These failure mechanisms that are not accounted for include: plate rupture, block shear failure, bearing/tearing, as well as shear lag if applicable.

For the design of a slip-critical connection, the following expression is recommended by Fisher and Struik (1973)

$$P_{slip} = k_s m \sum_{i=1}^{n} T_i \qquad\qquad \text{Eq. 3}$$

P_{slip} = slip resistance of bolted connection

k_s = slip coefficient

m = number of slip planes

T_i = bolt tension

Eq. 3 provides an easily adoptable model for designers to use for design of slip-critical connections. The equation presented above is very similar to that of the current AISC model depicted in Eq. 4 (AISC 2016). However, this model accounts for bolt pretension overstrength as well as the use of fillers.

$$R_n = \mu D_u h_f T_b n_s \qquad\qquad \text{Eq. 4}$$

μ = mean slip coefficient for Class A or B surfaces

D_u =1.13, a multiplier that reflects the ratio of the mean installed bolt pretension to specified minimum bolt pretension

h_f = factor for fillers

T_b = minimum fastener tension

n_s = number of slip planes required to permit the connection to slip

The current AISC model for available slip resistance (Eq. 4) is currently used when computing the available strength of a connection using bolts and welds in combination. Therefore, this model will be adopted in this study.

1.2   FILLET WELD STRENGTH

Similar to the bolted components in a combination connection, the load-deformation behavior of longitudinal fillet welds will influence the connection performance. The model developed by Fisher (Eq. 1) was also used by Butler and Kulak (1971) to investigate the fillet weld behavior as a function of the load direction. Their experimental study produced the empirical variables, R_{ult}, μ, and λ, based on an E60 weld electrode and 1/4-in. fillet welds. The variables are highlighted below, where θ is the angle in degrees between the direction of the applied load and longitudinal axis of the weld and Δ_{max} is the maximum weld deformation.

$$R_{ult} = \frac{10 + \theta}{0.92 + 0.0603\theta} \qquad\qquad \text{Eq. 5}$$

$$\mu = 75e^{0.0114\theta} \qquad\qquad \text{Eq. 6}$$

2

$$\lambda = 0.4e^{0.0146\theta} \hspace{5cm} \text{Eq. 7}$$

$$\Delta_{max} = 0.225(\theta + 5)^{-0.47} \hspace{4cm} \text{Eq. 8}$$

The variables may be used in conjunction with Eq. 1 to describe the load-deformation of a fillet welded connection where $\theta = 0°$ for longitudinal welds and $\theta = 90°$ for transverse welds.

Originally, the shear strength of fillet welds was designed according to an allowable stress acting on the weld throat. In 1928, the American Welding Society (AWS) Code for Fusion Welding and Gas Cutting in Building Construction permitted a shear stress of 11.3 ksi on the weld throat (Quinn 1991). The appropriateness of this stress level would be confirmed by an expansive testing program by the Structural Steel Welding Committee in 1931. The committee tested over 1,300 connections whose results supported the 1928 stress levels based on a desired factor of safety (Bowman and Quinn 1994, Quinn 1991). Further testing by Godfrey and Mount in (1940) allowed for a substantial 20% increase in the allowable shear stress to 13.6 ksi. This was due to the additional strength that was provided by covered electrodes versus bare wire electrodes. Finally, a study by Higgins and Preece (1969) concluded that an allowable stress equal to 30% of the weld tensile strength would be satisfactory for design. This new stress limit allowed for the accommodation of higher strength weld electrodes needed for high strength steel construction.

When load-resistance factor design (LRFD) was introduced, the Eq. 9 was presented by Fisher et al. (1978) to compute the nominal weld resistance. The allowable weld shear stress is assumed to be 60% of the specified minimum tensile strength of the weld electrode. This factor assumes that the weld is under pure shear and that the plastic flow can be described by the maximum distortion energy criterion, also known as von Mises theory (Fisher et al. 1978). This theory commonly describes the experimental behavior of ductile materials, including the longitudinal fillet welds (Ugural and Fenster 2011).

$$R_n = 0.60F_{EXX}A_w \hspace{4cm} \text{Eq. 9}$$

In the above nominal strength equation, A_w is the effective weld throat area and F_{EXX} is the specified minimum weld tensile strength. The model by Fisher et al. (1978) can be expanded to the current AISC model shown in Eq. 10, where the weld throat area, A_w, is expressed in terms of the weld size D and length l (AISC 2017).

$$R_n = 0.60F_{EXX}\left(\frac{\sqrt{2}}{2}\right)\left(\frac{D}{16}\right)l \hspace{3cm} \text{Eq. 10}$$

D = weld size in sixteenths of an inch

l = length, in

In addition to the current AISC nominal weld strength equation, there exists other models that deviate from the 0.6 factor for the weld shear strength computation. The Canadian Institution of

Steel Construction (CISC) model uses a 0.67 factor cited in the Handbook of Steel Construction (CISC, 2006). Additionally, research by Kwan and Grondin (2008) used a factor of 0.78 that represented the actual shear strength of the weld. This was empirically computed based on the experimental data presented by Deng et al. (2003).

Other studies have also shown that transverse fillet welds have a higher capacity compared to longitudinal fillet welds. For instance, Kato and Morita (1969) indicated that transverse welds have approximately 50% higher capacity than that of a longitudinal weld of the same length and size. The angle of inclination between the longitudinal weld axis and the load direction plays an important role in understanding the behavior of a welded connection and accurately predicting its ultimate capacity. Lesik and Kennedy (1990) developed an empirical formula to describe the load-deformation behavior and predict the ultimate capacity of weld lines as a function of the angle between the weld longitudinal axis and the applied load. Their model, which has been adopted by the AISC (2017) to calculate weld strength, predicts the ultimate strength by accounting for the loading angle through the coefficient $(1.00 + 0.50 * sin^{1.5}\theta)$.

Predicting the load-deformation behavior with respect to loading angle of welds is essential in quantifying the behavior of eccentrically loaded welds. Resisting the moment due to eccentric loading causes the internal force at discrete points along the weld to have different angles between the force resultant and the longitudinal axis of weld. Thus, the ultimate weld strength at discrete points changes along the length of the weld. Figure 1.1 shows the load-deformation behavior of fillet welds for different angles between the weld longitudinal axis and the load direction.
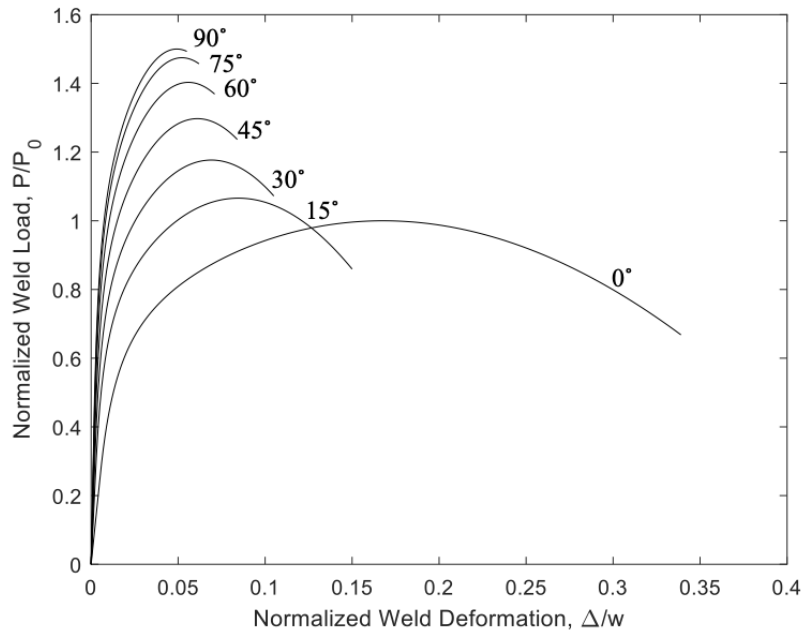
Figure 1.1 : Load-deformation of fillet weld with different loading angles

1.3 STRENGTH OF ECCENTRICALLY LOADED CONNECTIONS

Several approaches are available in literature for determining the capacity of connecting elements under eccentric loads. These approaches include elastic analysis, plastic analysis, and instantaneous center of rotation (IC). For bearing-type bolted connections, elastic analysis resolves the applied force into components applied at the center of gravity of the bolt group and finds the force on each bolt using elastic stress analysis (Higgins 1971). This method identifies the critical bolt and ensures that it has the minimum required capacity given the applied load and bolt group configuration. This method neglects the plastic capacity of bolts and tends to provide conservative estimate of the connection capacity (AISC 2017).

Crawford and Kulak (1968) developed a model to predict the ultimate capacity of eccentric bearing-type bolted connection that included the plastic deformation of bolts. The study defined the load-deformation behavior of 3/4-in diameter A325 bolts and implemented the instantaneous center of rotation method to predict the connection behavior based on equilibrium conditions. The model requires iterations over the location of the instantaneous center of rotation and calculates the resisting force of each bolt based on the proportion of the radii of the bolts to the IC and the load-deformation equation defined within the study. The bolt forces are summed, and equilibrium is checked against applied loads. The location of the IC is determined when equilibrium is reached. This model forms the basis of the AISC (2017) design method included in Tables 7-6 through 7-13 for eccentrically loaded bolted connections.

Kulak (1975) presented a paper that recognized that the IC Method and the associated load-deformation behavior for bearing-type bolts provides highly conservative load predictions for eccentrically loaded slip-critical joints. He demonstrated, analytically and experimentally, that the force resisted by each bolt should be equal to the ultimate slip force of that bolt and does not depend on the radius to the IC. By adopting this load-deformation behavior and using the IC Method, capacity predictions showed better agreement with experimental test results.

Butler et al. (1972) predicted the ultimate capacity of an eccentrically loaded welded connection by using the IC method. The research used the weld load-deformation model described by Eq. 5-8. The analytical study was complemented by experimental testing of eccentrically loaded longitudinal and C-shape welds. The capacity prediction based on the IC method showed good agreement with the experimentally obtained results. The AISC (2017) uses this method to calculate the nominal capacity of an eccentrically loaded welded connection with the following load-deformation relationship:

$$F_{nwi} = 0.6F_{EXX}(1.0 + 0.5sin^{1.5}\theta_i)[p_i(1.9 - 0.9p_i)]^{0.3} \qquad \text{Eq. 11}$$

1.4 COMBINATION CONNECTION STRENGTH

Several studies have been conducted to investigate the strength and behavior of combination connections. These studies have provided insight into the contributions of several variables to the connection strength; these include weld orientation, bolt hole clearance, bearing condition, bolt

tension, and randomness of bolt location relative to the bolt hole. Several experimental studies spanning from 1969 – 2020 are summarized below.

1.4.1   Steinhardt, Möhler, and Valtinat (1969)

Early efforts to understand the behavior of connections utilizing slip-critical bolts and longitudinal welds are discussed in the *Guide to Design Criteria for Bolted and Riveted Joints* by Fisher and Struik (1973). The 1969 study completed by Steinhardt et al. (1969) in Germany tested small tension butt splices featuring two bolts on each side of the splice. This experimental study included bolted-only, welded-only, and combination connections. A summary highlighting the load-deformation behavior of the test connections is depicted in Figure 1.2. The experimental results conclude that the capacity of the combination connection can be predicted as the sum of the bolted-only slip load and the ultimate load of the welded-only connection.
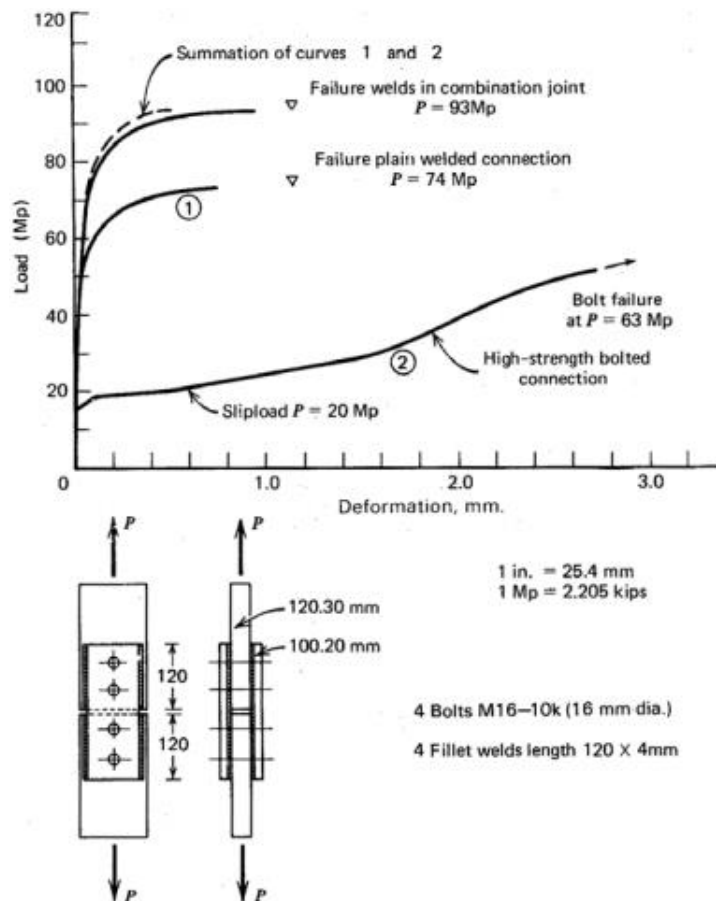
Figure 1.2 : Combination connection investigation results in Steinhardt et al. (1969)
[adapted from Fisher and Struik (1973)]

6

1.4.2 Holtz and Kulak (1970)

A research program conducted by Holtz and Kulak (1970) in Novia Scotia investigated the use of combination connections in two distinct configurations, tension splices and moment resistant beam-column connections.

The tension splice tests investigated the effect of weld orientation, longitudinal or transverse, as well as bolt hole clearance. The tension splices were double lap connections that included both bolts and welds. All test bolts were 3/4-in. diameter A325 grade. The welds were made with an E60 electrode and had a nominal fillet weld size of 1/4-in. The testing program consisted of three different configurations and each type featured three samples. The test configurations were:

1. Four lines of longitudinal fillet weld, each 3-in. long, and two high strength bolts. No clearance is provided between bolts and bolt holes (bolts are in direct bearing). Bolts are only installed as snug tight.
2. Four lines of longitudinal fillet weld, each 3-in. long, and two high strength bolts. Standard 13/16-in. holes are used. Bolts are pretensioned to 1/2 turn after snug tight condition.
3. Two lines of transverse fillet weld, each 7-in. long, and one high strength bolt. Standard hole 13/16-in. holes are used. Bolts are pretensioned to 1/2 turn after snug tight condition.

The moment connection tests used flange-plated fully restrained moment connection with welds connecting the flange-plate to the flanges of the supported beam and bearing-type bolts for the shear connection. These tests also studied the weld orientation to include longitudinal, transverse, and both welds. All welds were made with 1/4-in. fillet welds and E60 electrode. This testing had two specimens per weld configuration totaling 6 tests. All tests used three high-strength bolts in bearing and varied the weld geometry for the flange-pate connection as follows:

1. Four lines of longitudinal weld, each 8-in. long.
2. Two lines of transverse weld, each 8-in. long.
3. Four lines of longitudinal weld and two transverse welds, all 8-in. long.

The testing concluded that combination connections with transverse welds may not improve the connection capacity due to the limited ductility of welds. Longitudinal welds provided an increase in the deformation capacity and in turn a more efficient use when combined with bolts. The combination connections with bolts in direct bearing provided high factors of safety, but do not directly apply to typical construction practices due to the absence of bolt clearance. When hole clearance was provided, the joint underperformed compared to those with direct bearing conditions and therefore provided a lower factor of safety (Holtz and Kulak 1970).

1.4.3 Jarosch and Bowman (1986)

A similar study by Jarosch and Bowman (1986) was conducted at Purdue University. The research included the experimental testing of six double lap tension splice configurations, three of which were combinational. The tension splice tests investigated the effect of weld orientation,

longitudinal or transverse. All test bolts were 3/4-in. diameter A325 grade and featured standard 13/16-in. holes. Each bolt was also pretensioned to 1/2 turn after snug-tight condition. The welds were made with an E60 electrode and had a nominal fillet weld size of 1/4-in. The test configurations were:

1. Four lines of longitudinal fillet weld, each 4.5-in. long, and two high strength bolts.
2. Two lines of transverse fillet weld, each 5.5-in. long, and two high strength bolts.
3. Longitudinal welds (1), transverse welds (2), and two high strength bolts.

The study concluded that transverse welds should not be combined with slip-critical bolts due to ductility limitations. Furthermore, they indicated that the frictional load developed by the high-strength bolts is not reliable when transverse welds are utilized in a combination connection. For combination connections using only longitudinal welds, the ultimate load was accurately predicted by summing the weld shear strength and bolt slippage force (Jarosch and Bowman 1986).

1.4.4   Manuel and Kulak (2000)

In 2000 at the University of Alberta, Manuel and Kulak continued the research into the behavior of combination connections in tension splices (Manuel 1996, Manuel and Kulak 2000). They conducted an experimental testing program that included twenty-four axial lap specimens. Their test connections investigated the effect of weld orientation, bolt tension, and bolt bearing condition. While the effect of weld orientation, longitudinal or transverse, had been studied in the past, an extensive study had not yet been completed into the impact of bolt tension (snug tight or pretensioned) or the bearing condition. The bearing condition was defined as negative or positive bearing. For negative bearing, the connected parts would have the ability to slip over a distance equivalent to two times of the hole clearance before the bolts would engage in bearing. Positive bearing bolts engage in bearing on the onset of load application. The test bolts were 3/4-in. diameter A325 grade and featured standard hole clearance. For bolts that required pretension, a 1/2 turn after snug-tight condition was administered. All fillet welds featured a 0.236-in. (6-mm) weld size and utilized E48018-1 (E70) electrode. The testing program examined all possible combinations of the three testing variables resulting in twelve connection types. Additionally, each connection type contained two specimens. The tests specimens can be sorted in the following groups:

1. Four lines of longitudinal fillet weld, each 5.512-in. (140-mm) long, and four high strength bolts.
2. Two lines of transverse fillet weld, each 10.236-in. (260-mm) long, and four high strength bolts.
3. Longitudinal welds (1), transverse welds (2), and four high strength bolts.

Each group included combinations of bolt bearing (positive or negative) and bolt pretension (snug tight or pretensioned).

Similar to the study by Holtz and Kulak (1970) and Jarosch and Bowman (1986), it was concluded that transverse welds should not be combined with slip-critical bolts due to ductility limitations. The contribution of bolt pretension, occurring in the form of plate friction, was noticeable in the test program; however, it was not clearly understood. This additional capacity was dependent on the weld configuration and bearing condition. The influence of bolt pretension was noticed in the connections with longitudinal welds and bolts in negative bearing. The effect of bearing condition was shown to be an influential factor in evaluating the performance of the connection. Bolts in positive bearing resulted in a capacity increase that reached up to 81% for certain configurations (Manuel and Kulak 2000).

The experimental work resulted in the following analytical model for estimating the ultimate capacity of combination connections:

$$R_{ult\ joint} = R_{friction} + R_{bolts} + R_{trans} + R_{long} \qquad \text{Eq. 12}$$

The model provided a simplified approach for designers when the load-deformation behavior of fasteners is not available. In the model, $R_{friction}$ is taken as 25% of the total slip resistance for the bolted connections. When the connection utilizes transverse welds or it is known that the bolts are in negative bearing, the bolt shear strength, R_{bolts}, is not included. If the bolts are in positive bearing, R_{bolts} is 75% of the bolt shear capacity. However, bolts in intermediate bearing (middle of the hole) would incorporate 50% of the shear capacity. This is used to simulate field bolted conditions. Finally, the longitudinal fillet weld strength, R_{long}, is reduced to 85% when used with transverse fillet welds (Manuel and Kulak 2000).

1.4.5 Kulak and Grondin (2003)

Another testing program at the University of Alberta in 2003 was conducted by Kulak and Grondin (2003). Their experimental work was a continuation of the research conducted by Manuel and Kulak (2000) by investigating the effect of the randomness in the bolt bearing condition. Recall that the bearing condition contributed to the capacity of combination connections; however, the location of the bolts relative to the bearing surface is not easily controlled under construction field conditions. The testing program included nineteen axial lap test specimens that were nominally the same, except for the bolt bearing condition. This was the only variable studied during the experimental work. Each connection was constructed of four 3/4-in. diameter A325 grade test bolts with hole clearance and pretensioned to 1/2 turn after snug-tight condition. The test connection also included four lines of longitudinal fillet weld, each 5.512-in. (140-mm) long. All fillet welds featured a 0.236-in. (6-mm) weld size and utilized E48018-1 (E70) electrode.

The experimental results were compared against the model presented by Manuel and Kulak (2000) in Eq. 12. The bolt location relative to the holes was assumed to be intermediate bearing for the prediction. The model was capable of predicting the experimental results with sufficient accuracy (Kulak and Grondin 2003).

1.4.6 Shi., et al. (2011)

A study by Shi et al. in 2011 at Tsinghua University, China investigated the ultimate capacity of combination connections experimentally (Shi et al. 2011a) and numerically with the finite element method (FEM) (Shi et al. 2011b). Shi et al. (2011a) tested six double lap tension splice configurations, two of which were combination connections (Shi et al. 2011a). The experimental specimens included high strength bolts utilizing 3/4-in. diameter A490 (M20 – 10.9) bolts. The longitudinal and transverse fillet welds featured a 0.236-in. (6-mm) and 0.276-in. (7-mm) weld size, respectively. The welds were made of an E50 welding rod. The combination test configurations were:

1. Four lines of longitudinal fillet weld, each 2.362-in. (60-mm) long, and two high strength bolts.
2. Four lines of longitudinal fillet weld, each 2.362-in. (60-mm) long, and two lines of transverse fillet weld, each 3.150-in. (80-mm) long. Two high strength bolts.

The FEM models included a spectrum of high strength bolt diameters ranging 3/4-in. to 1-1/8-in. (M20 – M27), as well as two bolt grades, A325 and A490 (8.8.3 and 10.9). The modeled fillet weld sizes ranged from 0.157-in. to 0.394-in. (4-mm to 10-mm) and included lengths of 1.575-in. to 3.937-in. (40-mm to 100-mm). The weld electrode was modeled as E50. Fourteen different models were built consisting of four bolts and four longitudinal welds.

The experimental and numerical work concluded that the connection capacity may depend on the ratio between bolt capacity and weld capacity. The authors developed the following model based on the variable a that describes the bolt to weld capacity ratio (Shi et al. 2011b).

$$a = \frac{R_{friction}}{R_{long.\ welds}}, R_{ult} = \begin{cases} R_{long.\ welds} & for\ a < 0.5 \\ 0.75R_{long.\ welds} + R_{friction} & for\ 0.5 \leq a < 0.8 \\ 0.9R_{long.\ welds} + 0.8R_{friction} & for\ 0.8 \leq a \leq 2 \\ R_{long.\ welds} + 0.75R_{friction} & for\ 2 < a \leq 3 \\ R_{friction} & for\ a > 3 \end{cases} \qquad Eq.\ 13$$

1.4.7 Kim and Lee (2020)

Kim and Lee (2020) conducted a series of combined bolted and welded lap joint tests to investigate the effects of the steel grade of base metal, bolt bearing condition and weld configuration. It was concluded that the steel grade of base metal had little effect on the load-deformation behavior of the joints, while the capacity in the positive bearing condition could be higher than negative one by around 15%. Based on the test results and the load-deformation relationship in previous literature, Kim and Lee (2020) proposed a strength equation for combination connections with longitudinal fillet welds and bolts as

$$R_{ult} = 0.8R_{bolt} + U \times R_{long.welds} \qquad Eq.\ 14$$

where R_{bolt} is the ultimate strength of bearing-type bolt, l is the connection length, W is the plate width, and U was defined as a shear lag factor and was calculated as 1.0 ($l \geqslant 2\ W$), 0.87 ($2\ W > l \geqslant 1.5\ W$), or 0.75 ($1.5\ W > l \geqslant W$).

1.4.8 AISC Specification for Structural Steel Buildings (2016)

The current *Specification for Structural Steel Buildings* provides guidelines for connections with bolts and welds in combination in Section J1.8 (AISC 2016). These connections are permitted only in the design of shear connections on common faying surfaces with the consideration of strain compatibility. However, the specification permits the determination of available strength, ϕR_n and R_n/Ω, of a joint by combining the strengths of slip-critical bolts and longitudinal fillet welds. The nominal slip resistance, R_n, is defined in Equation J3-4 according to the requirements of a slip-critical connection (AISC 2016). The nominal weld strength, R_n, is defined in Section J2.4 (AISC 2016). The nominal strength of the combination connection may be taken as the sum of bolts and welds when the following apply:

a) $\phi = 0.75$ (LRFD); $\Omega = 2.00$ (ASD) for the combined joint
b) When the high-strength bolts are pretensioned using the turn-of-nut method, the longitudinal fillet welds shall have an available strength of not less than 50% of the required strength of the connection.
c) When the high-strength bolts are pretensioned using any method other than the turn-of-nut method, the longitudinal fillet welds shall have an available strength of not less than 70% of the required strength of the connection.
d) The high-strength bolts shall have an available strength of not less than 33% of the required strength of the connection.

Finally, the combined connection strength need not be taken as less than either the strength of slip-critical bolts or strength of longitudinal fillet welds alone (AISC 2016).

Based on this literature survey, the past research in combination connections studied how bolt pretension, bearing condition, and weld orientation impacts the capacity and load-deformation behavior of combination connections. However, there exists additional variables that may also influence the behavior of the connection. These variables include bolt pattern, bolt grade, bolt size, pretensioning technique, and faying surface class. In addition, although the weld/bolt strength ratio was investigated in Shi et al. (2011), the study outcomes were mainly based on the results of the numerical investigation. More research is needed in order to fully quantify the effect that the weld/bolt strength ratio has on the connection behavior and the capacity prediction. The next sections of this report discuss the results of a comprehensive experimental program conducted to address the knowledge gaps in the performance of connections utilizing slip-critical bolts and longitudinal fillet welds in combination.

2 CONCENTRIC CONNECTION TESTING

This section discusses the experimental methods used to investigate both the strength and load-deformation behavior of concentric connections using slip-critical bolts with longitudinal fillet welds in combination. This includes a discussion regarding the overall test specimen design, as well as the testing equipment and experimental procedures.

2.1 TEST SPECIMENS

Two sizes of axial lap double shear configurations are included in the study, 2×2 connections and 2×3 connections. The specimen configuration was designed such that the load is applied through the centroid of the fasteners. Both test specimen sizes are made of three parts: the tested connection, the anchorage zone, and the connection grip. Each of the three parts utilize A572 Gr.50 steel. Figure 2.1 shows a 3-D view of a typical test specimen.
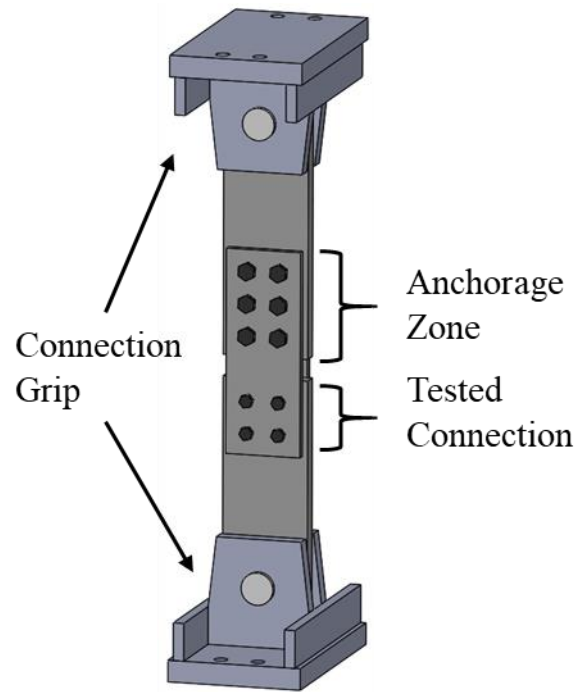
Figure 2.1: Typical 2×2 test specimen

2.1.1 Test Matrix

This portion of the experimental testing program is made up of two parts, 2×2 connections and 2×3 connections. The test specimens represent an effort to analyze different combinations of important test variables. The variables include bolt pattern, bolt grade, bolt size, tensioning technique, faying surface class, and weld/bolt strength ratio. Table 2.1 depicts the experimental test matrix consisting of 75 connections with 23 different combinations of connection variables. Of these, 47 are of the 2×2 connection size and 28 are 2×3. The connection nomenclature used for testing is based purely off the test matrix (Test 1 – Test 23). Each test series contains multiple

specimens to be named A, B, C, etc. (e.g., 2A, 2B, 2C). This naming system was chosen due to the large amount of connection variables and the inability to efficiently name each connection based purely on the test variables.

Table 2.1: Experimental test matrix: double-shear tension splices

	Test No.	Bolt Pattern	Bolt Grade	Bolt Pretensioning Method	Faying Surface Class	Weld Geometry (Size × length) [†]	R_{n_W}/ R_{n_B}	No. of Samples
Bolted-Only	1	2×2	A325	ToN	B	-	-	5
	2	2×2	A325	ToN	A	-	-	3
	3	2×2	A490	ToN	B	-	-	3
	4	2×2	A325	TC	A	-	-	3
	5	2×2	A490	ToN	A	-	-	3
Welded-Only	6	-	-	-	-	5/16 × 3.0	-	3
Bolted & Welded	7	2×2	A325	ToN	B	5/16 × 5.0	1.5	3
	8	2×2	A325	ToN	B	5/16 × 2.25	0.67	3
	9	2×2	A325	ToN	B	5/16 × 3.5	1.0	3
	10	2×2	A325	TC	B	5/16 × 2.25	0.67	3
	11	2×2	A490	ToN	B	5/16 × 2.75	0.67	3
	12	2×2	A325	ToN	A	5/16 × 1.25	0.67	3
	13	2×2	A325	ToN	A	5/16 × 2.0	1.0	3
	14	2×2	A325	ToN	A	5/16 × 3.0	1.5	3
	15*	2×2	A325	ToN	A	5/16 × 3.5	1.0	3
Bolted-Only	16	2×3	A325	ToN	A	-	-	5
Welded-Only	17-2	-	-	-	-	5/16 × 2.0	-	3
	17-4	-	-	-	-	5/16 × 4.0	-	2
Bolted & Welded	18	2×3	A325	ToN	A	5/16 × 2.0	0.67	3
	19	2×3	A325	ToN	A	5/16 × 3.0	1.0	3
	20	2×3	A325	ToN	A	5/16 × 4.0	1.33	3
	21	2×3	A325	ToN	A	5/16 × 6.25	2.0	3
	22	2×3	A325	TC	A	5/16 × 3.0	1.0	3
	23	2×3	A490	ToN	A	5/16 × 2.0	0.50	3

NOTE: All bolts are 3/4-in. diameter (oversized holes) unless noted otherwise.
TC = Tension control bolt; ToN = Turn of nut method
R_{n_W} = Nominal shear capacity of welds; R_{n_B} = Nominal slip capacity of bolts
[†] Four fillet weld lines of the specified geometry per connection. Units are inches.
* Bolts are 1-in. diameter A325 in oversized holes.

Tests 1 – Test 15 cover the 2×2 connections and provide a comprehensive investigation into each of the critical variables. Test 1 – Test 5 in the experimental test matrix consist of bolted-only connections that isolate the bolt grade, bolt tensioning method, and faying surface class. These tests provide a baseline understanding of the influence of discrete variables on the inherent strength and ductility of the connections. Additionally, each test includes three individual

specimens to better characterize the statistical variation in the capacity. Two additional specimens were added to Test 1 during the program to better understand the variation in the Class B faying surface. The connections in Test 1 – Test 5 will also be used to evaluate the mean slip coefficient associated with the specific steel material and fabrication technique. The welded-only specimens in Test 6 feature 3-in. welds and are used to estimate the weld shear strength and to understand the load-deformation behavior of the specific weld electrode used for the research program. Finally, Test 7 – Test 15 are combination connections that investigate the load-sharing capability of the bolts and welds. These tests vary the weld/bolt strength ratio as well as the faying surface, bolt grade, bolt pretensioning technique, and bolt diameter. The weld/bolt ratio for the 2×2 combination connections vary from 0.67 – 1.5 for Class A and Class B surfaces.

Test 16 – Test 23 study the 2×3 connections and only investigate Class A surfaces. Similar to the 2×2 connections, Test 16 and Test 17 are aimed at quantifying the capacity of individual connecting elements. Test 16 includes five bolted-only specimens and Test 17 includes five welded-only connections studying two different lengths of weld, 2-in. (Test 17-2) and 4-in. (Test 17-4). Three 2-in. samples and two 4-in. samples are tested. The combination connections in Test 18 – Test 23 vary the weld/bolt strength ratio as well as bolt grade and bolt pretensioning technique. The weld/bolt ratio for the 2×3 combination connections vary from 0.67 – 2.0. Again, each combination test includes three specimens.

Class A connections are a clean mill scale and Class B connections feature a SSPC-SP6 commercial blast cleaning. The blast cleaning removes all visible rust, mill scale, paint and foreign matter; however, staining is permitted on no more than 33% of each 9-in.[2] of the plate surface (AISC 2017). The Class B plates used in this program exceeded these SSPC-SP6 requirements. All welded connections, both welded-only and combination, use four equally sized longitudinal fillet welds, one on each side of the two splice plates. The weld lengths were chosen based on the desired weld/bolt strength ratio cited in Table 2.1. All longitudinal fillet welds are 5/16-in. size and are made with an E70 electrode.

2.1.2   Test Connection Design & Details

As previously highlighted in Figure 2.1, each connection consists of three parts: the tested connection, the anchorage zone, and the connection grip. The test connection details for each specimen are depicted in Figure 2.2. The zones for each configuration, 2×2 and 2×3, were designed according to the highest expected load within the test matrix. These correspond to Test 7 and Test 21, respectively for the 2×2 and 2×3 connection layouts. The steel plates are designed to ensure the following inequality:

$$R_n(Plates) > R_n(Bolt\ Slip) + R_n(Weld) \qquad \text{Eq. 15}$$

$R_n(Plates) = $ nominal plate capacity

$R_n(Bolt\ Slip) = $ nominal slip resistance of pretensioned slip-critical bolts

$R_n(Weld) = $ nominal capacity of longitudinal fillet welds

The connecting elements are designed to fail before plate failure. Each connection zone was designed considering the following modes of failure: gross yielding, plate rupture, block shear, bolt shear, pin failure, and bolt bearing and tear out.

The *tested connection* indicates the portion of the sample that will be analyzed, meaning that failure is designed to occur here first. The bolts in this zone, four for 2×2 and six for 2×3, are slip-critical and will be combined with four longitudinal fillet welds at varying lengths according to Table 2.1. The bolt holes in this location are oversized and the plates are assembled in negative bearing to measure the full slip distance. For negative bearing, the connected parts can slip a distance equivalent to twice the hole clearances before the bolts would engage in full bearing. Plate rupture through the splice plate holes for oversized 1-in. diameter bolts (Test 15) is the controlling failure mode for the *tested connection*.

The *anchorage zone* supplies the necessary resistance to tie-down the specimen during loading. The resistive force is applied by bolts in positive bearing to transfer the load to the specimen. Six 1-in. diameter A490 bolts are used for the 2×2 specimens and eight 7/8-in. A490 bolts for 2×3 specimens. Unlike the tested connection, all bolt holes are standard hole size. Similar to the tested connection plates, plate rupture through the splice plate holes is the controlling failure mode for the *anchorage zone*.

The *connection grip* is the load transfer mechanism from the header beams of the test frame to the specimen. This component is made up of two parts: the pin connection and the beam clevis. The pin connection is designed simply to transfer the force in double shear using a 3-in. steel cylinder with 130 ksi yield stress. The clevis plates were checked for gross yielding, plate rupture, bearing and tear out, as well as all local effects due to stress concentration. During load application, the connection grip can experience high amounts of bending at the top header beam. Therefore, longitudinal stiffeners are added to resist the stress.

The specimens are fabricated according to AISC and industry standards at W&W|AFCO Steel in Oklahoma City. The fabricator also completed all Class B SSPC-SP6 sand blasting. All test connections were assembled at the Bert Cooper Engineering Laboratory (BCEL) according to industry standard. Connection fillet welds are placed by the lab manager who is a certified welder.

Figure 2.2: Test connection details (units are in inches)
a) 2×2 connection, b) 2×3 connection

16

2.2   EXPERIMENTAL TEST FRAME

A custom load frame was designed and constructed to test the 2×2 and 2×3 test specimens in this study. The test frame is designed for a 500-kip load. This load provides a factor of safety of 1.5 against the largest expected connection capacity (Test 21). The frame was designed in accordance with the 2016 AISC Specifications. Figure 2.3**Error! Reference source not found.** depicts a 3-D rendering of the test frame.
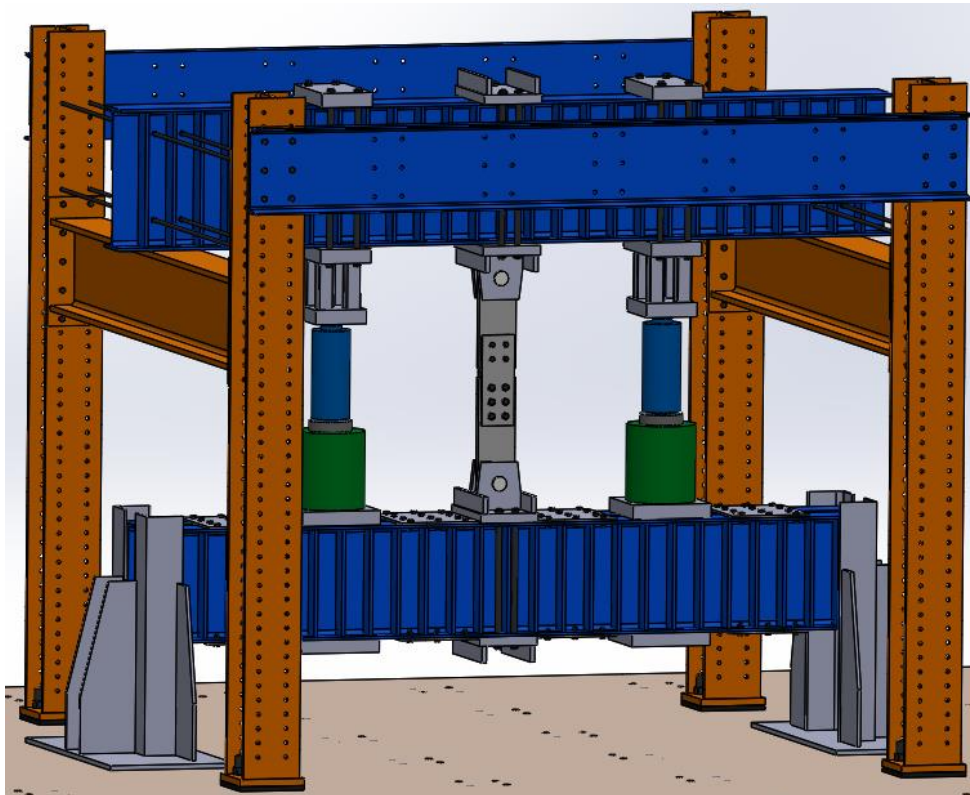
Figure 2.3: 3-D rending of load frame

2.2.1   Frame Structure

The test frame is designed so that all loading is balanced within the test frame itself. The only loads transmitted to the laboratory floor is the self-weight of the test frame plus specimens. The testing load is contained within the bottom and top header beam(s). Each header beam has been designed for shear, moment, stability, and local effects. Stiffeners throughout the section have been specified to counteract local effects such as web buckling and web yielding/crippling. All frame plates are constructed using A572 Gr. 50 steel.

The bottom header beams are two W24×68 sections that are bolted together with 1/2-in. plates. The beams work together as a box-girder section to supply the needed resistance for testing. Two beams were chosen for the bottom to accommodate the hydraulic cylinder attachment. The top header beam is a single W30×99. Each test specimen attaches to the load frame at midspan of the section. To withstand the high test loads, the *connection grip* is attached

17

to the test frame using 1-1/4-in. diameter A354-BD threaded rods. The rods run through top and bottom sandwich plates that are designed to resist the high bending that will occur during the load test. Additionally, the threaded rods are pretensioned to reduce clearances due to rod elongation during the test. Finally, two MC18X58 channels are added outside the frame for global stability. Load application occurs on each side of the test specimen through a load column. Each load column features a base plate, hydraulic cylinder, load cell, and a built-up column. The load column is attached to the test specimen by utilizing sandwich plates and threaded rods. Figure 2.4 depicts a detailed connection test frame with an assembled 2×2 connection.

All test frame components, including the top and bottom header beams, lateral stability components, channels, and the built-up columns, were fabricated and provided by W&W|AFCO Steel Co. The total test frame is shown in Figure 2.5.
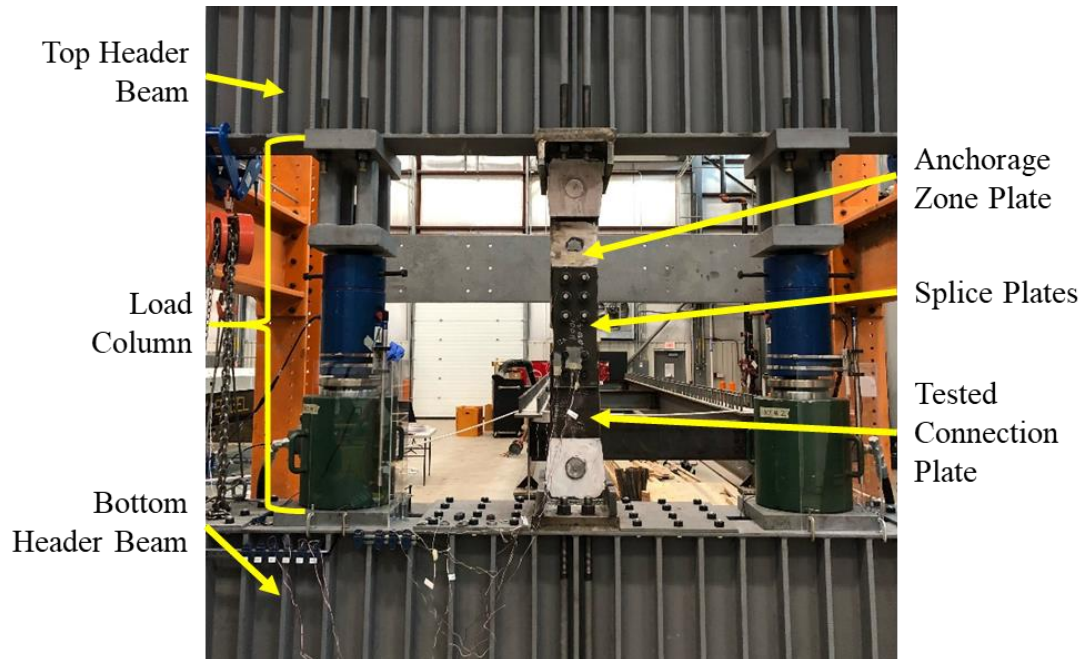
Figure 2.4: Test setup components

Figure 2.5: Constructed 500-kip test frame

2.2.2   Frame Hydraulics & Control

The BCEL features an MTS SilentFlo 90-GPM pump to provide hydraulic power throughout the laboratory. Loads for our testing were controlled using an MTS FlexTest 60 controller. This equipment allows for accurate control of the test load at all times. The load is applied using two 565-ton Simplex hydraulic cylinders operating at 3,000-psi. Each cylinder is fitted with an MTS servo valve and connected to an MTS hydraulic service manifold (HSM). This allows for

automated control of the test system. Each cylinder is also accompanied by a 6-in. stroke linear variable displacement transducer (LVDT) and 250-kip load cell. These components allow for flexibility of the load application to either be controlled by load or displacement. During a test, the two cylinders extend simultaneously at a rate of 0.02-in/min (0.5-mm/min) which lower the bottom header beam and apply tension force to the test connection. One of the two hydraulic load columns is shown below in Figure 2.6.
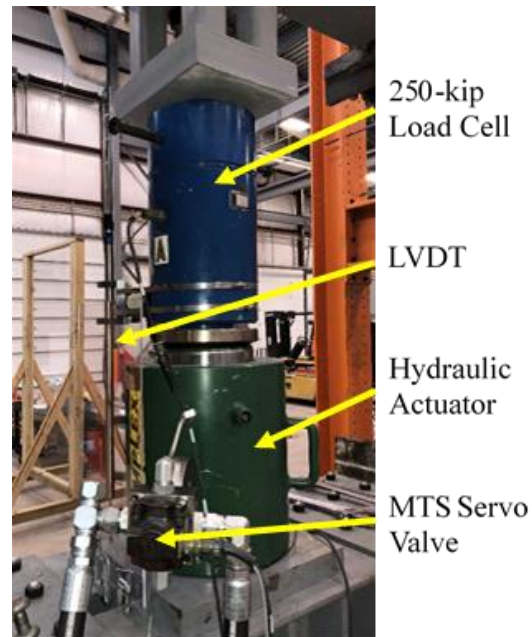
Figure 2.6: Hydraulic load column

2.3 INSTRUMENTATION

To record measured displacements, strains, connection forces, and bolt pretension values, three instrumentation tools are utilized to collect data during the test: LVDTs, strain gages, and load cells. A National Instruments (NI) cDAQ-9178 is utilized for data acquisition along with LabVIEW NXG 3.0 (NI, 2018) to measure and record all experimental data. Figure 2.7 illustrates the NI cDAQ used during the experimental work as well as the various accessories needed to read and record the different data types. Figure 2.8 shows the instrumentation layout for both the 2×2 and 2×3 connections.
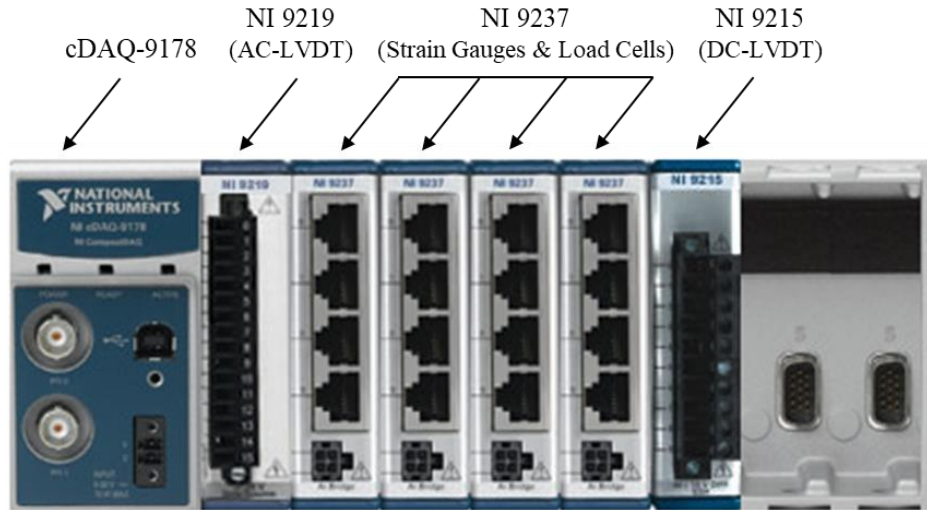
Figure 2.7: Data acquisition system

For displacement measurements, two types of LVDTs are used at various locations, high accuracy AC-LVDTs and long-stroke DC-LVDTs. The four AC-LVDTs measure the slip of the splice plates up to 0.2-in. Larger slip behavior is tracked with two DC-LVDTs that measure the relative displacement between the two center plates. The LVDTs are attached to the connection using strong magnets and are shown in Figure 2.9, images a) and b).

Strain data is acquired using foil-type strain gauges. Two strain gauges are placed on the tested connection near the top of the welds and one is placed in-between the top bolt row. Two additional strain gauges are attached on both sides of the anchorage plate to detect any load eccentricities.

The test force is measured using two load cells. One of the load cells is pictured in Figure 2.6 depicting a typical load column. The load data is fed into both the MTS FlexTest 60 controller as well as the NI cDAQ-9178. Finally, the bolt pretension force is detected with bolt load cells that fit along the bolt shaft in-between the plate and the nut. The bolt load cells are depicted in Figure 2.9, image c).
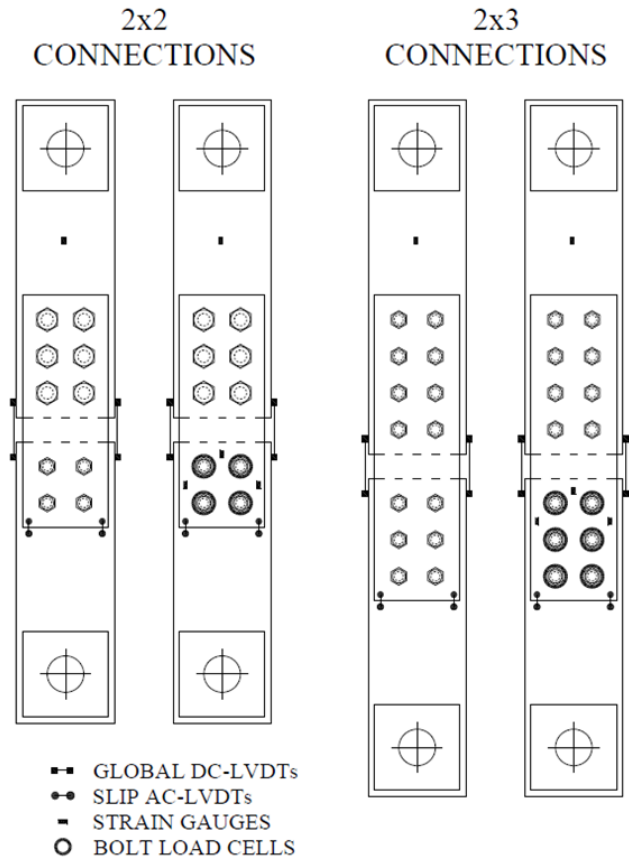
Figure 2.8: Specimen instrumentation plan

The bolt pretension force has a key influence on the strength of bolted-only and combination connections. Therefore, additional bolt pretension data was captured using a Skidmore Wilhelm bolt tension calibrator. Before every connection assembly, three bolts that match the connections bolt type were tested in the Skidmore Wilhelm bolt tension calibrator. This assured that the pretensioning device is operational and provided additional bolt pretension data. This device was also used to calibrate the bolt load cells. The bolt pretension data was later used in this report to evaluate the as-built strength of the connection.
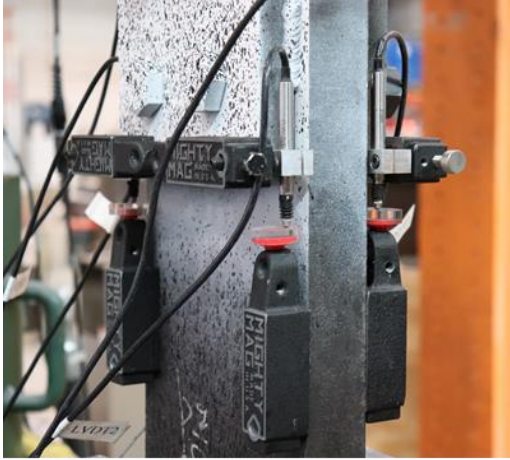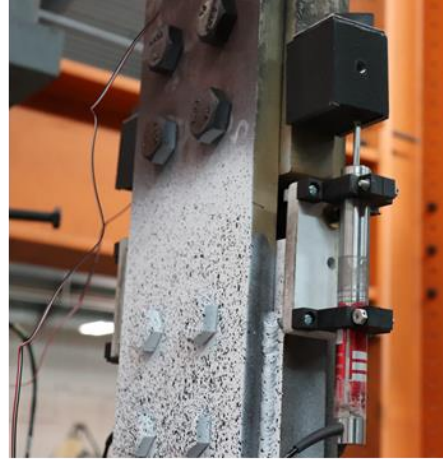
Figure 2.9: Connection instrumentation
a) AC-LVDT, b) DC-LVDT, c) bolt load cells

2.4 TEST PROCEDURE

The following testing procedure was created to ensure that all specimens are assembled and tested consistently.

1. Clean tested connection faying surfaces with degreaser to remove any dirt or oil that would contaminate the faying surface. This cleaning process is only for Class A connections. Class B connections are not cleaned with the degreaser to prevent cross-contamination of the blast-cleaned faying surface.
2. Lift the anchorage zone center plate into the upper connection grip and secure into place with the 3-in. diameter pin.
3. Lift the tested connection center plate into the lower connection grip and secure into place with the 3-in. diameter pin.

4. Attach the two splice plates to the anchorage zone and hand tighten bolts into positive bearing position. These are NOT the test bolts.
5. Use the hydraulic system to manually raise the bottom header beam, which will also lift the tested connection center plate. The beam should be raised until the tested connection holes are in the negative bearing position.
6. Before assembling the test bolts, test three bolts in the Skidmore Wilhelm bolt tension calibrator and record values.
7. Assemble bolts/bolt load cells and pretension tested connection bolts based on RCSC specification (Table J3.1 AISC).
    a. For turn of nut (ToN) method – GWY TN-24EZA-1 ToN Tightening Wrench.
    b. For tension control (TC) bolts – GWY GS-111EZ Shear Wrench.
8. Record bolt pretension forces obtained from bolt load cells.
9. Wrap bolt load cells with tape for protection during welding.
10. Weld specimen according to the test matrix and wait 30 min to cool.
    a. Note any change in pretension force.
    b. Record as-built weld dimensions.
11. Attach final instrumentation according to the instrumentation plan.
    a. Strain gauges
    b. LVDTs
    c. Logitech Webcams

Run the test in displacement control using the MTS FlexTest 60 Controller. Tests are conducted in displacement control at a rate of 0.020-in./min (0.5-mm/min). After the tested connection is removed, the fractured welds are both measured and photographed.

3   EXPERIMENTAL RESULTS: CONCENTRIC CONNECTIONS

A total of 75 individual specimens were tested in the 500-kip load frame constructed for this research program. Each connection was loaded to its capacity (i.e., full slip for bolted-only and bolted-welded; and ultimate fracture for welded-only) or to the point where the connection reached the maximum available slip of 0.375-in. For the most part, the maximum slip force was achieved prior to this displacement level; however, there were some cases where tension forces increased just prior to the 0.375-in. of slip which may indicate the initiation of the bolt bearing behavior. The 75 tests cover a spectrum of critical test variables including bolt pattern, bolt grade, bolt size, tensioning technique, faying surface class, and weld/bolt strength ratio. The results section is organized based on the connection type: bolted-only, welded-only, and combination connections.

3.1   CONNECTION CAPACITY CRITERIA

The nominal strength for each connection was computed using the current AISC Specification. This capacity is noted as the AISC R_n. The AISC R_n is related to the theoretical nominal strength of the bolted and/or welded component. This also corresponds to the capacity that a design engineer would compute. Additionally, the methods used to size the weld lengths based on weld/bolt strength ratio given in the experimental test matrix are based on this formulation. To compute the AISC R_n, equations prescribed by the AISC Steel Specification and AISC Steel Construction Manual were utilized (Eq. 16 and Eq. 17) (AISC 2016, AISC 2017) were the AISC R_n is the summation of the capacities provided by bolts and welds.

Slip-Critical Bolts:

$$R_n = \mu D_u h_f T_b n_s \qquad\qquad \text{Eq. 16}$$

μ = mean slip coefficient for Class A or B surfaces. $\mu = 0.3$ for Class A; $\mu = 0.5$ for Class B

D_u =1.13, a multiplier that reflects the ratio of the mean installed bolt pretension to specified minimum bolt pretension

$h_f = 1.0$; factor for fillers (no fillers)

T_b = minimum fastener tension for A325 or A490 bolts. $T_b = 28$ kips for 3/4-in. A325 bolts; $T_b = 35$ kips for 3/4-in. A490 bolts; $T_b = 51$ kips for 1-in. A325 bolts (AISC Table J3.1) (AISC 2016)

$n_s = 2$; number of slip planes

Fillet Welds:

$$R_n = 0.60F_{EXX}\left(\frac{\sqrt{2}}{2}\right)\left(\frac{D}{16}\right)l \qquad\qquad \text{Eq. 17}$$

$F_{EXX} = 70$ ksi; using an E70 weld electrode

$D = 5$; weld size in sixteenths of an inch

$l =$ weld length, in.

3.2 DETERMINATION OF CONNECTION CAPACITY FROM TEST DATA

This section discusses the methods adopted in interpreting the experimental results to determine the reported test capacity, denoted herein as Test R_n. The Research Council on Structural Connections (RCSC) outlines typical load-deformation behaviors for slip-critical connections as depicted in Figure 3.1 (RCSC 2014). Additionally, the RCSC has defined techniques for determining the slip load for each behavior scenario. Although the standard test for determining the friction coefficient was not conducted, these techniques have been adopted to attain the slip load in this study. The slip load corresponds to the connection capacity for all experimental tests utilizing slip-critical bolts.

Case (a): Slip load is the maximum load provided that this maximum occurs before a slip of 0.02-in.

Case (b): Slip load is the load at which the slip rate increases suddenly.

Case (c): Slip load is the load corresponding to a deformation of 0.02-in. This definition applies when the load vs. slip curve shows a gradual change in response.

It should be noted that the reported test results for the Class A surfaces followed a load-deformation behavior similar to Case (c) while the Class B surfaces followed a response closer to Case (a) shown in Figure 3.1. These curves were adopted to determine the connections capacity or Test R_n.

3.3 BOLTED-ONLY TESTS

To establish a baseline understanding of the load-deformation (i.e., load-slip) behavior of the bolted connections, six types of bolted-only connections were tested, and each test included at least three test specimens. These connections varied several critical variables including bolt pattern, bolt grade, bolt tensioning method, and faying surface class. Table 3.1 depicts the specific connection characteristics for each test.
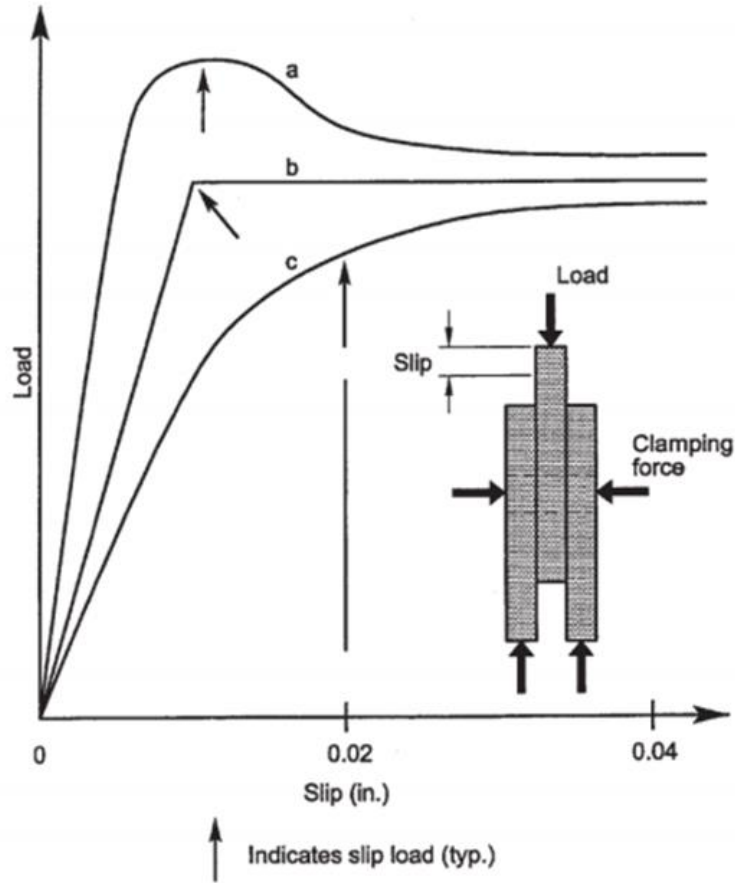
Figure 3.1: Load-slip curves defined by AISC
[adapted from (RCSC 2014)]

Table 3.1: Bolted-only connection characteristics

	Test No.	Bolt Pattern	Bolt Type	Bolt Tensioning Method	Faying Surface Class	Weld Geometry (Size × length)	R_{n_W}/ R_{n_B}	No. of Samples
	1	2×2	A325	ToN	B	-	-	5
	2	2×2	A325	ToN	A	-	-	3
	3	2×2	A490	ToN	B	-	-	3
Bolted-Only	4	2×2	A325	TC	A	-	-	3
	5	2×2	A490	ToN	A	-	-	3
	16	2×3	A325	ToN	A	-	-	5
NOTE: All bolts are 3/4-in. diameter (oversized holes) unless noted otherwise.								
TC = Tension control bolt; ToN = Turn of nut method								
R_{n_W} = Shear capacity of welds; R_{n_B} = Slip capacity of bolts								

3.3.1 2×2 Class A Connections

A total of nine 2×2 Class A bolted-only connections were tested. These connections are Test 2, Test 4, and Test 5. The connections vary the bolt grade, A325 or A490, and the bolt pretensioning method, ToN or TC. Each Class A connection was constructed as outlined in the test procedure. Figure 3.2 – Figure 3.4 depict the load-deformation behavior for the Class A bolted-only tests. Each test consisted of three specimens and the results of each individual test are shown in Table 3.2. Note also that the strength of each connection was increasing with the increase in slip, but that some tests were stopped short of bolt bearing for safety concerns at the beginning of the test program. The reported test capacity, Test R_n, for each test is the connection force recorded at 0.02-in. of slip.
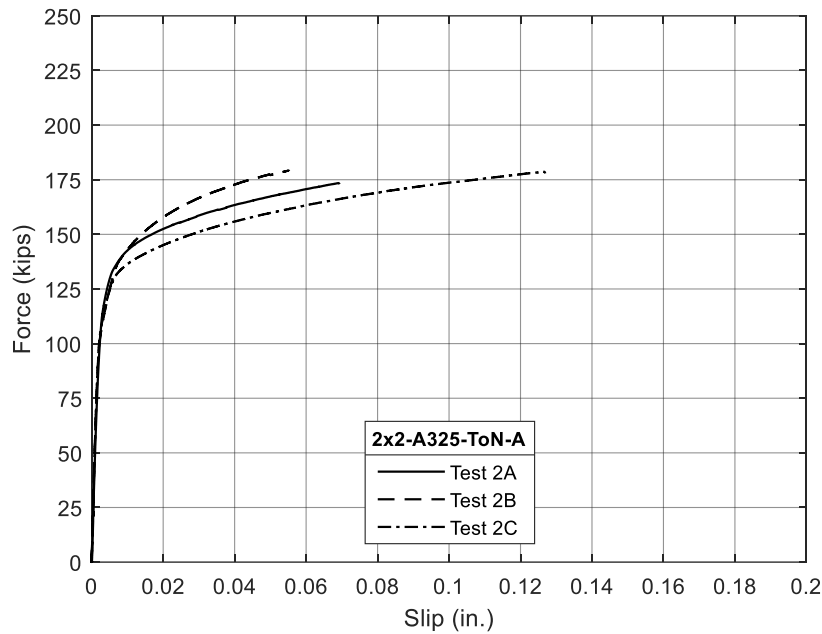
Figure 3.2: Test 2 load-slip curve
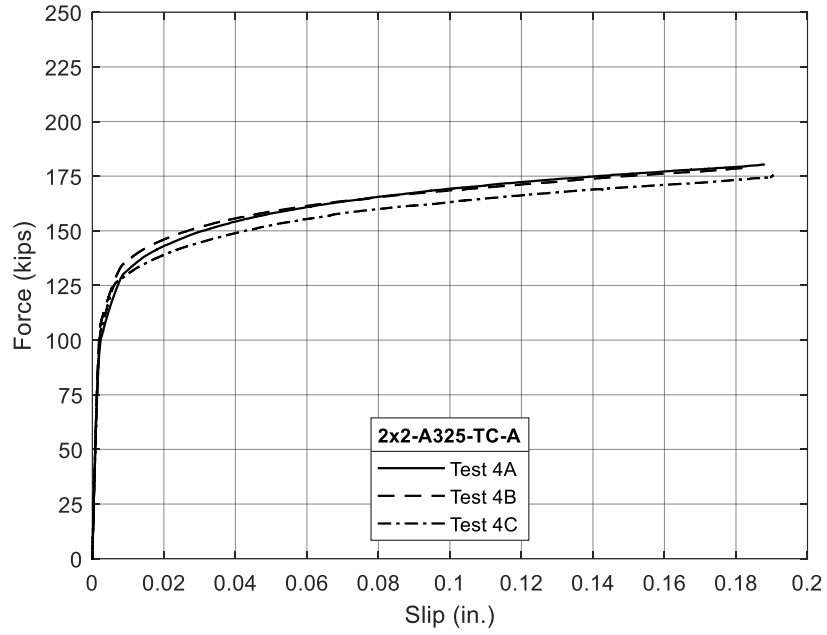
Figure 3.3: Test 4 load-slip curve
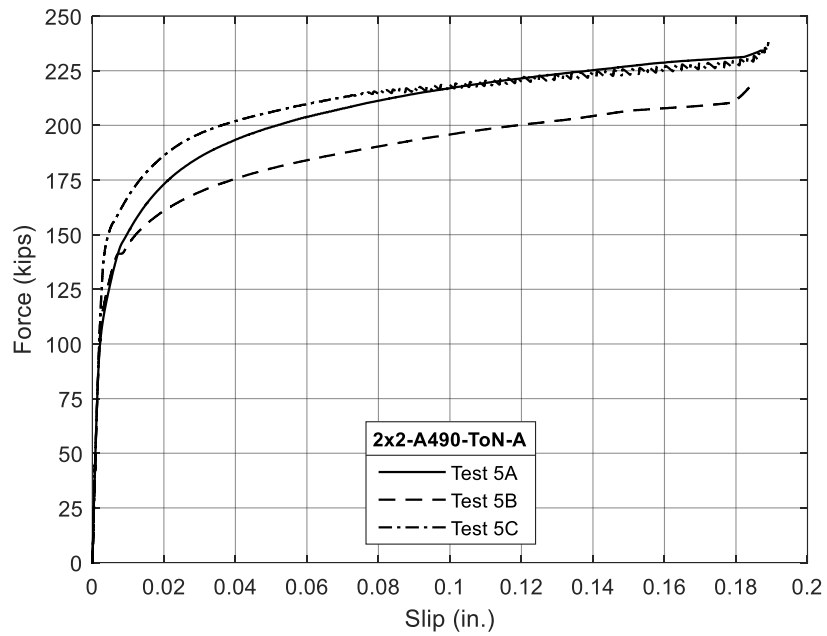
Figure 3.4: Test 5 load-slip curve

For the tests shown in Figure 3.2 (Test 2), the loading was stopped at approximately 180 kips which is the shear capacity of the bolts. These connections were the first specimens tested in the frame. However, later tests were pushed to 0.18-in. of slip and beyond, as indicated by the LVDT reading. All load-slip curves are ended at 0.2-in. of slip due to the limiting stroke of the four high accuracy AC-LVDTs. However, slip was still tracked using large-stroke DC-LVDTs up to 0.375-in.

Table 3.2 highlights the connections' nominal strength (i.e., AISC R_n), as well as the slip load (i.e., Test R_n) for each test. The load-deformation behavior for Test 2, Test 4, and Test 5 followed closely the behavior outlined as Case (c) by the RCSC in Figure 3.1. The slip load for these bolted-only connections is the load corresponding to 0.02-in. of slip. Finally, the connections factor of safety, Test R_n / AISC R_n, is computed and included in Table 3.2.

Table 3.2: 2×2 bolted-only results – Class A faying surface

	Specimen	AISC R_n (kips)	Test R_n (kips)	Test R_n / AISC R_n
Test 2	A	75.9	152.5	2.01
	B	75.9	157.8	2.08
	C	75.9	145.1	1.91
Test 4	A	75.9	143.0	1.88
	B	75.9	146.0	1.92
	C	75.9	139.0	1.83
Test 5	A	94.9	173.1	1.82
	B	94.9	160.9	1.70
	C	94.9	186.2	1.96
NOTE: The Test R_n is the load at 0.02-in. of deformation. AVG = Average value; SD = Standard Deviation; CV = Coefficient of variation				**AVG = 1.902** **SD = 0.112** **CV = 5.90%**

As seen in Figure 3.2 – Figure 3.4 and Table 3.2, 2×2 Class A bolted-only connections (Test R_n) provided a capacity that is on average 90% higher than the nominal AISC capacity (AISC R_n). It is noted that, despite the Test R_n exceeding the AISC R_n by 90% on average, the standard deviation in the Test R_n / AISC R_n is 0.112 and the coefficient of variation is only 5.9%.

3.3.2 2×2 Class B Connections

A total of eight Class B bolted-only connections were tested. These connections are Test 1 and Test 3 and their respective test characteristics are highlighted in Table 3.1. The Class B connections vary only the bolt grade, A325 or A490. Figure 3.5 – Figure 3.6 depict the load-deformation behavior for the Class B bolted-only tests and the results of each individual test are shown in Table 3.3. Each Class B bolted-only connection was constructed as outlined in the test procedure. However, Class B connections are not cleaned with the degreaser. This cleaning process can contaminate the faying surface if shop towels are not clean and may cause premature failure as evident by the results of Test 1B. This test had a reduction in capacity as shown in

Figure 3.5 below. Note that in most of these tests, the maximum strength of each connection was achieved right before the occurrence of sudden slip. The reported test capacity, Test R_n, for each test is the maximum connection force recorded before 0.02-in. of slip.
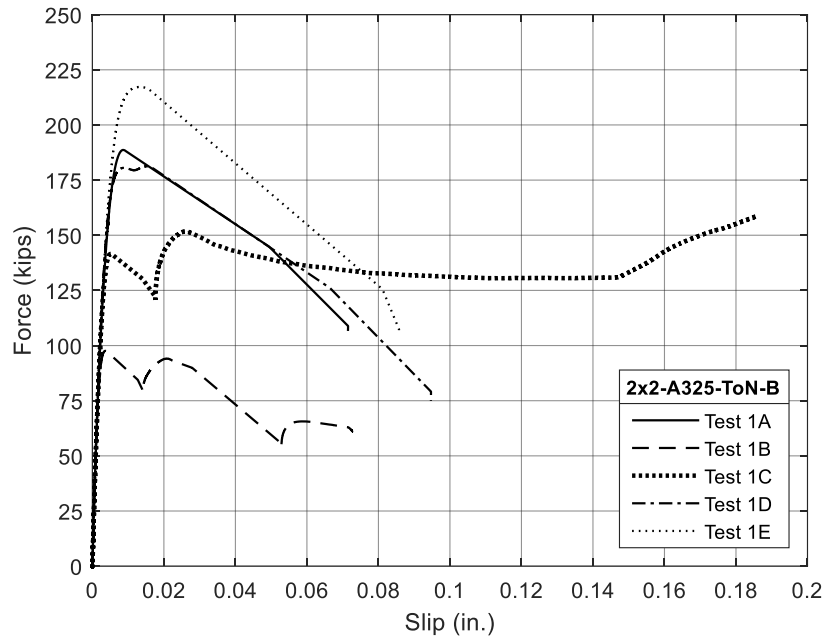
Figure 3.5: Test 1 load-slip curve

The connection tests shown in Figure 3.5 highlight Test 1. As indicated above, Test 1B was stopped prematurely just after 0.07-in. of slip. Test 1B was the Class B connection that had a contaminated faying surface. Once the sudden slip occurred at a low force, the test was stopped so the problem could be assessed. Other connection tests, Test 1A, 1D, and 1E, exhibited a sudden slip that triggered a safety break detect that was built into the load application procedure. If the controller detects a load drop of 50% or more, the force application stops, and the connection is unloaded. Test 1C did not slip suddenly and was loaded to bearing. Each connection slips past 0.02-in of deformation in a manner resembling Case (a) outlined by the RCSC in Figure 3.1.

The connections in Test 3, depicted in Figure 3.6, behaved similarly to the connections in Test 1. Test 3A slipped suddenly and triggered the break detect, while Test 3B and 3C were loaded to bearing. Each connection slips past 0.02-in of deformation and resembles Case (a) outlined by the RCSC in Figure 3.1. Table 3.3 highlights the connections' nominal strength, AISC R_n, as well as the slip load, Test R_n, for each test. The load-deformation behavior for Test 1 and Test 3 followed the behavior outlined as Case (a) by the RCSC in Figure 3.1. The slip load for these bolted-only connections corresponds to the maximum load before 0.02-in. of slip. Finally, the connections factor of safety, Test R_n / AISC R_n, is computed and shown in Table 3.3.
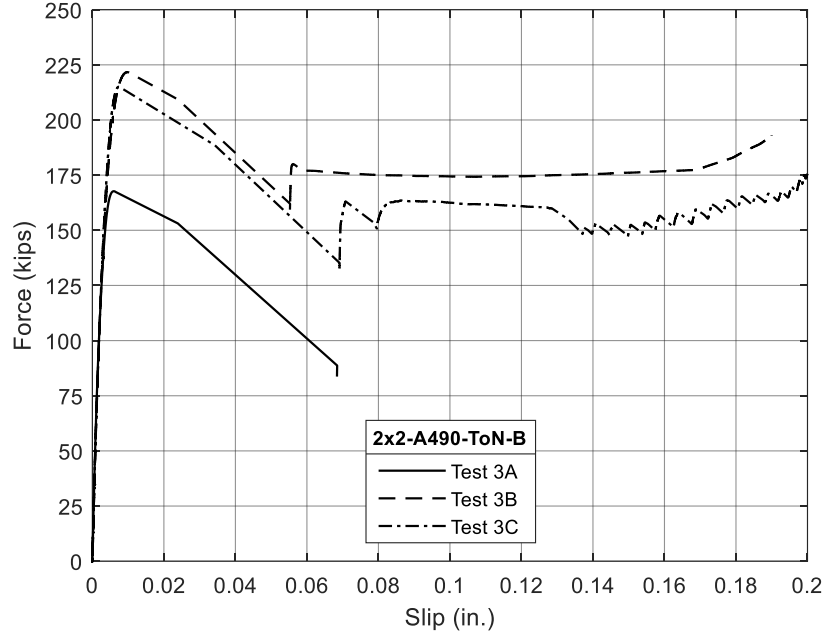
Figure 3.6: Test 3 load-slip curve

Table 3.3: 2×2 bolted-only results – Class B faying surface

	Specimen	AISC R_n (kips)	Test R_n (kips)	Test R_n / AISC R_n
Test 1	A	126.6	188.7	1.49
	B	126.6	97.6*	-
	C	126.6	141.5	1.12
	D	126.6	181.3	1.43
	E	126.6	217.3	1.72
Test 3	A	158.2	167.7	1.06
	B	158.2	221.7	1.40
	C	158.2	215.1	1.36
NOTE: The Test R_n is the maximum slip load before 0.02-in. of deformation. AVG = Average value; SD = Standard Deviation; CV = Coefficient of variation * Test 1B had a contaminated surface and does not represent traditional Class B slip load strength.				**AVG = 1.368 SD = 0.223 CV = 16.33%**

As seen in Figure 3.5 – Figure 3.6 and Table 3.3, 2×2 Class B bolted-only connections (Test R_n) provided a capacity that is on average 37% higher than the nominal AISC capacity (AISC R_n). While this overstrength is lower than the Class A connections, the variability in the data is higher with standard deviation of 0.223. Additionally, the coefficient of variation is 16.3%.

3.3.3 2×3 Class A Connections

Test 16 consists of five bolted-only connections with 2×3 bolt patterns and Class A faying surfaces. These specimens utilized A325 bolts and were tensioned with the turn-of-nut method (ToN). Each connection was assembled according the construction practices outlined in the test procedure. The load-deformation behavior of the tested connections is shown in Figure 3.7. Test 16 consisted of five test specimens and the results of each individual test are shown in Table 3.4. Note that the reported test capacity of each connection was dependent on the load-deformation behavior of the specimen which was not uniform across all connections.
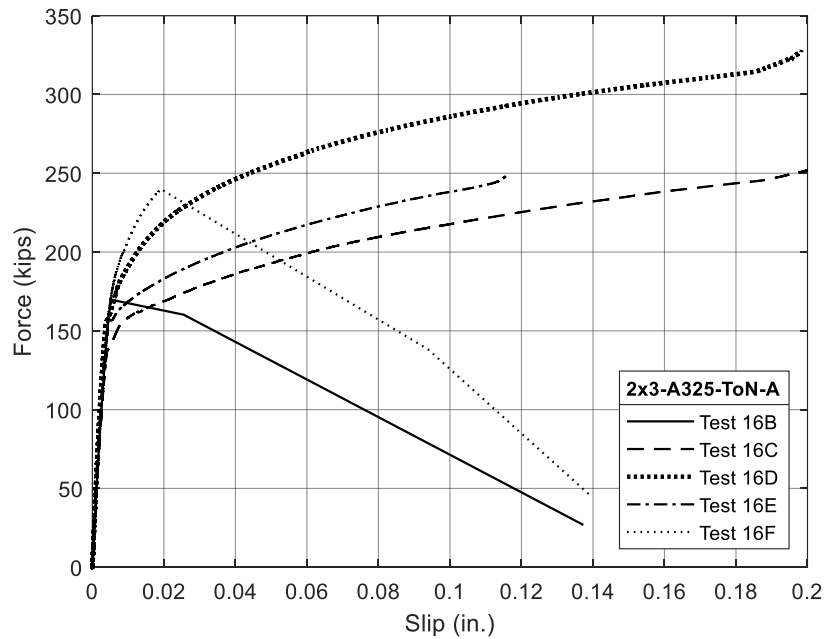
Figure 3.7: Test 16 load-slip curve

The load-deformation behavior of Test 16 connection series varies between connections. Test 16B and Test 16F failed suddenly without warning. This behavior is not consistent with the previous 2×2 Class A connections. This may be due to the differences in the faying surface of the 2×3 plates. The loading on Test 16E was stopped and did not fail before reaching 0.12-in. of deformation. This was due to a malfunction in one of the LVDTs. However, enough data was acquired during the test to make an adequate judgment in regard to the connection strength and load-deformation characteristics.

Table 3.4 highlights the connections' nominal strength, AISC R_n, as well as the slip load, Test R_n, for each test. The load-deformation behavior for Test 16B, Test 16C, and Test 16D followed closely the behavior outlined as Case (c) in Figure 3.1. The slip load for these three Class A bolted-only connections is the load corresponding to 0.02-in. of slip. The load-deformation behavior of Test 16B and Test 16F follows Case (a) in Figure 3.1. Their respective

capacity corresponds to the maximum force before 0.02-in. of slip. Regardless of slip behavior, each connection exceeded the AISC R_n. Lastly, the connections factor of safety, Test R_n / AISC R_n, is shown in Table 3.4.

Table 3.4: 2×3 bolted-only results – Class A faying surface

	Specimen	AISC R_n (kips)	Test R_n (kips)	Test R_n / AISC R_n
Test 16	B	113.9	169.6*	1.49
	C	113.9	168.8	1.48
	D	113.9	218.9	1.92
	E	113.9	183.0	1.61
	F	113.9	239.8*	2.11
NOTE: The Test R_n is the slip load at 0.02-in. of deformation. AVG = Average value; SD = Standard Deviation; CV = Coefficient of variation * The Test R_n is the maximum slip load before 0.02-in. of deformation.				**AVG = 1.721** **SD = 0.279** **CV = 16.25%**

As seen in Figure 3.7 and Table 3.4, the 2×3 Class A bolted-only connections (Test R_n) provided a capacity that is on average 72% higher than the nominal AISC capacity (AISC R_n). This overstrength is more similar to the 2×2 Class A connections, but with a higher variability in the prediction ability. The factor of safety data has a standard deviation of 0.279 and a coefficient of variation of 16.3%.

3.4   WELDED-ONLY TESTS

To establish a baseline understanding of the load-deformation behavior of the welded connections and determine the experimental weld shear strength, three welded-only tests were conducted, Test 6, Test 17-2, and Test 17-4. Test 6 uses the 2×2 Class A plates while Test 17-2 and Test 17-4 uses the 2×3 Class A plates. While it was noted that the coefficient of friction may contribute to variations in the bolted-only connection strength, the welded-only connections are not reliant on the friction between plate surfaces to develop the connection capacity. The welding rods were provided by W&W|AFCO Steel Co. and are Lincoln Electric Excalibur 7018 MR rods. Table 3.5 cites the specific weld geometry of the welded-only connections. The load-deformation behavior of these connections is highlighted in Figure 3.8. The results for each test are highlighted in Table 3.6. The reported test capacity, Test R_n, for each test is the ultimate load before fracture.

Table 3.5: Welded-only connection characteristics

	Test No.	Bolt Pattern	Bolt Type	Bolt Tensioning Method	Faying Surface Class	Weld Geometry (Size × length)	R_{n_W}/ R_{n_B}	No. of Samples
Welded-Only	6	-	-	-	-	5/16 × 3.0	-	3
	17-2	-	-	-	-	5/16 × 2.0	-	3
	17-4	-	-	-	-	5/16 × 4.0	-	2
NOTE: Four fillet weld lines of the specified geometry per connection. Units are inches R_{n_W} = Shear capacity of welds; R_{n_B} = Slip capacity of bolts								
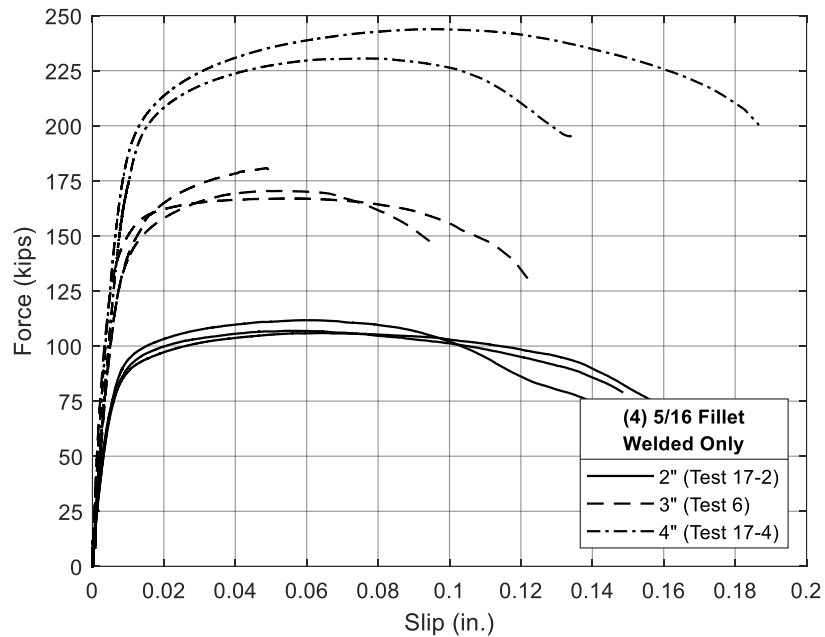
Figure 3.8: Welded-only load-deformation curve

Test 6A, shown in Figure 3.8, was stopped at a force level similar to the first set of bolted-only connections. This stop shown at approximately 0.05-in. of slip indicates the intentional ending of the test. The later welded-only tests were loaded to fracture. Table 3.6 highlights the connections' nominal strength, AISC R_n, as well as the ultimate load, Test R_n, for each test. In addition to the measured dimensions of the weld before the test, the post-test fracture area of the weld was photographed and measured. Finally, the connections factor of safety, Test R_n / AISC R_n, is computed and shown in Table 3.6.

Table 3.6: Welded-only results

	Specimen	AISC R_n (kips)	Test R_n (kips)	Test R_n / AISC R_n
Test 6	A	111.4	180.8	1.62
	B	111.4	170.4	1.53
	C	111.4	167.0	1.50
Test 17-2	A	74.2	106.9	1.44
	B	74.2	111.7	1.50
	C	74.2	105.9	1.53
Test 17-4	D	148.5	230.5	1.55
	E	148.5	243.8	1.64
NOTE: The Test R_n is the ultimate load before fracture. AVG = Average value; SD = Standard Deviation; CV = Coefficient of variation				**AVG = 1.527** **SD = 0.078** **CV = 5.08%**

35

As seen in Figure 3.8 and Table 3.6, the welded-only connections (Test R_n) provided a capacity that is on average 53% higher than the nominal AISC capacity (AISC R_n). It is noted that, despite the Test R_n exceeding the AISC R_n by 53% on average, the factor of safety data has a standard deviation of 0.078 and that the coefficient of variation is only 5.1%.

3.5   COMBINATION TESTS

The main purpose of this this portion of the testing program is to investigate the behavior of concentric connections utilizing both bolts and welds in combination. The experimental test matrix (Table 2.1) consists of fifteen combination tests, nine 2×2 tests and six 2×3 tests. Of the nine 2×2 tests, four use Class A surfaces and five use Class B. All 2×3 connection tests use Class A surfaces. These completed tests also vary other critical variables including bolt size, bolt grade, bolt tensioning method, and weld/bolt strength ratio.

3.5.1   2×2 Class A Connections

A total of twelve 2×2 Class A combination samples were tested according to the experimental test matrix. These connections are Test 12, Test 13, Test 14, and Test 15. The first three tests vary only the weld/bolt strength ratio, which inherently changes the weld lengths from 1.25-in. to 3.0-in. However, Test 15 utilizes 1-in. diameter bolts to study the effect of larger bolt sizes. Each Class A connection was assembled in negative bearing and tested according to the previously discussed testing procedure. The specific connection characteristics are highlighted in Table 3.7. Figure 3.9 – Figure 3.12 depict the load-deformation behavior for the 2×2 Class A combination connections. Each test consisted of three specimens and the results of each individual test are shown in Table 3.8. Since these combination connections are in essence slip-critical joints, the reported test capacity, Test R_n, for each test, is the connection strength recorded at 0.02-in. of slip.

Table 3.7: 2×2 combination connection characteristics – Class A faying surface

	Test No.	Bolt Pattern	Bolt Type	Bolt Tensioning Method	Faying Surface Class	Weld Geometry (Size × length)	$R_{n\_w}/$ R_{n_B}	No. of Samples
Bolted & Welded	12	2×2	A325	ToN	A	5/16 × 1.25	0.67	3
	13	2×2	A325	ToN	A	5/16 × 2.0	1.0	3
	14	2×2	A325	ToN	A	5/16 × 3.0	1.5	3
	15*	2×2*	A325	ToN	A	5/16 × 3.5	1.0	3
NOTE: All bolts are 3/4-in. diameter (oversized holes) unless noted otherwise. ToN = Turn of nut method; Four fillet weld lines of the specified geometry per connection. Units are inches. R_{n_W} = Shear capacity of welds; R_{n_B} = Slip capacity of bolts * Bolts are 1-in. diameter A325 in oversized holes.								
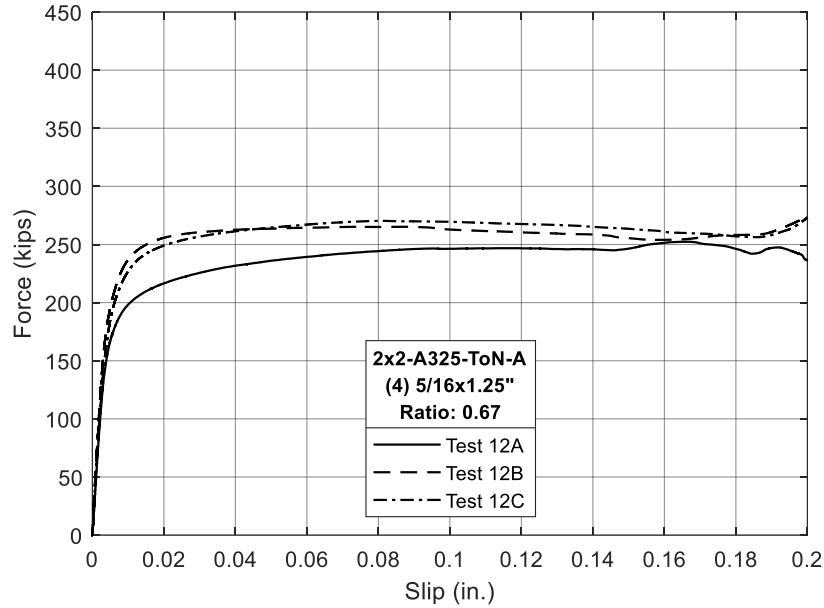
Figure 3.9: Test 12 load-slip curve

Table 3.8 highlights the nominal strength of the connection (i.e., AISC R_n) as well as the slip load (i.e., Test R_n) for each test. The load-deformation behavior for Test 12, Test 13, Test 14, and Test 15 followed the behavior outlined as Case (c) in Figure 3.1. The slip load for these twelve combination connections is the load corresponding to 0.02-in. of slip. Finally, the connections factor of safety, Test R_n / AISC R_n, is computed.
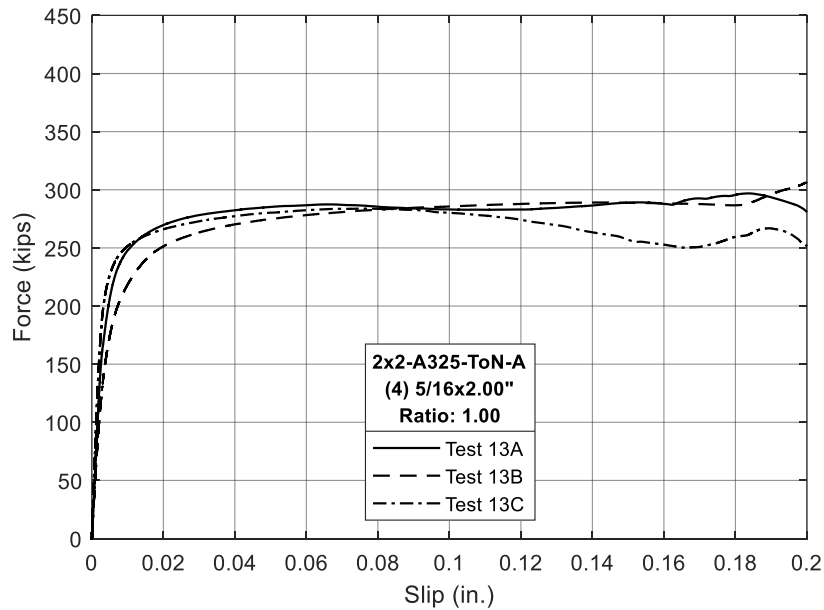
Figure 3.10: Test 13 load-slip curve
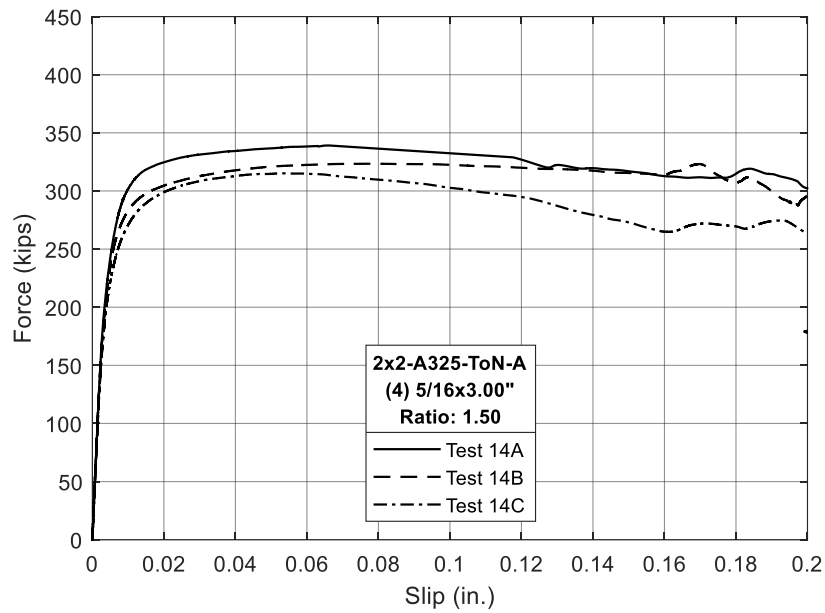
Figure 3.11: Test 14 load-slip curve
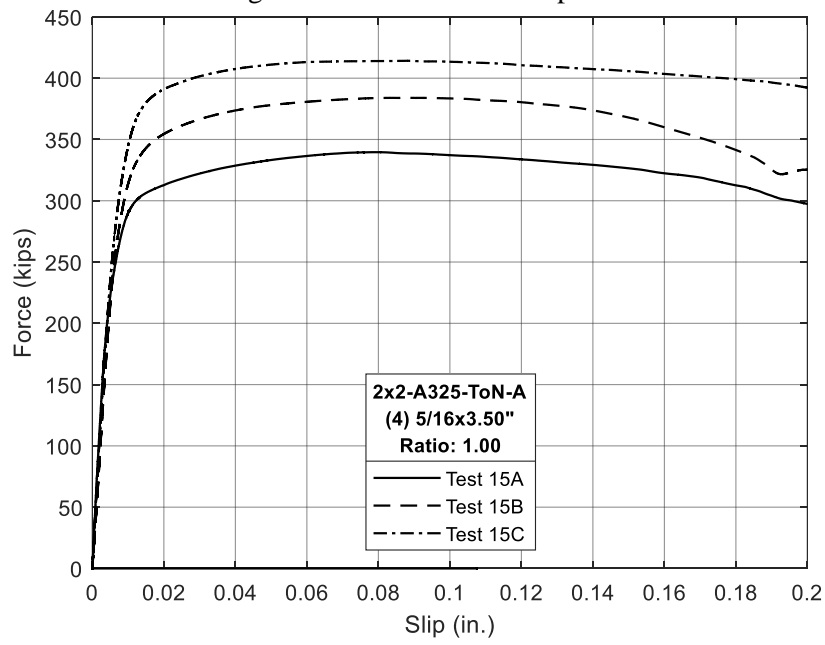
Figure 3.12: Test 15 load-slip curve

Table 3.8: 2×2 combination results – Class A faying surface

	Specimen	AISC R_n (kips)	Test R_n (kips)	Test R_n / AISC R_n
Test 12	A	122.3	216.6	1.77
	B	122.3	255.8	2.09
	C	122.3	249.0	2.04
Test 13	A	150.2	269.7	1.80
	B	150.2	251.3	1.67
	C	150.2	266.0	1.77
Test 14	A	187.3	324.7	1.73
	B	187.3	304.6	1.63
	C	187.3	299.0	1.60
				AVG = 1.788 **SD = 0.171** **CV = 9.54%**
Test 15*	A	268.2	312.7	1.17
	B	268.2	354.4	1.32
	C	268.2	390.0	1.45
NOTE: The Test R_n is the slip load at 0.02-in. of deformation. AVG = Average value; SD = Standard Deviation; CV = Coefficient of variation * Test 15 bolts are 1-in. diameter.				**AVG = 1.314** **SD = 0.144** **CV = 10.98%**

As seen in Figure 3.9 – Figure 3.12 and Table 3.8, 2×2 Class A combination connections (Test R_n) provided a capacity higher than the nominal AISC capacity (AISC R_n). The Test R_n of combination connections using 3/4-in. diameter bolts exceeded the prediction model by an average 79%, while connections with 1-in. diameter bolts outperformed the model by 31%. Despite the Test R_n exceeding the AISC R_n at different margins for different bolt sizes, the variability in the data is similar and have a standard deviation of 0.171 and 0.144 for 3/4-in. diameter bolts and 1-in. diameter bolts, respectively. Additionally, the coefficient of variation for these bolt groups is 9.5% and 11.0%, respectively.

3.5.2   2×2 Class B Connections

A total of fifteen 2×2 Class B combination samples were tested according to the experimental test matrix. These connections are Test 7, Test 8, Test 9, Test 10, and Test 11. The first three tests vary only the weld/bolt strength ratio, which inherently changes the weld lengths from 2.25-in. to 5.0-in. The specimens in Test 10 investigate the bolt tensioning method by using TC bolts rather than the ToN method. The final three specimens in Test 11 use A490 bolts and complement the Class B combination connection group to understand the effect of using higher bolt grades. Each Class B connection was assembled in negative bearing and tested according to the previously discussed testing procedure. The specific connection characteristics are highlighted in Table 3.9. Figure 3.13 – Figure 3.17 depict the load-deformation behavior for the 2×2 Class B combination connections. Each test consisted of three specimens and the results of

each individual test are shown in Table 3.10. The reported test capacity, Test R_n, for each test is the maximum connection strength recorded before 0.02-in. of slip.

Table 3.9: 2×2 combination connection characteristics – Class B faying surface

	Test No.	Bolt Pattern	Bolt Type	Bolt Tensioning Method	Faying Surface Class	Weld Geometry (Size × length)	$R_{n\_W}/$ R_{n_B}	No. of Samples
Bolted & Welded	7	2×2	A325	ToN	B	5/16 × 5.0	1.5	3
	8	2×2	A325	ToN	B	5/16 × 2.25	0.67	3
	9	2×2	A325	ToN	B	5/16 × 3.5	1.0	3
	10	2×2	A325	TC	B	5/16 × 2.25	0.67	3
	11	2×2	A490	ToN	B	5/16 × 2.75	0.67	3
NOTE: All bolts are 3/4-in. diameter (oversized holes) unless noted otherwise.								
TC = Tension control bolt; ToN = Turn of nut method								
Four fillet weld lines of the specified geometry per connection. Units are inches.								
R_{n_W} = Shear capacity of welds; R_{n_B} = Slip capacity of bolts								
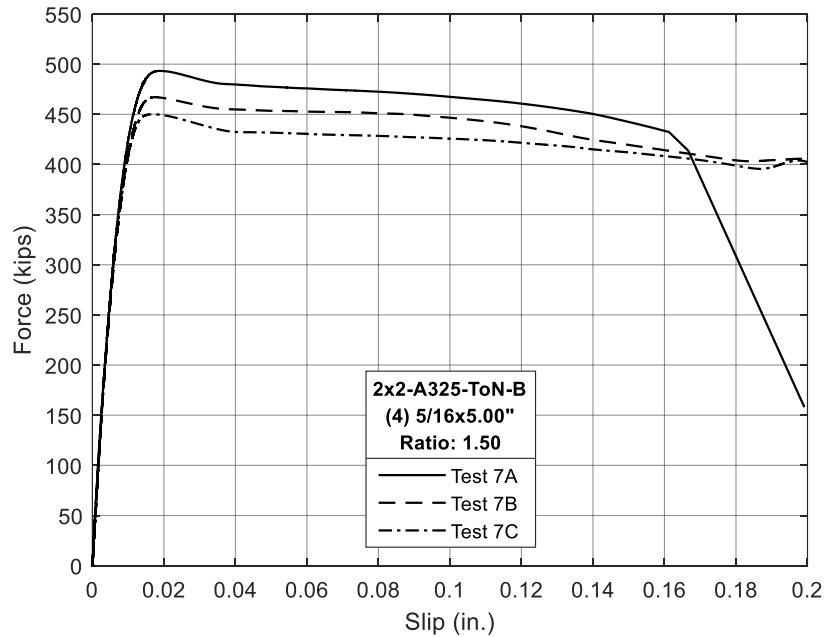
Figure 3.13: Test 7 load-slip curve
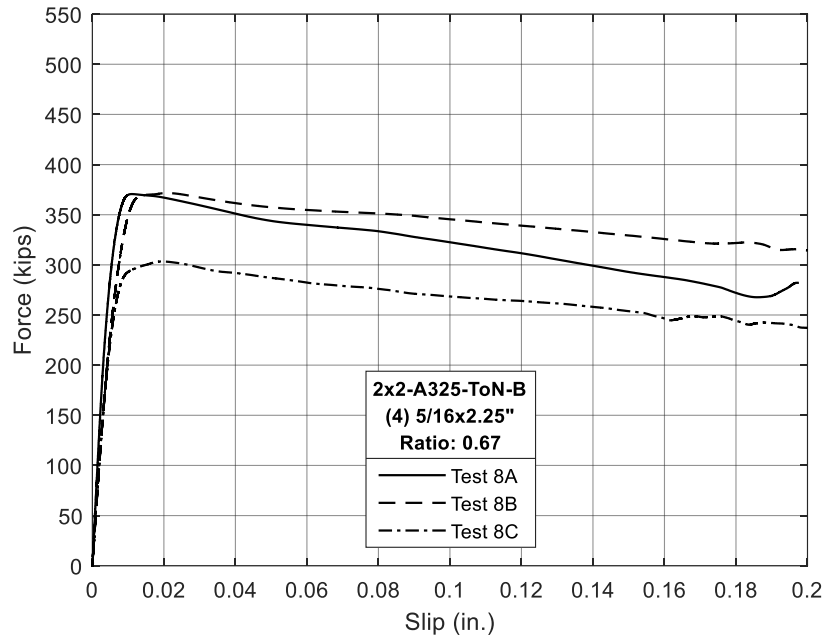
Figure 3.14: Test 8 load-slip curve
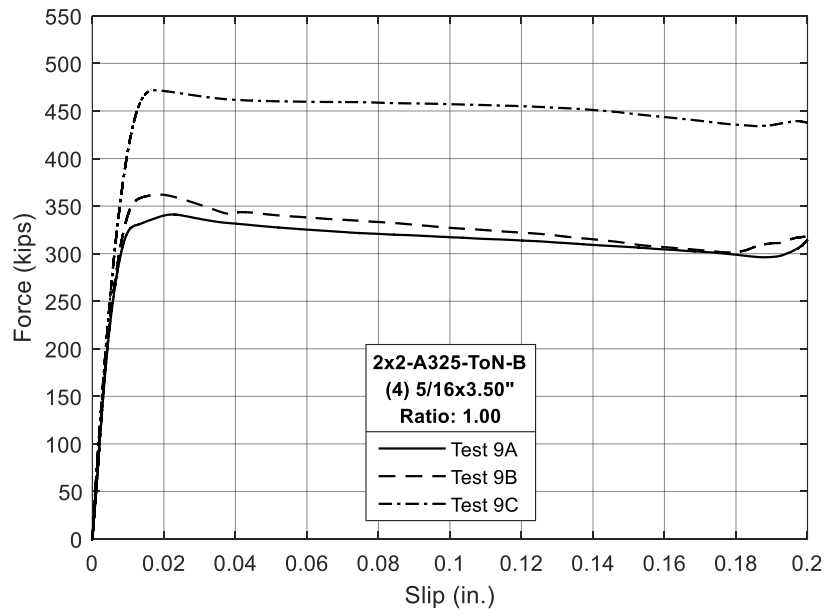
Figure 3.15: Test 9 load-slip curve

41
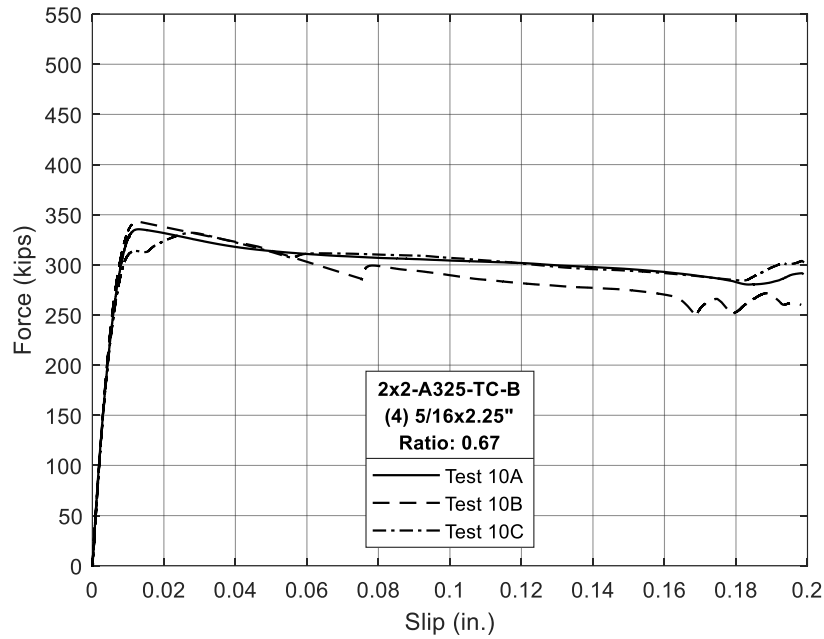
Figure 3.16: Test 10 load-slip curve
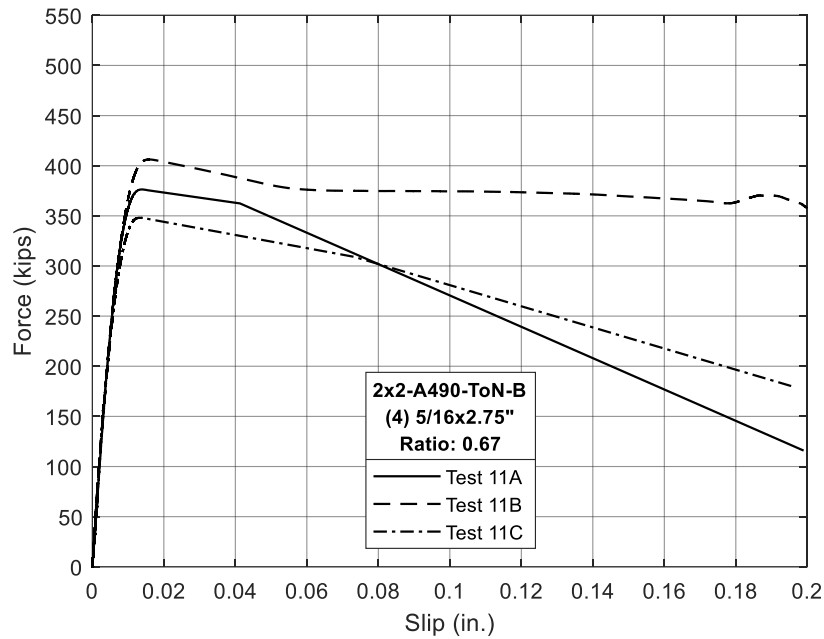
Figure 3.17: Test 11 load-slip curve

Table 3.10 highlights the connections' nominal strength, AISC R_n, as well as the slip load, Test R_n, for each test. The load-deformation behavior for Test 7, Test 8, Test 9, Test 10, and Test 11 followed the behavior outlined as Case (a) in Figure 3.1. The slip load for each of the fifteen

Class B combination connections was assumed to be the maximum load that occurred before 0.02-in. of slip. Finally, the connections factor of safety, Test R_n / AISC R_n, is computed.

As seen in Figure 3.13 – Figure 3.17 and Table 3.10, 2×2 Class B combination connections (Test R_n) provided a capacity that is on average 54% higher than the nominal AISC capacity (AISC R_n). While this overstrength is lower than the Class A combination connections, the variability in the data is similar with standard deviation of 0.155. It is also noteworthy that the presence of weld reduces the coefficient of variation in the capacity of Class B connections from 16.3% to 10.1%.

Table 3.10: 2×2 combination results – Class B faying surface

	Specimen	AISC R_n (kips)	Test R_n (kips)	Test R_n / AISC R_n
Test 7	A	312.1	493.3	1.58
	B	312.1	467.1	1.50
	C	312.1	450.1	1.44
Test 8	A	210.1	370.6	1.76
	B	210.1	370.0	1.76
	C	210.1	303.4	1.44
Test 9	A	256.5	340.0	1.33
	B	256.5	362.1	1.41
	C	256.5	471.7	1.84
Test 10	A	210.1	335.5	1.60
	B	210.1	343.0	1.63
	C	210.1	313.9	1.49
Test 11	A	260.3	376.3	1.45
	B	260.3	406.2	1.56
	C	260.3	348.1	1.34
NOTE: The Test R_n is the maximum slip load before 0.02-in. of deformation. AVG = Average value; SD = Standard Deviation; CV = Coefficient of variation				**AVG = 1.542** **SD = 0.155** **CV = 10.07%**

3.5.3   2×3 Class A Connections

A total of eighteen 2×3 Class A combination samples were tested according to the experimental test matrix. These connections are Test 18, Test 19, Test 20, Test 21, Test 22, and Test 23. The first four tests vary only the weld/bolt strength ratio, which inherently changes the weld lengths from 2.0-in. to 6.25-in. The test specimens in Test 22 investigate the bolt tensioning method by using TC bolts rather than the ToN method. The final three test specimens in Test 23 use A490 bolts and complement the Class A combination connection group to understand the effect of using higher grade bolts. Each Class A connection was assembled in negative bearing and tested according to the previously discussed testing procedure. The specific connection characteristics are highlighted in Table 3.11. Figure 3.18 – Figure 3.23 depict the load-deformation behavior for the 2×3 Class A combination connections. Each test consisted of three specimens and the results of each individual test are shown in Table 3.12. The reported test capacity, Test R_n, for each test is the connection strength recorded at 0.02-in. of slip.

43

Table 3.11: 2×3 combination connection characteristics – Class A faying surface

	Test No.	Bolt Pattern	Bolt Type	Bolt Tensioning Method	Faying Surface Class	Weld Geometry (Size × length)	$R_{n\_W}/$ R_{n_B}	No. of Samples
Bolted & Welded	18	2×3	A325	ToN	A	5/16 × 2.0	0.67	3
	19	2×3	A325	ToN	A	5/16 × 3.0	1.0	3
	20	2×3	A325	ToN	A	5/16 × 4.0	1.33	3
	21	2×3	A325	ToN	A	5/16 × 6.25	2.0	3
	22	2×3	A325	TC	A	5/16 × 3.0	1.0	3
	23	2×3	A490	ToN	A	5/16 × 2.0	0.50	3
NOTE: All bolts are 3/4-in. diameter (oversized holes) unless noted otherwise. TC = Tension control bolt; ToN = Turn of nut method Four fillet weld lines of the specified geometry per connection. Units are inches. R_{n_W} = Shear capacity of welds; R_{n_B} = Slip capacity of bolts								

Figure 3.18: Test 18 load-slip curve
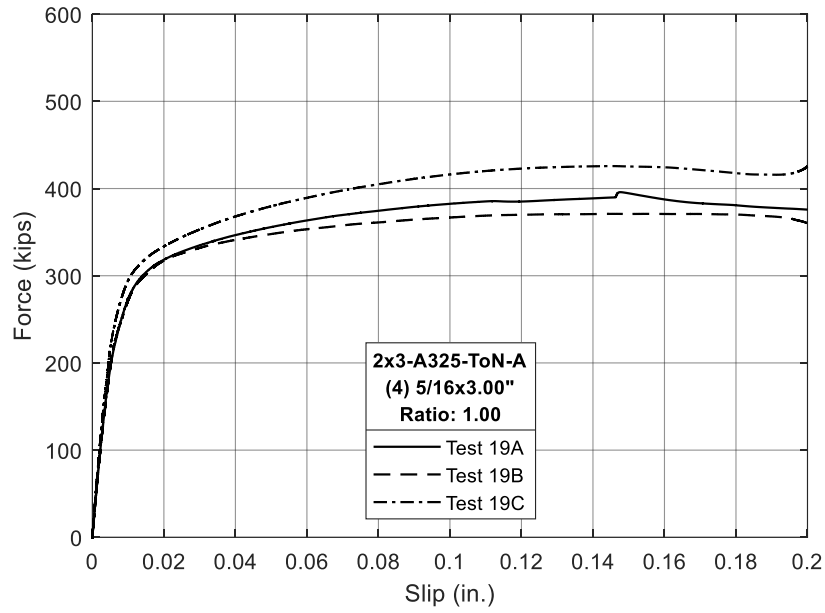
Figure 3.19: Test 19 load-slip curve
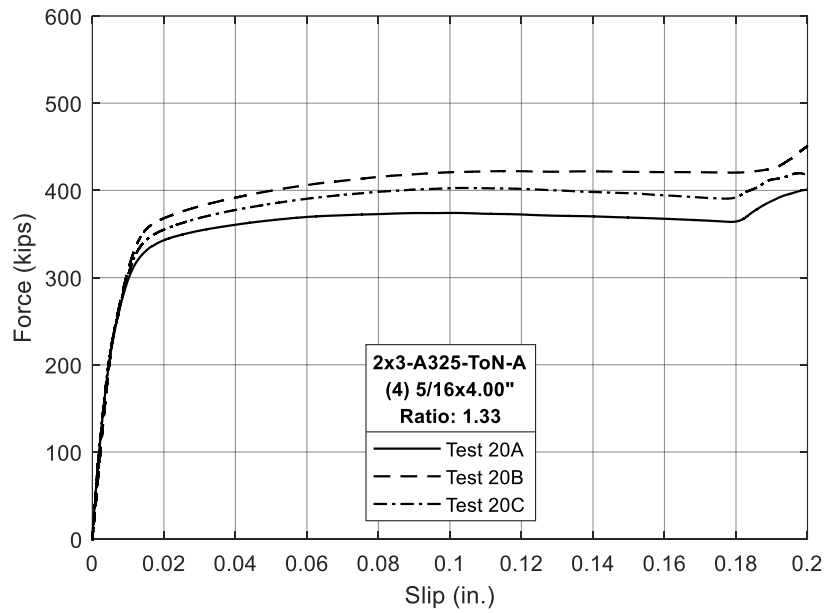
Figure 3.20: Test 20 load-slip curve
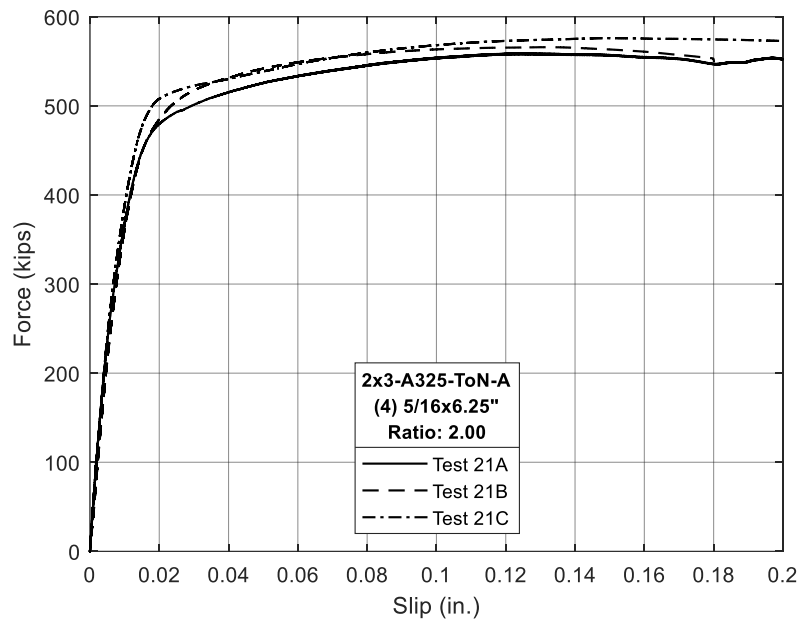
Figure 3.21: Test 21 load-slip curve
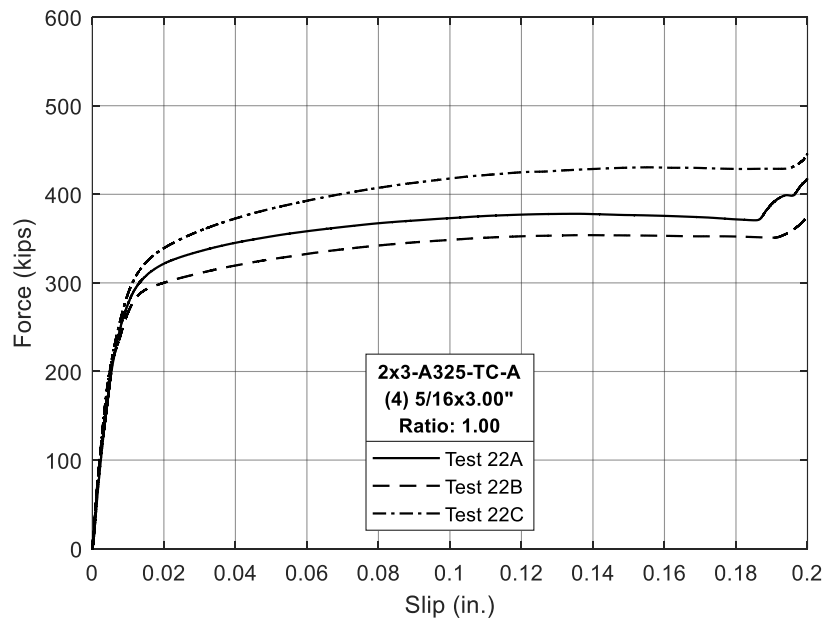
Figure 3.22: Test 22 load-slip curve
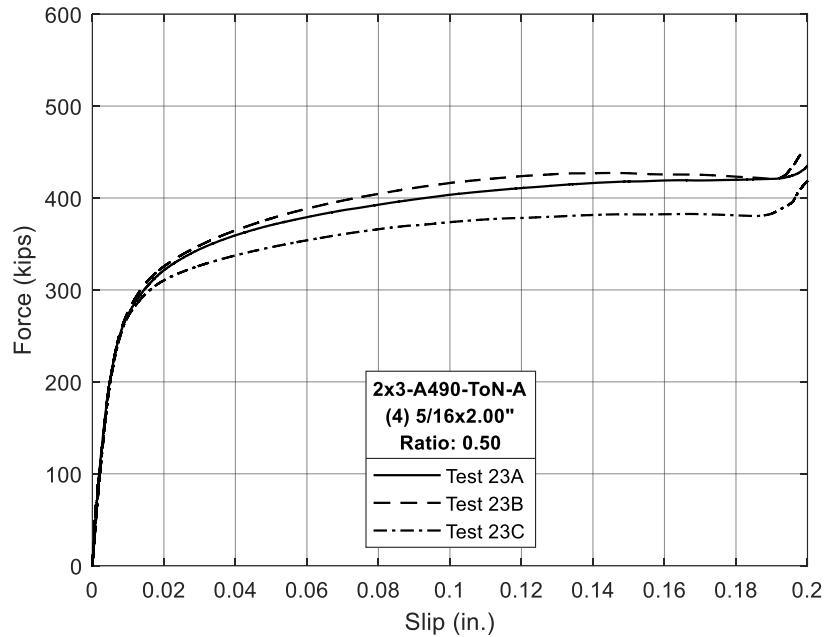
Figure 3.23: Test 23 load-slip curve

All eighteen 2×3 combination connections were tested past 0.18-in. of bolt slip or until the bolt bearing condition initiated. Test 19A in Figure 3.19 displays a small load increase at approximately 0.145-in. of connection slip. The test was actually conducted over two days and this point corresponds to the initiation of load application during the second test.

Table 3.12 highlights the connections' nominal strength, AISC R_n, as well as the slip load, Test R_n, for each test. The load-deformation behavior for Test 18, Test 19, Test 20, Test 21, Test 22, and Test 23 followed closely the behavior outlined as Case (c) in Figure 3.1. The slip load for these eighteen combination connections is the load corresponding to 0.02-in. of slip. Finally, the connections factor of safety, Test R_n / AISC R_n, is computed.

As seen in Figure 3.18 – Figure 3.23 and Table 3.12, 2×3 Class A combination connections (Test R_n) provided a capacity that is on average 42% higher than the nominal AISC capacity (AISC R_n). While this overstrength is lower than the 2×2 Class A combination connections, the variability in the data is lower with standard deviation of 0.079. Additionally, the coefficient of variation is 5.6%.

Table 3.12: 2×3 combination results – Class A faying surface

	Specimen	AISC R_n (kips)	Test R_n (kips)	Test R_n / AISC R_n
Test 18	A	188.1	257.4	1.37
	B	188.1	299.8	1.59
	C	188.1	239.2	1.27
Test 19	A	225.3	318.2	1.41
	B	225.3	317.5	1.41
	C	225.3	333.6	1.48
Test 20	A	262.4	342.8	1.31
	B	262.4	367.9	1.40
	C	262.4	354.9	1.35
Test 21	A	345.9	479.4	1.39
	B	345.9	484.6	1.40
	C	345.9	507.0	1.47
Test 22	A	225.3	321.7	1.43
	B	225.3	300.2	1.33
	C	225.3	339.9	1.51
Test 23	A	216.6	321.2	1.48
	B	216.6	325.6	1.50
	C	216.6	310.4	1.43
NOTE: The Test R_n is the slip load at 0.02-in. of deformation. AVG = Average value; SD = Standard Deviation; CV = Coefficient of variation				**AVG = 1.419** **SD = 0.079** **CV = 5.58%**

3.6   EVALUATION OF THE NOMINAL AISC CAPACITY

For each connection, the AISC R_n was plotted against its respective Test R_n to gain insight into the ability of the ASIC model to predict the capacity, and inherently, the factor of safety provided (Test R_n / AISC R_n). This is shown below in Figure 3.24. Recall that the AISC equations, Eq. 16 and Eq. 17, include the nominal slip coefficients, minimum bolt pretension forces, and assume 70 ksi for the tensile strength of the weld electrode.

All test connections exceed the AISC R_n, expect for Test 1B. The experimental results show that the capacity of the tested combination connections is on average 42-79% beyond the nominal AISC R_n. Figure 3.24 visually describes this observation as many of these connections are centered on the 1.5:1 ratio line. The average factor of safety (Test R_n / AISC R_n) is 1.53 considering all combination tests. Again, this comparison is based on the nominal properties of the welds and bolts and does not reflect the true ability of the AISC model to predict the capacity.
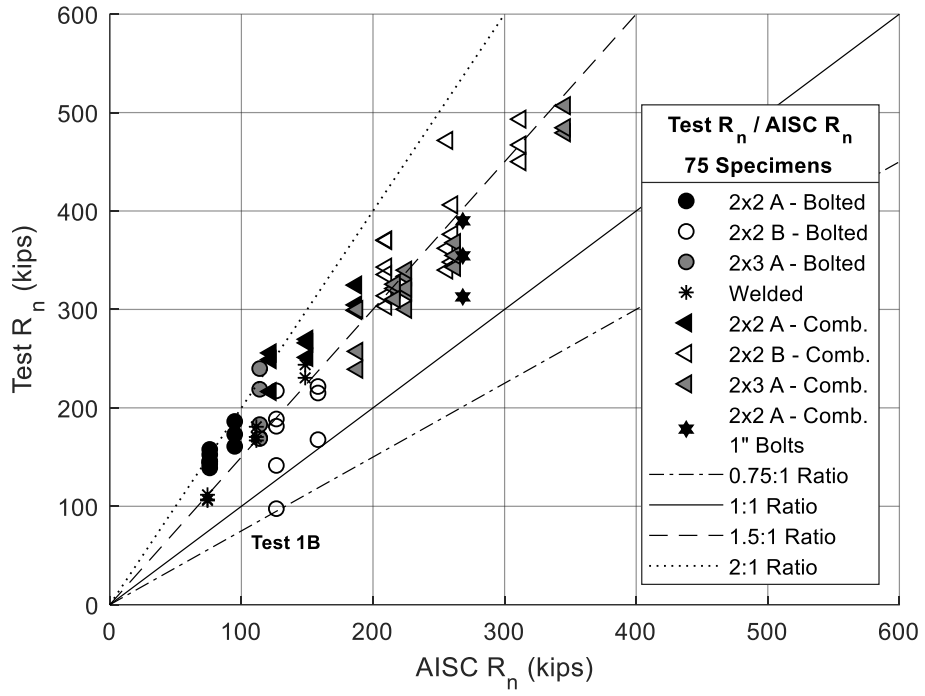
Figure 3.24: Factor of safety plot of concentric connections: Nominal AISC Model

4 DISCUSSION: CONCENTRIC CONNECTIONS

The test program provided insight into the performance of connections utilizing both slip-critical bolts and longitudinal fillet welds in combination. This section evaluates the bolt pretension, faying surface friction coefficients, and weld shear strength for predicting the connection capacity based on the as-built characteristics of the connection. This prediction procedure, denoted herein as the As-Built prediction, is based on the AISC specification, while incorporating known material characteristics rather than nominal values. Then, a proposed prediction model based on the established material properties is used to predict the capacity. In addition, the influence of different connection variables is investigated by comparing the load-deformation behavior and capacity of connections with different configurations.

4.1 EVALUATION OF THE BOLT PRETENSION

To better predict the capacity of connections utilizing both bolts and welds in combination, it is necessary to study the uncertainty in the forces that are being applied by the bolts. Over 190 Skidmore tests were conducted during the test program encompassing four different bolt configurations. Additionally, the bolt pretension force was regularly acquired using bolt load cells.

The largest group of bolts was 3/4-in. diameter A325-ToN and included 129 Skidmore tests. When designing a slip-critical connection utilizing these bolts, the AISC specifies a minimum pretension of $T_b = 28$ kips (AISC 2016). The current AISC procedure multiplies the minimum bolt pretension by 1.13 in expectation that additional force will be applied as the bolt is pretensioned. The 1.13 factor brings the expected bolt tension to 31.6 kips. Before every test, three bolts were tested in the Skidmore Wilhelm bolt tension calibrator and their pretension values were recorded. It is noteworthy that every Skidmore test exceeded the 31.6 kips value. The mean and standard deviation of bolt pretention associated with different bolt groups are presented in Table 4.1. Additionally, a histogram highlighting the probability density of the pretension force Skidmore data corresponding to the 3/4-in. diameter A325-ToN is depicted in Figure 4.1.

Table 4.1: Skidmore probabilistic measurements

	3/4-in A325-ToN	3/4-in A325-TC	3/4-in A490-ToN	1-in A325-ToN
# of Samples	129	27	36	9
Mean	42.73 kips	38.47 kips	46.79 kips	64.07 kips
Standard Deviation	1.99 kips	2.76 kips	2.30 kips	3.07 kips
NOTE: TC = Tension control bolt; ToN = Turn of Nut				
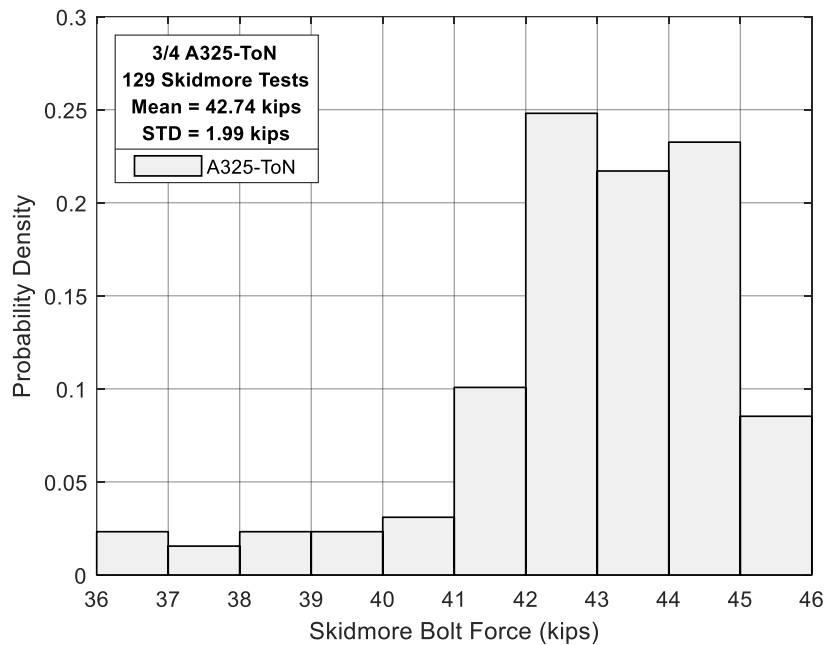
Figure 4.1: 3/4-in. A325-ToN Skidmore histogram

During the experimental testing program, bolt pretension was also measured by bolt load cells. A histogram describing the collected bolt pretension data for the 3/4-in. diameter A325-ToN bolt group is shown Figure 4.2. This data set represents approximately 75% of the total bolts used in this group. The remaining quarter of the data was not captured due to equipment malfunction due to the repeated use. The load cells recorded a mean pretension force of 39.3 kips with a standard deviation of 5.42 kips. The standard deviation of the bolt pretension measured by the load cells is much higher than that of the Skidmore Wilhelm bolt tension calibrator. This can be attributed to the high measurement error associated with the bolt load cells. Since no detailed probabilistic analysis is conducted to account for this error, the Skidmore pretension data shown in Table 4.1 is used herein to determine the slip coefficient of the faying surfaces and the bolt pretension in the as-built prediction.
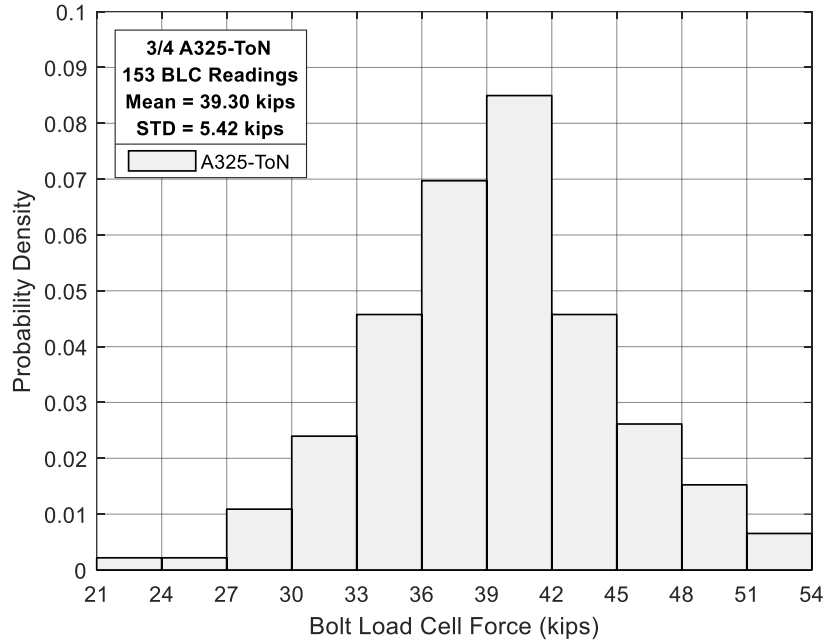
Figure 4.2: 3/4-in. A325-ToN bolt load cell histogram

4.2   DETERMINATION OF THE SLIP COEFFICIENT

Another variable that must be properly quantified is the slip coefficient of the tested connection faying surfaces. An estimate of the experimental slip coefficient, μ, is computed for 2×2 Class A, 2×2 Class B, and 2×3 Class A faying surfaces. A separate computation for the 2×2 and 2×3 Class A surfaces was necessary due to the different rust patina on the steel utilized for these two groups of plates. The RCSC provides a guide for computing the slip coefficient for an individual faying surface, k_s, and Eq. 18 was adopted for this computation (RCSC 2014). The computation is based on the bolted-only slip loads (i.e., Test R_n) and the average bolt pretension forces from the Skidmore dataset shown in Table 4.1.

$$k_s = \frac{slip\ load}{2 \times clamping\ force}$$

Eq. 18

k_s = slip coefficient for an individual specimen

$slip\ load$ = Test R_n

$clamping\ force$ = total number of bolts multiplied by average Skidmore pretension force shown in Table 4.1 for the specific bolt group

A slip coefficient was computed for each bolted-only test specimen. This computation accounted for the different faying surfaces as well as the specific bolt groups used in the connection. For each faying surface group, the average of all individual slip coefficients corresponded to the group experimental slip coefficient. This specific computation is highlighted in Table 4.2. The

slip coefficient for the 2×2 Class A surface was found to be 0.457 which is significantly higher than the AISC minimum of 0.3 for Class A surfaces (AISC 2016). The 2×2 Class A surface test data is very consistent with a standard deviation of 0.022 and coefficient of variation of 4.9%. Similarly, the experimental slip coefficient for the 2×2 Class B surface also exceeded the AISC minimum (0.5 for Class B) but displayed higher variability. The slip coefficient was found to be 0.535 with a standard deviation of 0.079 and coefficient of variation of 14.8%. This value for Class B surfaces is very close to the mean value of 0.524 reported in Grondin et al. (2007). A two-sided Z-test was conducted with the null hypothesis referring to the case in which the mean of samples is equal to the population mean reported in Grondin et al. (2007). The p-value was calculated as 0.764, which indicated that the sample mean lies well within the acceptance region. Accordingly, a mean value of 0.535 is adopted for capacity prediction.

Finally, the experimental mean slip coefficient for the 2×3 Class A surfaces was found to be 0.382 considering the five bolted-only specimens. However, the coefficient of variation for 2×3 Class A surfaces is found to be 16.3% which is significantly higher than the 4.9% from 2×2 Class A surfaces. Grondin et al. (2007) reported a mean value of 0.301 and coefficient of variation of 23.3% for Class A faying surfaces. In addition, considering the high variability in the behavior of the 2×3 Class A surface shown in Figure 3.7, the authors were not confident that the higher values would properly represent the frictional characteristics of this surface. To improve the confidence in the friction coefficient value to be used in the subsequent analysis, a two-sided Z-test is adopted herein to validate the properties of the five 2×3 Class A surfaces tests. The null hypothesis defines the case in which the mean of samples is equal to the mean value reported in Grondin et al. (2007), specifically 0.301, and the alternative hypothesis is that the samples mean does not belong to the population. A p-value is computed as 0.009 which means that, at 10% level of significance, the null hypothesis is rejected in favor of the alternative hypothesis. Thus, it is unlikely that the mean value estimated from the five tests would represent the frictional coefficient of the Class A surface. Accordingly, for the 2×3 Class A surfaces, the three tests with relatively lower capacity are considered for calculating the mean slip coefficient. This resulted in a mean value of 0.339, which lies well within the acceptance region of the Z-test with 10% level of significance. Accordingly, a mean friction coefficient of 0.339 is used in the capacity prediction of the 2×3 connections utilizing Class A faying surfaces.

4.3   DETERMINATION OF THE WELD SHEAR STRENGTH

The final variable that must be properly quantified to predict the connection strength is the weld shear strength. This computation is based purely on the welded-only connection tests encompassing weld lengths of 2-in., 3-in., and 4-in. The weld shear stress, τ, was computed for each individual connection using Eq. 19. The computation is inherently similar to the model in Eq. 9; however, the $0.6F_{EXX}$ term is replaced with the weld shear stress, τ, and the effective weld throat area, A_w, corresponds to the effective throat size times the length of the weld that were measured before tests. Finally, the equation is rearranged and the computed weld shear stress

values for each connection are averaged to attain the experimental weld shear strength. The weld shear strength computation is highlighted below in Table 4.3.

$$\tau = \frac{Test\ R_n}{A_w} \qquad \text{Eq. 19}$$

Table 4.2: Slip coefficient evaluation data based on test results

Faying Surface	Bolt Type	Test	Skidmore (kips)	Clamping Force (kips)	Test R_n (kips)	k_s
2×2 Class A	A325 ToN	2A	42.73	170.92	152.5	0.446
		2B			157.8	0.462
		2C			145.1	0.424
	A325 TC	4A	38.47	153.88	143.0	0.465
		4B			146.0	0.474
		4C			139.0	0.452
	A490 ToN	5A	46.79	187.16	173.1	0.462
		5B			160.9	0.430
		5C			186.2	0.497
						AVG = 0.457 **SD = 0.022** **CV = 4.89%**
2×2 Class B	A325 ToN	1A	42.73	170.92	188.7	0.552
		1C			141.5	0.414
		1D			181.3	0.530
		1E			217.3	0.636
	A490 ToN	3A	46.79	187.16	167.7	0.448
		3B			221.7	0.592
		3C			215.1	0.575
						AVG = 0.535 **SD = 0.079** **CV = 14.77%**
2×3 Class A	A325 ToN	16B	42.73	256.38	169.6	0.331
		16C			168.8	0.329
		16E			183.0	0.357
NOTE: All bolts are 3/4-in. diameter (oversized holes) unless noted otherwise. AVG = Average value; SD = Standard Deviation; CV = Coefficient of variation TC = Tension control bolt; ToN = Turn of nut method						**AVG = 0.339** **SD = 0.016** **CV = 4.59%**

The welded-only test data shown in Table 4.3 conclude that the experimental weld shear strength is approximately 69.53 ksi with a standard deviation of 3.77 ksi and coefficient of variation of 5.42%. This computed shear stress is around 30% higher than previous experimental research using similar weld electrode, where a range of 47.4-55.1 ksi for longitudinal fillet welds was reported (Manuel 1996). This analysis was also complemented by testing weld coupons that were fabricated based on AWS B4 (2016) and tested at the BCEL. Two coupons were fabricated from the same box of weld electrodes used for the specimens and were shown to have a yield stress of

74 ksi and ultimate stress of 83 ksi. Three more electrodes from another box of weld electrodes with the same specifications were also fabricated and tested; however, these three samples resulted in 65 ksi and 75 ksi for the average yield stress and tensile strength, respectively. Given this variation, it was decided to use weld electrodes from the first box for the entire testing program (i.e., concentric and eccentric testing). Accordingly, the high shear stress can be attributed to (a) the superior mechanical properties associated with the used weld electrodes and (b) the use of effective throat area measured before testing for computing the shear stress rather than the actual weld fracture area. Research by Deng et al. (2003) indicates that the actual fracture area of the fillet welds is on average 27% higher than the effective throat area measured before testing. This was also confirmed by the measurements taken during this experimental program. Using the fracture area led to an average ultimate weld shear stress of 54.36 ksi, which correlates well with the values reported in literature. However, the higher value of 69.53 will be used in the remaining parts of this report along with the effective throat area (measured before fracture) as it is more convenient to use these quantities in analytical modeling and numerical analysis.

Table 4.3: Experimental weld shear strength evaluation

Weld Size	Test	Effective Throat Area (in^2)	Test R_n (kips)	Weld Shear Stress (ksi)
5/16 × 3-in	6A	2.494	180.8	72.49
	6B	2.472	170.4	68.93
	6C	2.359	166.9	70.75
5/16 × 2-in	17-2A	1.645	106.9	65.00
	17-2B	1.642	111.7	68.02
	17-2C	1.649	105.9	64.24
5/16 × 4-in	17-4D	3.227	230.5	71.44
	17-4E	3.234	243.8	75.38
NOTE: Four fillet weld lines of the specified geometry per connection. Units are inches. AVG = Average value; SD = Standard Deviation; CV = Coefficient of variation Average effective weld throat: 0.194-in.				**AVG =69.53** **SD = 3.77** **CV = 5.42%**

4.4 CAPACITY PREDICTION OF CONCENTRIC CONNECTIONS

This section assesses the accuracy of the AISC model and attempts to achieve a better prediction of the capacity of the concentric connections. Two different models for capacity prediction are assessed: (a) the As-Built AISC prediction, which represent an effort to predict the capacity of the connection using the AISC equation (AISC 2016) based on the as-built dimensions and the estimated material properties and (b) a proposed capacity prediction based on As-Built properties but considering the weld behavior at the onset of bolt slip. The as-built properties include bolt pretension measured by Skidmore tests, slip coefficient estimated from bolted-only tests, and the weld shear strength obtained from welded-only tests. Additionally, each weld was measured before the test in order to estimate the effective throat area of the weld. To compute the As-Built AISC capacity, the equations prescribed by the AISC Steel Specification and AISC Steel Construction Manual were modified to account for the known connection attributes (AISC 2016,

AISC 2017). The equations are highlighted below for slip-critical bolts and fillet welds, respectively. Similar to the AISC R_n, the As-Built R_n is the summation of the bolted and welded components.

The nominal slip resistance of the bolted component (i.e., Eq. 20) uses the Skidmore average bolt pretension and experimental slip coefficient computed in Table 4.1 and Table 4.2, respectively. Since an estimate of the bolt pretension is known from the Skidmore data, the 1.13 factor highlighted in Eq. 16 is omitted. The remaining factors for fillers and number of slip planes remain the same. The nominal strength of the welded component includes the experimental weld shear strength shown in Table 4.3, as well as the known dimensions of the constructed fillet weld. These dimensions are the effective throat length, t_e, and fillet weld length, l. The effective throat length is computed by the measured size of each leg of the fillet weld and accounts for unequal leg sizes. Then, the throat is computed using the expression shown in Eq. 21 (Salmon et al. 2009). The effective throat length and weld length measurements allow for a more accurate computation of the failure area.

As-Built Capacity of Slip-Critical Bolts:

$$R_b = \mu h_f n_s T_B \qquad \text{Eq. 20}$$

μ = experimental slip coefficient for Class A or B surfaces. $\mu = 0.457$ for Class A (2×2); $\mu = 0.339$ for Class A (2×3); $\mu = 0.535$ for Class B *(experimental slip coefficient evaluated from Table 4.2)*

$h_f = 1.0$; factor for fillers (no fillers)

$n_s = 2$; number of slip planes

T_B = fastener pretension: $T_b = 42.73\ kips$ for 3/4-in. A325 – ToN; $T_b = 38.47\ kips$ for 3/4-in. A325 – TC; $T_b = 46.79\ kips$ for 3/4-in. A490 – ToN; $T_b = 64.07\ kips$ for 1-in. A325 – ToN *(experimental bolt pretension data from Table 4.1)*

As-Built Capacity of Fillet Welds:

$$R_w = \tau t_e l \qquad \text{Eq. 21}$$

$\tau = 69.53$ ksi; weld shear strength *(experimental weld shear strength evaluated from Table 4.3)*

$t_e = \frac{ab}{\sqrt{a^2+b^2}}$; the shortest distance of the weld from the root to the face of the weld, where a and b are the measured leg sizes of the fillet weld. This accommodates unequal leg sizes (Salmon et al. 2009).

l = weld length, in.

Then the As-built capacity of the combination connection is

$$R_n = R_b + R_w \qquad \text{Eq. 22}$$

The As-Built R_n was evaluated for each combination connection and the test series average is presented below in Table 4.4. Additionally, the average Test R_n for the test series is used to compute the factor of safety for each connection and for the faying class group (Test R_n / As-Built R_n).

Table 4.4: As-Built prediction results for combination connections

	Test	AVG As-Built R_n (kips)	AVG Test R_n (kips)	AVG Test R_n / As-Built R_n	SD Test R_n / As-Built R_n	Group Test R_n / As-Built R_n
2×2 Class A	Test 12	235.3	240.5	1.02	0.071	**AVG = 0.977**
	Test 13	277.6	262.3	0.94	0.027	**SD = 0.054**
	Test 14	320.8	309.4	0.96	0.037	**CV = 5.55%**
	Test 15*	439.0	352.4	0.80	0.082	-*
2×2 Class B	Test 7	460.1	470.2	1.02	0.045	
	Test 8	320.5	348.0	1.09	0.130	**AVG = 1.071**
	Test 9	376.2	391.3	1.04	0.175	**SD = 0.106**
	Test 10	288.8	330.8	1.15	0.091	**CV = 9.94%**
	Test 11	355.3	376.9	1.06	0.082	
2×3 Class A	Test 18	291.8	265.5	0.91	0.111	
	Test 19	334.8	323.1	0.97	0.049	**AVG = 0.958**
	Test 20	393.6	355.2	0.90	0.038	**SD = 0.069**
	Test 21	518.2	490.3	0.95	0.027	**CV = 7.25%**
	Test 22	326.8	320.6	0.98	0.065	
	Test 23	306.2	319.1	1.04	0.013	
NOTE: * Test 15 uses 1-in. diameter bolts and is not included in the 2×2 Class A group statistics. Test 15: AVG = 0.80; SD = 0.082; CV = 10.22% AVG = Average value; SD = Standard Deviation; CV = Coefficient of variation						

As shown in Table 4.4, the As-Built AISC equation slightly overpredicts the capacity in several of the conducted tests, especially for 2×3 Class A tests. This can be attributed to the fact that the ultimate capacity of the welds is considered in As-Built equation, whereas the bolt capacity is computed at or before 0.02-in of slip. The proposed prediction model attempts to resolve this issue by using the weld stress corresponding to the onset of bolt slip rather than the ultimate weld shear strength. This accounts for the load-deformation compatibility of bolt and weld in the combination connection. Accordingly, the weld shear stress at 0.02-in of slip displacement is considered in the proposed capacity prediction. The mean value of the weld shear stress at 0.02-in is obtained, from the welded-only tests, as 63.99 ksi and the ratio of weld shear stress at 0.02-in of slip to the ultimate weld shear strength is 0.92 for the tested 5/16-in welds. Accordingly, the proposed capacity prediction equation can be expressed as

$$R_n = R_b + C_w R_w \qquad\qquad \text{Eq. 23}$$

where C_w is the ratio of weld shear stress at 0.02-in of slip to the ultimate weld shear strength, taken as 0.92 for tested 5/16-in welded connections.

The prediction results from Eq. 23 are listed in Table 4.5. As shown, the proposed equation is capable of predicting the connection capacity with sufficient accuracy. The factor of safety plot is depicted in Figure 4.3. It should be noted that both prediction equations are conservative with respect to the connections with Class B faying surface.

Table 4.5: Prediction results for combination connections using the proposed model

	Test	R_{n_W} / R_{n_B}	AVG Proposed R_n (kips)	AVG Test R_n (kips)	AVG Test R_n / Proposed R_n	SD Test R_n / Proposed R_n	Group Test R_n / Proposed R_n
2×2 Class A	Test 12	0.67	229.0	240.5	1.05	0.074	**AVG = 1.011**
	Test 13	1.00	267.9	262.3	0.98	0.028	**SD = 0.053**
	Test 14	1.50	307.6	309.4	1.01	0.038	**CV = 5.29%**
	Test 15*	1.00	422.6	352.4	0.83	0.086	**-***
2×2 Class B	Test 7	1.5	437.9	470.2	1.07	0.047	
	Test 8	0.67	309.5	348.0	1.12	0.134	**AVG = 1.114**
	Test 9	1.00	360.8	391.3	1.08	0.183	**SD = 0.108**
	Test 10	0.67	278.8	330.8	1.19	0.092	**CV = 9.73%**
	Test 11	0.67	342.9	376.9	1.10	0.085	
2×3 Class A	Test 18	0.67	282.3	265.5	0.94	0.114	
	Test 19	1.00	321.9	323.1	1.00	0.048	
	Test 20	1.33	376.0	355.2	0.94	0.040	**AVG = 0.998**
	Test 21	2.00	490.6	490.3	1.00	0.029	**SD = 0.070**
	Test 22	1.00	313.2	320.6	1.02	0.068	**CV = 7.01%**
	Test 23	0.50	296.9	319.1	1.07	0.014	
NOTE: * Test 15 uses 1-in. diameter bolts and is not included in the 2×2 Class A group statistics. Test 15: AVG = 0.83; SD = 0.086; CV = 10.26% AVG = Average value; SD = Standard Deviation; CV = Coefficient of variation							

58
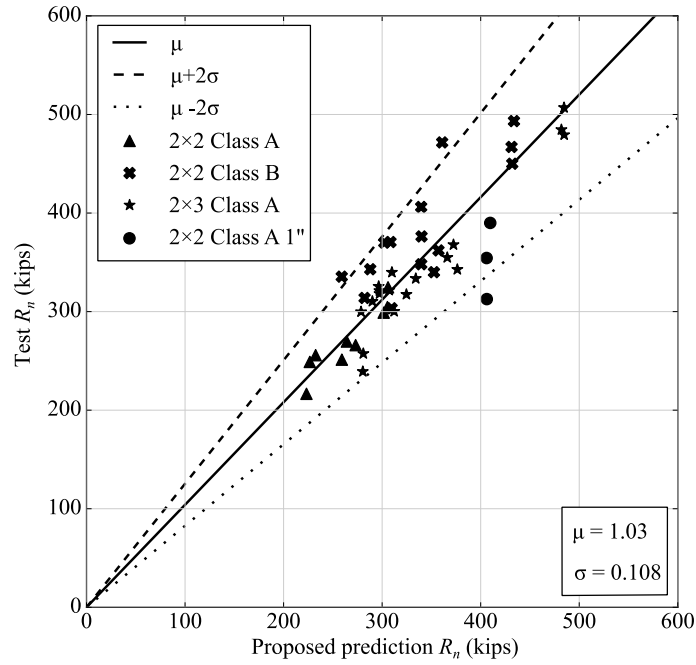
Figure 4.3: Factor of safety plot: Proposed equation prediction

The adopted value of C_w in Eq. 23 considers only the tested connections with 5/16-in weld size. As indicated in Lesik and Kennedy (1990), the load-deformation behavior of welded connections depends on the fillet weld size. In order to account for the effect of weld size on the factor C_w, the load-deformation model for fillet welds adopted by the AISC (2017) is utilized. In this model, the deformation of welds at ultimate capacity Δ_u is

$$\Delta_u = 0.209(\theta + 2)^{-0.32} w \qquad \text{Eq. 24}$$

where θ is the weld orientation considered 0 for longitudinally loaded fillet welds and w is the weld size (in). The ratio, $f(\Delta)$, of the weld strength at a specific deformation Δ to the ultimate strength at Δ_u is defined as

$$f(\Delta) = \left[\frac{\Delta}{\Delta_u} \left(1.9 - 0.9 \frac{\Delta}{\Delta_u} \right) \right]^{0.3} \qquad \text{Eq. 25}$$

By setting $\Delta = 0.02$-in, the factor C_w becomes

$$C_w = f(0.02) = \left(\frac{0.227w - 0.013}{w^2} \right)^{0.3} \qquad \text{Eq. 26}$$

For connections with 5/16-in weld size, the value of C_w obtained using Eq. 26 is 0.86. This value is lower than the one obtained from current experimental tests. However, the difference is to be expected given the variability in the weld mechanical properties, dimensions, and quality. It should be noted that Eq. 26 will yield lower values of C_w for larger weld sizes. For example, a 1-

59

in weld size will lead to C_w of 0.63. However, the lack of experimental load-deformation data in literature for large fillet welds prevented a more detailed analysis into the estimation of C_w for larger fillet welds. Accordingly, more experimental work is needed for better characterization of the load-deformation behavior of fillet welds with sizes exceeding 5/16-in.

4.5 INFLUENCE OF INVESTIGATED CONNECTION VARIABLES

This section studies the influence of the investigated variables by comparing the experimental load-slip curves of tested connections and studying their ductility and ultimate capacity. The following sections describe the impact that bolt pattern, bolt grade, bolt size, tensioning technique, faying surface class, and weld/bolt strength ratio have on the performance of combination connections.

4.5.1 Bolt Pattern

The bolt pattern of the combination connection is studied in a comparative analysis shown in Figure 4.4 and Figure 4.5 for weld/bolt strength ratios of 0.67 and 1.0, respectively. Each comparison shows the combination connections good ductility characteristics. However, the 2×3 connections continue to carry load as the deformations increase whereas the load carrying of 2×2 connections will flatten out and begin to drop earlier. This can be due to the different friction characteristics of the of plates used for these two connection types. When comparing the proposed prediction capacity to the Test R_n at the considered weld/bolt strength ratios, most cases fail at loads higher than predicted ones as shown in Table 4.5. Test 18 provided a capacity that is on average 5% lower than the proposed prediction capacity R_n. This can be attributed to the higher variability associated with the 2×3 Class A slip coefficient. It is noteworthy that two of the considered 2×2 connections in Test 12 had a slip load similar to that of two 2×3 connections in Test 18. This is due to the higher friction coefficient of the 2×2 Class A plates used in this study and the high variability of the friction coefficient of the utilized 2×3 Class A plates. Figure 4.6 shows a comparison between the 2×2 and 2×3 connections with a similar weld length of 2.0-in. Due to the lower friction coefficient of the 2×3 plates, two of the connections had a slip load that is lower than that of the 2×2 connections with the same weld length. In summary, it seems that the number of bolts has a minimal effect on the accuracy of the capacity prediction process.
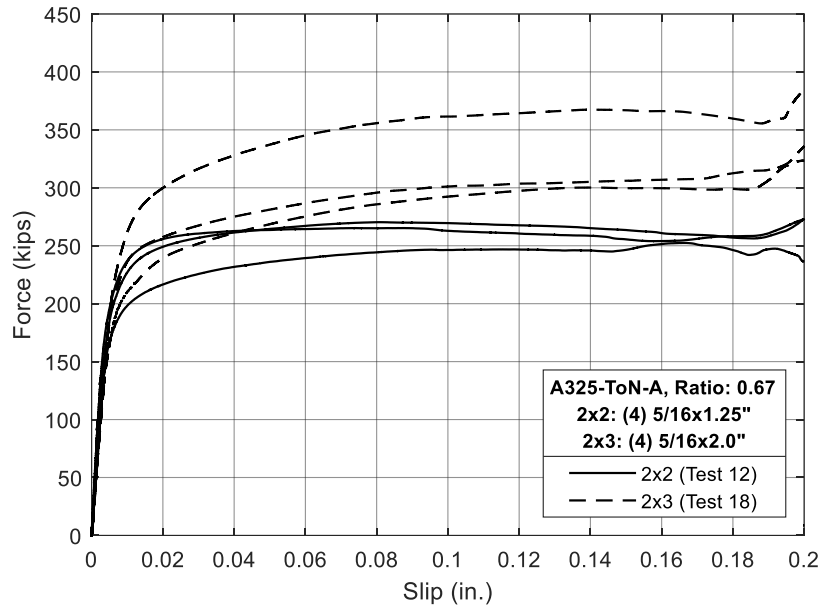
Figure 4.4: Bolt pattern comparison – 2×2 vs 2×3 (Ratio: 0.67)
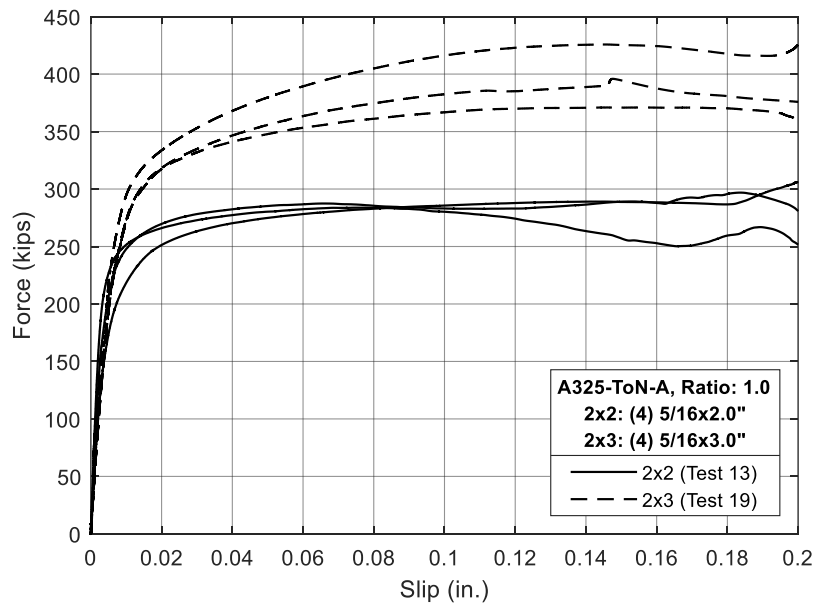
Figure 4.5: Bolt pattern comparison – 2×2 vs 2×3 (Ratio: 1.0)

61
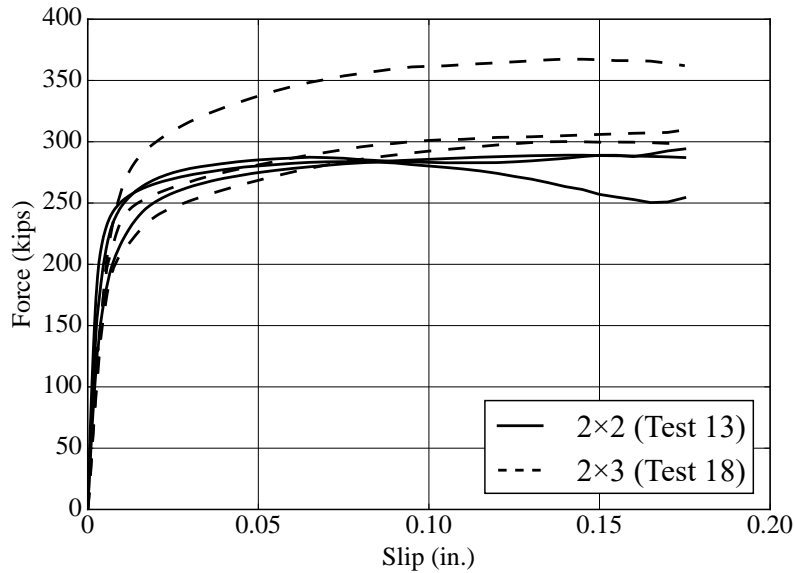
Figure 4.6 Bolt pattern comparison – 2×2 vs 2×3 (2-in weld length)

4.5.2   Bolt Grade

Most connections in the test program use A325 bolts; however, two combination test series were chosen to highlight the effect of higher bolt grades (A490), i.e., Test 11 and Test 23. The first comparison in Figure 4.7, features a 2×2 Class B connection with ToN bolts. The combination connections are constructed with a weld/bolt strength ratio of 0.67; thus, providing longer welds for the A490 connections. As shown in Table 4.5, the A325 bolts (Test 8) provided an average factor of safety of 1.130 with standard deviation of 0.11 and the A490 (Test 11) bolts provided 1.11 with standard deviation of 0.075. Overall, these combination connections provide similar levels of conservatism. Additionally, they display similar load-deformation behavior and follow the traditional Class B combination trends noticed throughout the experimental test program.

Figure 4.8 compares the bolts grades in a different manner. Instead of using similar weld/bolt strength ratios between the two tests, the weld lengths are kept constant. The highlighted connections are 2×3 Class A specimens with ToN bolts. Each combination connection features 2-in. welds to provide weld/bolt strength ratios of 0.67 and 0.50 for Test 18 and Test 23, respectively. According to the connection results in Table 4.5, connections utilizing A325 bolts (Test 18) have an average slip load of 265.8 kips and connections with A490 bolts (Test 23) have an average slip load of 319.1 kips. As expected, the increase in strength is due to the higher pretension load associated with the A490 bolt grade. Again, regardless of the bolt grade, the overall load-deformation behavior remains the same.
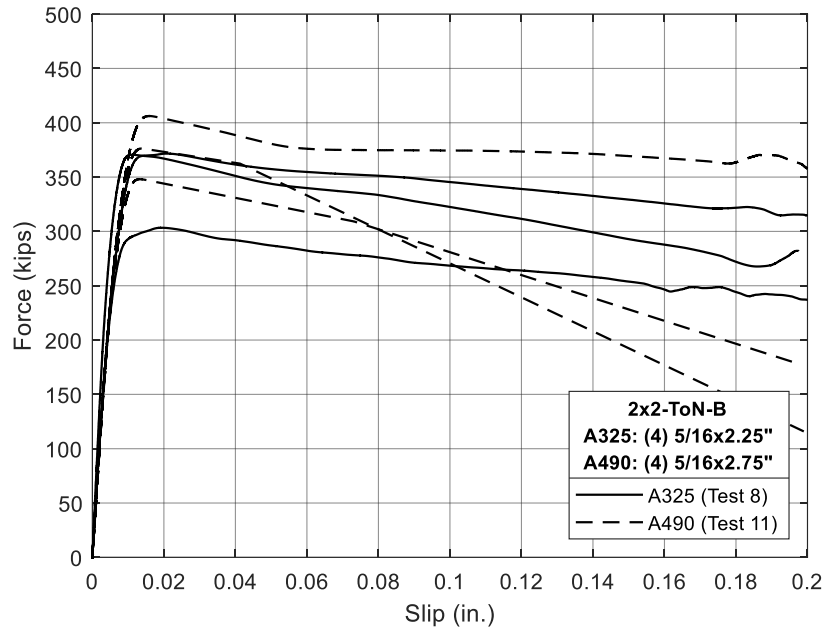
Figure 4.7: Bolt grade comparison – A325 vs A490 (2×2 – Class B)
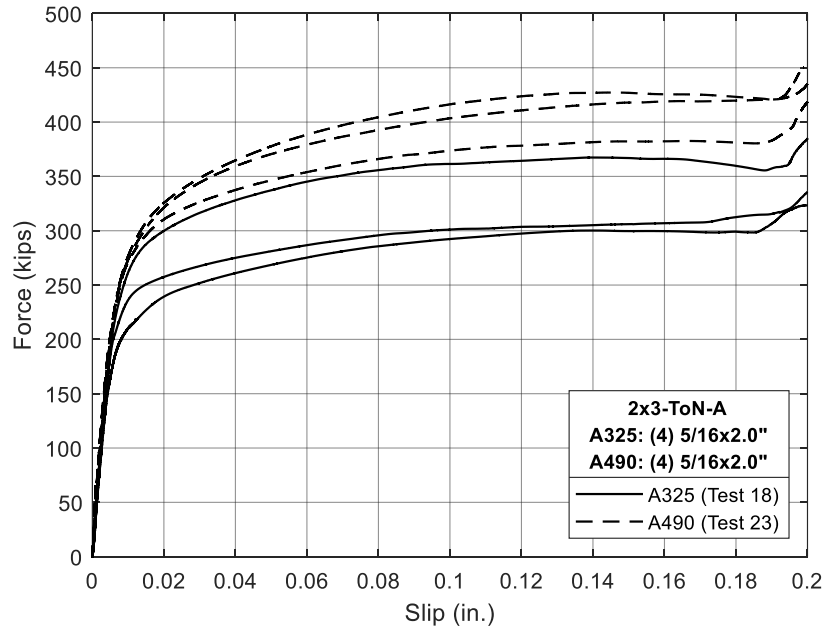
Figure 4.8: Bolt grade comparison – A325 vs A490 (2×3 – Class A)

63

4.5.3 Bolt Size

All connections in the experimental test matrix utilize 3/4-in. diameter bolts except Test 15. These connections feature 1-in. diameter A325-ToN bolts. Figure 4.9 compares the load-deformation curves of these specimens, at weld/bolt strength ration of 1.0, against a similar connection with 3/4-in. diameter bolts, Test 13. Both connections exhibit similar ductile behavior, however the 1-in. bolts have a more variability in the capacity ranging nearly over 80 kips. According to Table 4.5, the proposed prediction model overpredicts the capacity for the 1-in. diameter bolts by roughly 14%, whereas the model is conservative for the 3/4-in. diameter bolts. This may be attributed to the large, oversized holes used in the tested connection with 1-in. diameter bolts. Allan and Fisher (1968) reported a 15% drop in the pretension force for 1-in. bolts when the size of the bolt holes changes from standard to oversized. A similar reduction in the slip capacity of bolted connections when larger bolts are used has been reported in Shoukry and Haisch (1970) and Heistermann et al. (2013). Heistermann et al. (2013) argued that the presence of these larger holes reduces the effective friction area of the plate. Accordingly, it seems that the higher bolt size, when combined with oversized holes, could have an effect on the capacity of slip-critical bolted connections.
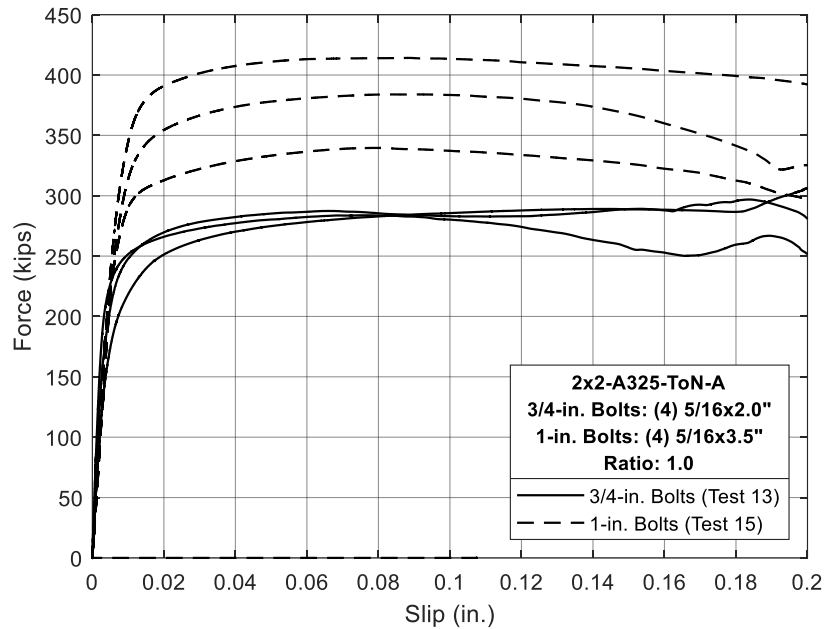
Figure 4.9: Bolt size comparison – 3/4-in. vs 1-in. bolts (2×2 – Class A)

4.5.4 Bolt Pretensioning Method

Most connections in the test program use the turn-of-nut tightening method (ToN); however, two combination test series were conducted to investigate the effect of using tension control (TC) bolts (i.e., Test 10 and Test 22). The first comparison in Figure 4.10 features a 2×2 Class B connection with A325 bolts. These combination connections are constructed with a weld/bolt

strength ratio of 0.67, thus providing the same weld lengths for each test series. According to the Skidmore data presented in Table 4.1, it was expected that the ToN connections would provide slightly higher capacities than connections with TC bolts. From Table 4.5, the connections in Test 8 utilizing the ToN method have an average slip load of 348.0 kips and the connections in Test 10 that use TC bolts have an average slip load of 330.8 kips. This represents a difference of approximately 5% in the capacity of the connection and follows the expectation from the Skidmore data.

Another bolt tensioning comparison pertaining to the 2×3 connections is presented in Figure 4.11. The 2×3 connections use Class A faying surface with A325 bolts. These combination connections are constructed with a weld/bolt strength ratio of 1.0 to provide the same weld lengths for each test series. The test data in Table 4.5 shows that the connections in Test 19 utilizing the ToN method have an average slip load of 323.1 kips and the connections in Test 22 that use TC bolts have an average slip load of 320.6 kips. This represents less than 1% drop in the capacity of the connection, which is less than the percentage reported in 2×2 Class B connections. It could be related to the high variability of the slip characteristics of the 2×3 Class A plates.

For both considered types, the behavior of the combined connection remains similar regardless of the bolt pretensioning method. Accordingly, it seems that the bolt pretensioning method (i.e., ToN vs. TC) has a negligible effect on the performance of combined bolted and welded concentric connections. This is contingent upon using the proper tightening techniques associated with the given bolt type to achieve the required bolt pretension.
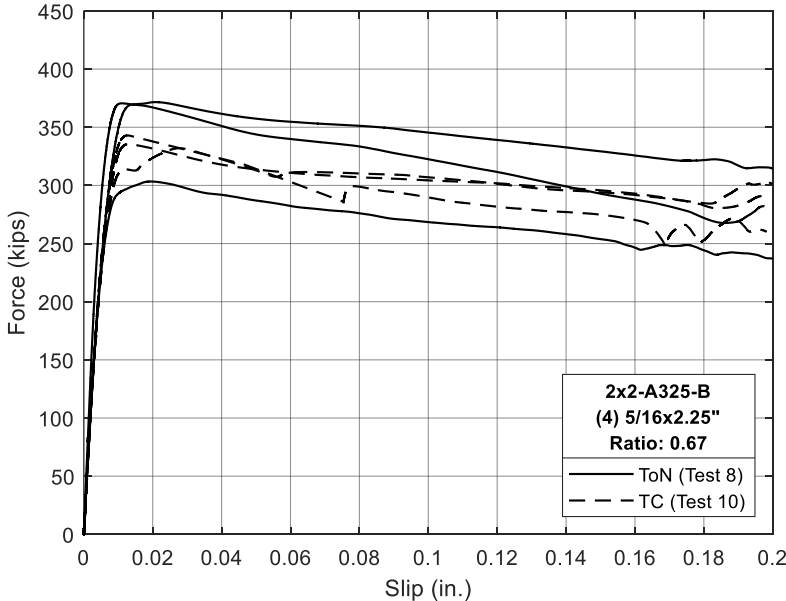
Figure 4.10: Bolt tensioning comparison – ToN vs TC (2×2 – Class B)
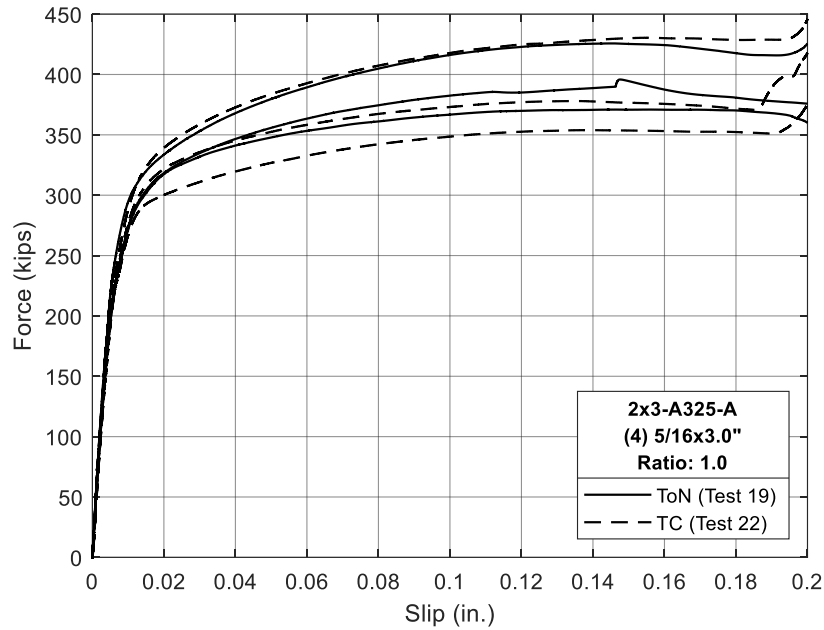
Figure 4.11: Bolt tensioning comparison – ToN vs TC (2×3 – Class A)

4.5.5   Faying Surface Class

A major factor in determining the capacity and behavior of combination connections is the faying surface. Three comparisons are presented to describe how the faying surface characteristics can impact the performance. Each connection uses a 2×2 bolt pattern with A325-ToN bolts. The connections in each comparison feature the same weld/bolt strength ratio. Due to the high slip coefficient of Class B connections, these specimens will have longer weld lengths. Figure 4.12, Figure 4.13, and Figure 4.14 describe the connection performance for weld/bolt strength ratios of 0.67, 1.0, and 1.5, respectively.

There is a noticeable difference in the overall load-deformation behavior between connections utilizing the two surface classes. The Class A faying surface, which is clean mill scale, is stiff in the elastic region of the connection. After approximately 0.01-in. of deformation, the Class A connections begin to soften and lose stiffness. The load-slip of connections with Class A faying surface softens gradually as the connection slip-hardens. During connection slip, load is sustained over large deformations and can continue as the bolts go into bearing, as shown in Figure 4.12 and Figure 4.13. The reported slip load for Class A combination connections corresponds to the load at 0.02-in. of deformation. This is according to the load-slip curve provided by the *Specification for Structural Joints Using High-Strength Bolts* shown in Figure 3.1 (RCSC 2014).

66

Combination connections with Class B surfaces display a similar load-deformation behavior to their bolted-only counterparts (Figure 3.5 and Figure 3.6), but with higher ductility provided by the longitudinal fillet welds. Similar to the Class A surface, the connections utilizing Class B are very stiff in the elastic region of their load-deformation curve. However, shortly after 0.01-in. of deformation, the connection slips. Unlike Class A faying surfaces where the connection gradually slips and sustains load, the load sustained by the connection drops as slip increases; the Class B combination connections do not display slip hardening behavior. This may be attributed to the interlocking nature of sand blasted steel surfaces; as the connection slips, this interlock is lost, and the frictional resistance is reduced causing the loss of slip capacity. The slip load for Class B combination connections corresponds to the maximum load before 0.02-in. of deformation.

Lastly, the factor of safety was evaluated for both Class A and Class B surfaces using the proposed prediction equation. The Class B surfaces provided a higher factor of safety averaging at 1.116 with standard deviation of 0.093, while Class A surfaces provided 1.021 with standard deviation of 0.039. For both faying surface classes, the test capacity is conservatively predicted using the proposed equation.
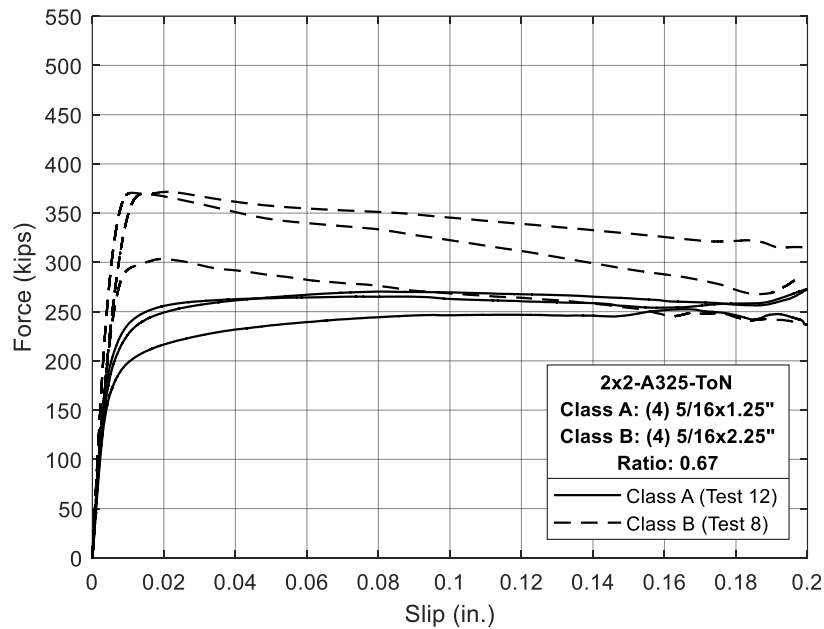
Figure 4.12: Surface class comparison – Class A vs Class B (2×2 – Ratio: 0.67)
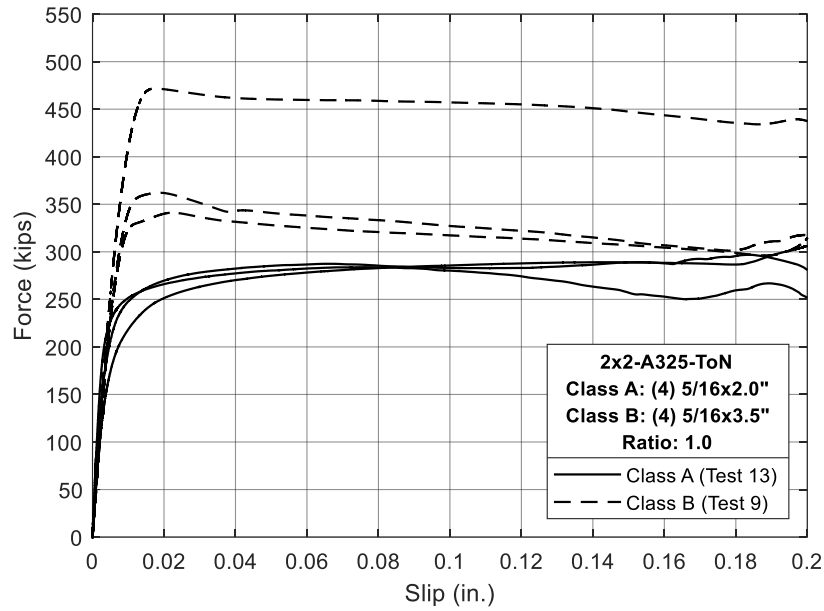
Figure 4.13: Surface class comparison – Class A vs Class B (2×2 – Ratio: 1.0)
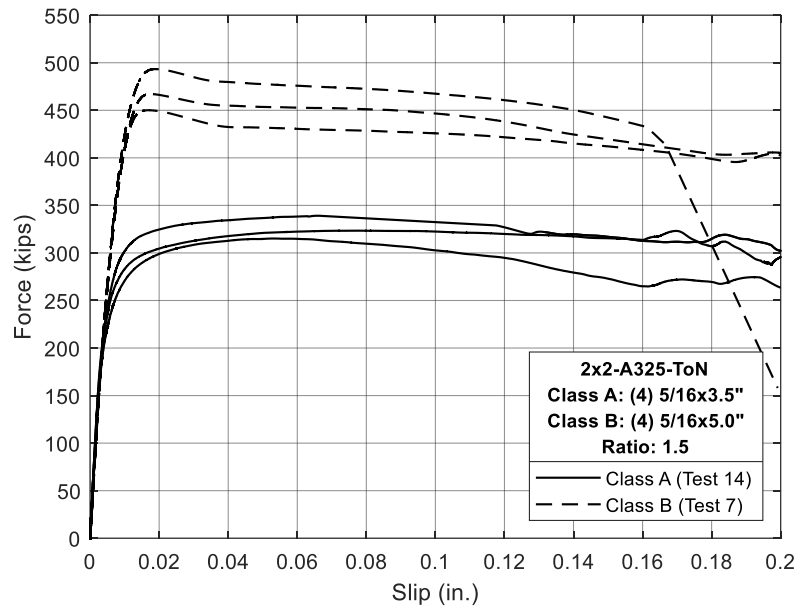
Figure 4.14: Surface class comparison – Class A vs Class B (2×2 – Ratio: 1.5)

4.5.6 Weld/Bolt Strength Ratio

The research conducted by Shi et al. (2011) concluded that the weld/bolt ratio may play a significant role in determining the combination connection capacity. This conclusion is assessed

in the following three comparisons highlighted in Figure 4.15 – Figure 4.17. The studied connections include 2×2 Class A, 2×2 Class B, and 2×3 Class A with weld/bolt strength ratios ranging from 0.67 – 2.0.

The comparison in Figure 4.15 shows the 2×2 Class A connections with ratios of 0.67, 1.0, and 1.5. The average slip load of the three groups of connections is 240.5 kips, 262.3 kips, and 309.4 kips for ratios of 0.67, 1.0, and 1.5, respectively. The increase in capacity is expected as additional weld is used in the connection. Additionally, the experimental slip load of the connection outperforms the capacity predicted using the proposed model with a negligible effect of the weld/bolt strength ratio. The probabilistic parameters of the safety factors are highlighted in Table 4.6.

The 2×2 Class B ratio comparison, shown in Figure 4.16, produces similar outcomes to the 2×2 Class A, but behaves slightly different. The average slip load of the connections are 348.0 kips, 391.3 kips, and 470.2 kips for ratios of 0.67, 1.0, and 1.5, respectively. Again, this increase is expected due to the addition of weld. Two of the 1.0 ratio connections (Test 9) slip at a load level lower than that achieved with 0.67 ratio and the other slips at a load level consistent with the 1.5 ratio. This large variability can be attributed to the high randomness associated with Class B faying surface conditions. However, all connections in Test 9 series outperformed the predicted capacity computed with the proposed formulation. Additionally, the average factor of safety is consistent across all connections, as shown in Table 4.6. However, the standard deviation differs between ratios, which is typical for Class B surfaces.

Finally, Figure 4.17 compares the behavior of 2×3 combination connections at ratios of 0.67, 1.0, 1.33, and 2.0. Their behavior is consistent with the other 2×2 Class A connections previously compared, in that the average slip load of the connection increases as the weld/bolt ratio increases. These loads are 265.5 kips, 323.1 kips, 355.2 kips, and 490.3 kips for weld/bolt strength ratios of 0.67, 1.0, 1.33, and 2.0, respectively. Lastly, the slip load of the connection meets the capacity of the proposed model for all test series groups with some fluctuations, such as Test 18, and Test 20.
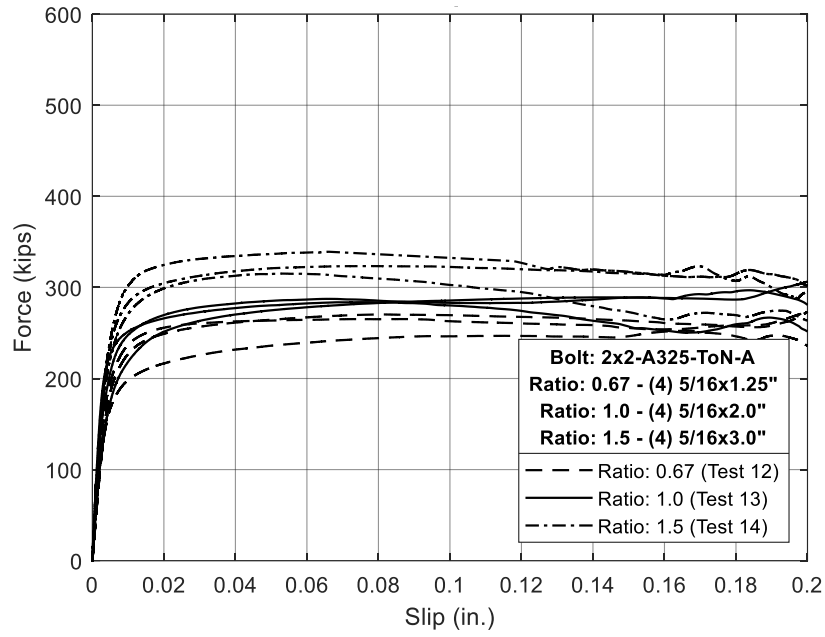
Figure 4.15: Weld/bolt strength ratio comparison (2×2 – Class A)
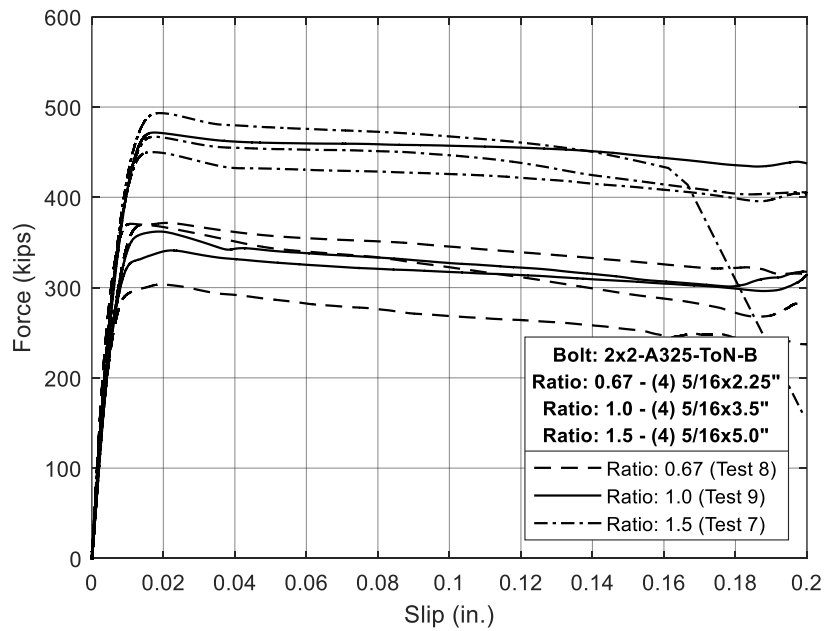
Figure 4.16: Weld/bolt strength ratio comparison (2×2 – Class B)
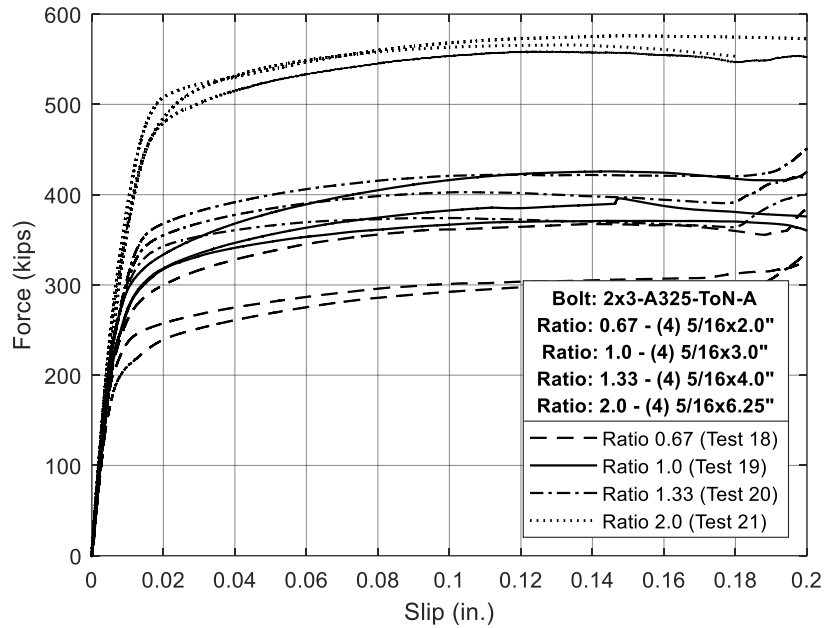
Figure 4.17: Weld/bolt strength ratio comparison (2×3 – Class A)

Table 4.6: Weld/bolt strength ratio comparison with respect to the factor of safety

Comparison	Test No.	$R_{n\_w}/$ R_{n_B}	Average Factor of Safety	Standard Deviation	Coefficient of Variation
2×2 – Class A (Figure 4.15)	Test 12	0.67	1.06	0.061	5.75%
	Test 13	1.0	0.99	0.023	2.32%
	Test 14	1.5	1.02	0.032	3.14%
2×2 – Class B (Figure 4.16)	Test 8	0.67	1.13	0.110	9.73%
	Test 7	1.0	1.10	0.151	13.73%
	Test 9	1.5	1.15	0.088	7.65%
2×3 – Class A (Figure 4.17)	Test 18	0.67	0.95	0.094	9.89%
	Test 19	1.0	1.01	0.039	3.86%
	Test 20	1.33	0.96	0.033	3.44%
	Test 21	2.0	1.01	0.024	2.38%

4.6   SUMMARY: DOUBLE SHEAR TENSION SPLICES

The test results presented above show that the capacity of a slip-critical axial lap bolted connection increases when combined with fillet welds. The increase in the capacity is relative to the dimensions of the weld lines used to retrofit the connection. Connections implementing both Class A and B faying surfaces experienced this increase in capacity. Figure 4.18 presents the results of Test 2 (bolted-only with Class A surface utilizing A325-ToN bolts), Test 6 (welded-only test with four longitudinal fillet welds at 5/16 × 3.0-in), and Test 14 is the combination connection using the same attributes of Tests 2 and 6. It was found that this combination

connection has higher stiffness in the elastic region than its bolted-only and welded-only counterparts. After the connection slips, it exhibits a ductile behavior and fails at a capacity close to the sum of the capacities of individual connecting elements.

To compare the experimentally obtained capacity to that achieved using the AISC (2016) model (i.e., summation of bolt and weld capacities), Figure 4.19 compares the average load-slip profiles for (a) bolted-only Class A 2×2 tests (i.e., Test 2), (b) welded-only 3-in tests (i.e., Test 6), the experimental profile (i.e., Test 14), and finally the summation of curves (a) and (b). As shown in Figure 4.19, the experimental profile shows a behavior that is similar to the one depicted by the summation curve; especially at slip values below 0.02 inches. It should be noted that the bolted, welded, and experimental profiles reflect the average values obtained from the three test specimens. Figure 4.20 highlights the effect of variability in the experimental tests when compared to the summation curve. As shown, the summation curve lies within the experimental results, especially for low slip values. A similar trend was also found for Class A 2×3 as shown in Figure 4.21; however, the lower bounds of the bolted-only tests were considered in this comparison due to the high variability associated with the 2×3 faying surface conditions. The prediction using the considered as-built values shows good agreement with the experimental test results as shown in Figure 4.22.

With respect to connections with Class B faying surfaces, Figure 4.23 shows the load-slip curves resulting from Test 1, Test 6, and Test 9. Test 9 has a weld length of 3.5-in while Test 6 has a weld length of 3.0-in. Regardless of the weld length, connections with Class B faying surface exhibit a considerable improvement in the load-deformation behavior when combined with welds. These connections tend to have significantly better ductility compared to the bolted-only counterparts which exhibited a sudden slip at their slip loads. Furthermore, the ultimate capacity of the connection can be conservatively predicted using the summation of the bolt and weld capacities at 0.02-in of slip as shown in Figure 4.24. The large difference between the summation curve and the experimental results is attributed to the high variability associated with bolted-only and combination connections utilizing blast cleaned surface highlighted in Figure 4.25. Following this discussion, it is apparent that there is enough evidence that the capacity of the concentrically loaded combination connection can be accurately computed using the summation of the weld force at 0.02-in of slip and the highest bolt capacity occurring at or before 0.02-in of slip.
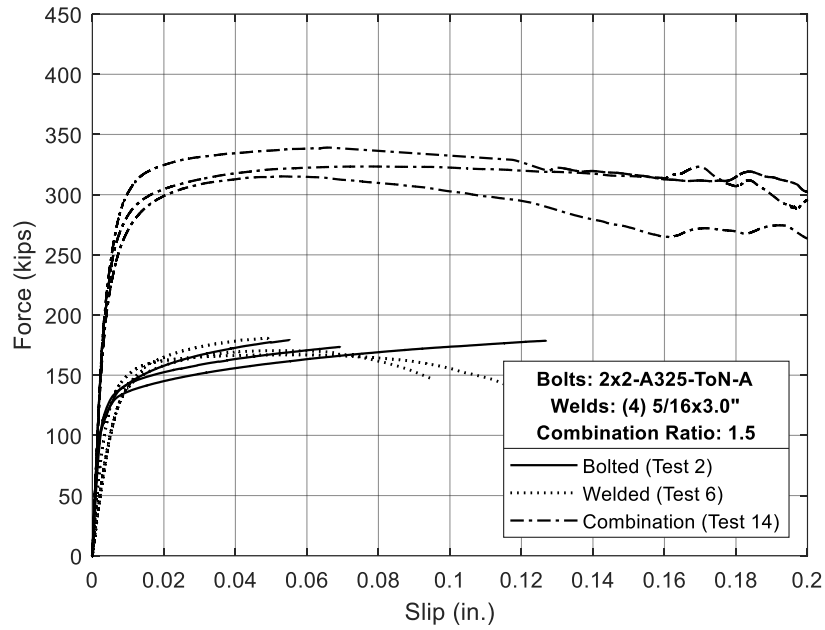
Figure 4.18: Component contribution analysis (2×2 – Class A – Ratio: 1.5)
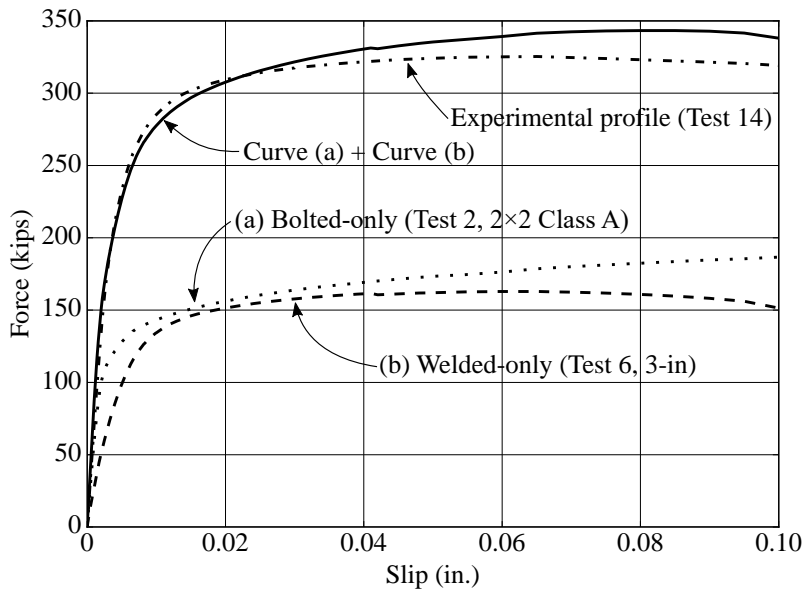
Figure 4.19: Comparison of prediction and test for Class A 2×2 bolt pattern

73
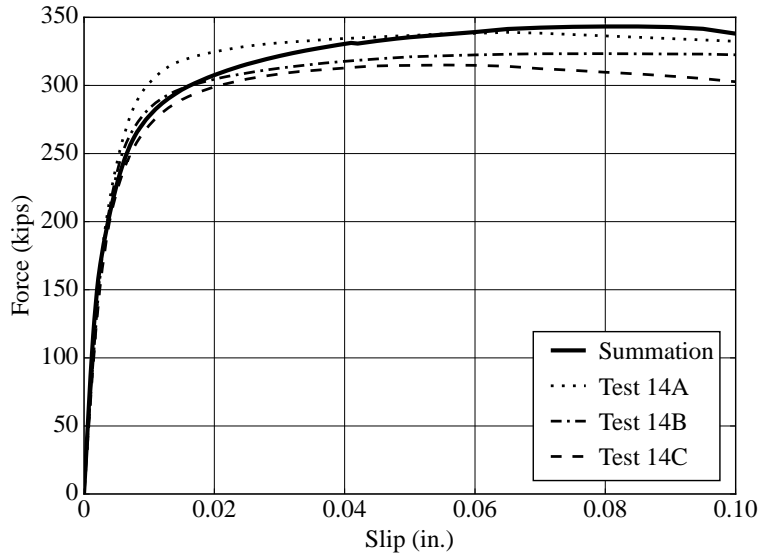
Figure 4.20: Variability of Class A 2×2 with 3.0 in weld
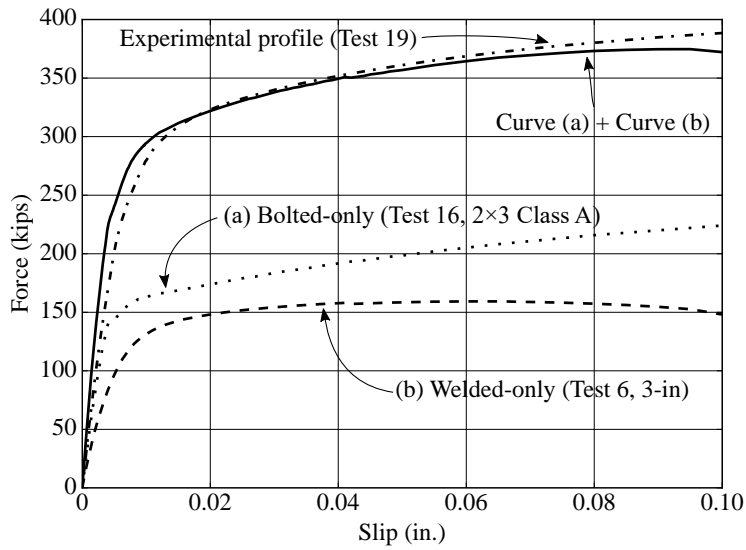
Figure 4.21: Comparison of prediction and experimental results for Class A 2×3 bolt pattern
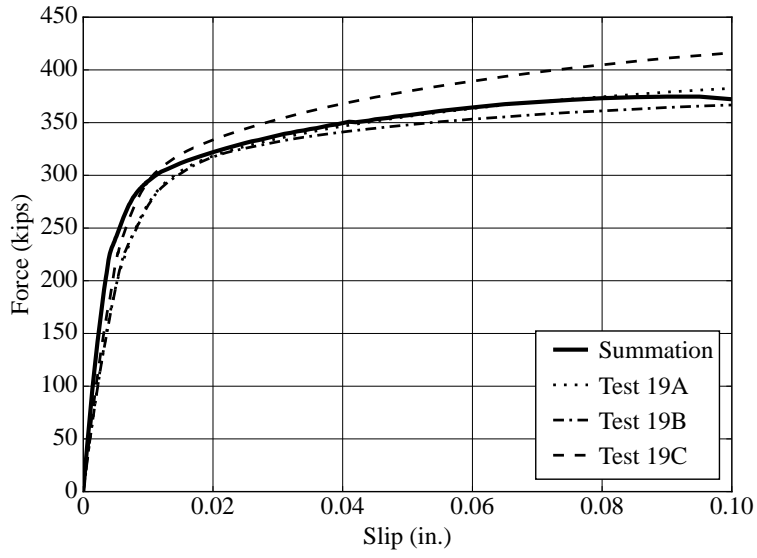
Figure 4.22: Variability of Class A 2×3 with 3.0 in weld
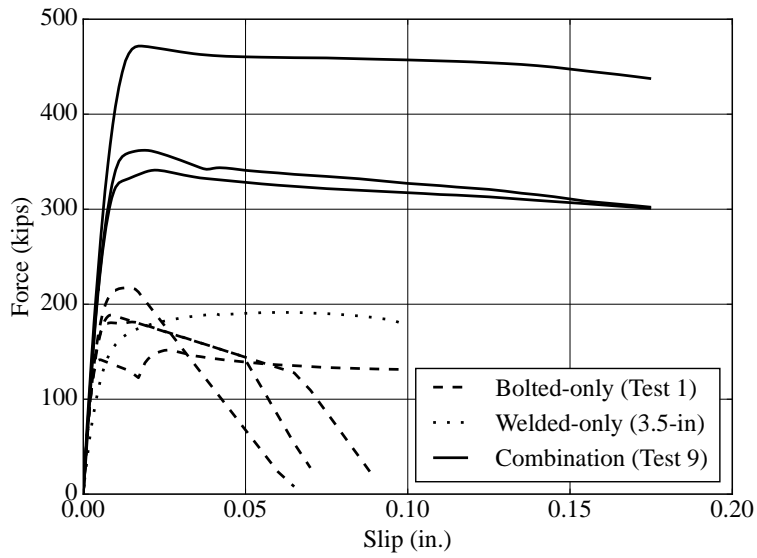
Figure 4.23: Component contribution analysis (2×2 - Class B - Ratio: 1.0)
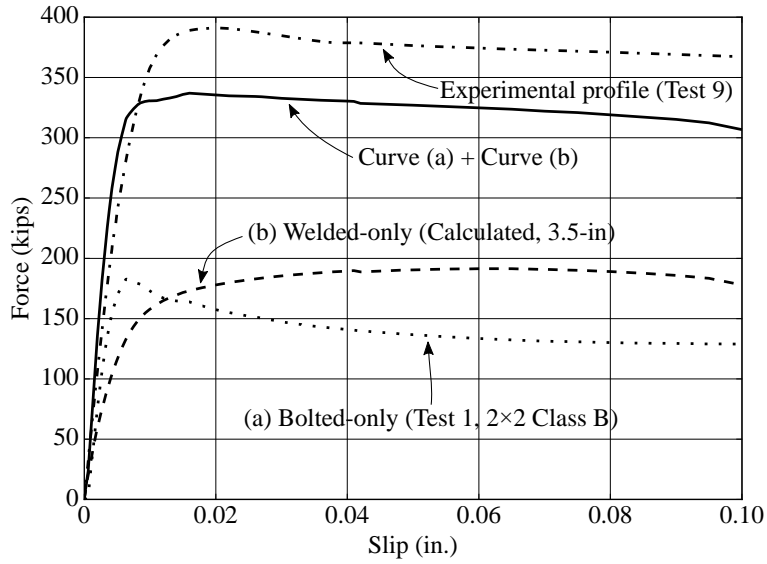
Figure 4.24: Comparison of prediction and test results for Class B 2×2 bolt pattern
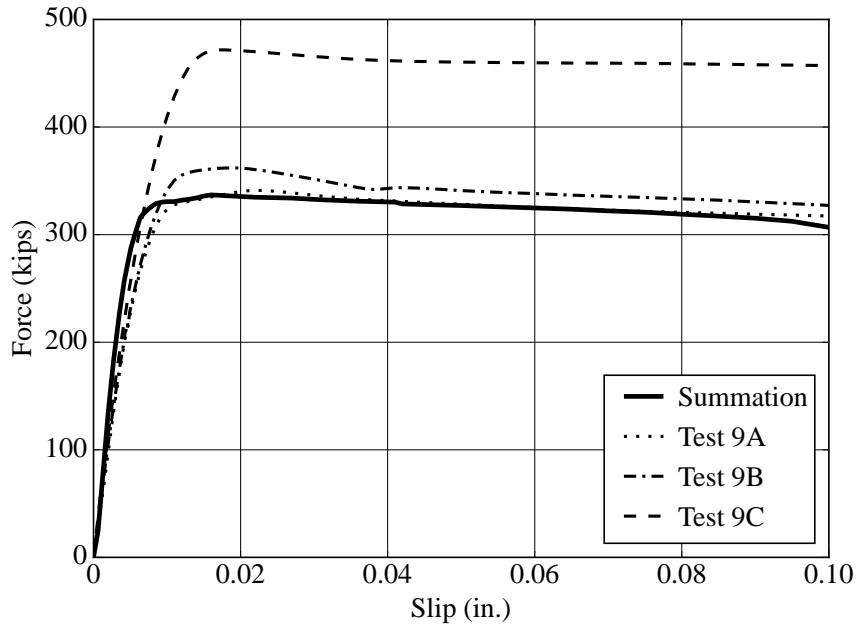
Figure 4.25: Variability of Class B 2×2 with 3.5 in weld

5   ECCENTRIC CONNECTION TESTING

This part of the study attempts to characterize the behavior of eccentrically loaded connections employing both welds and bolts in a single load sharing system. A total of 36 specimens covering 18 variations of input parameters were tested in this phase of the project. These tests attempt to evaluate the effect of key input parameters on the behavior of eccentrically loaded combination connections.

5.1   TEST SPECIMENS

The test specimens designed for this phase is a double shear connection with two different bolt patterns (i.e., 2×3 and 1×6) of slip-critical bolts. Figure 5.1 shows a 3-D view of the 1×6 connection while Figure 5.2 shows the details of these connection. There are two distinct regions for each connection: the tested connection and the anchorage zone (see Figure 5.2). All plates are fabricated using A572 Gr. 50 steel and have been designed to ensure failure of connecting elements before plate yielding or bearing failure at bolt holes.
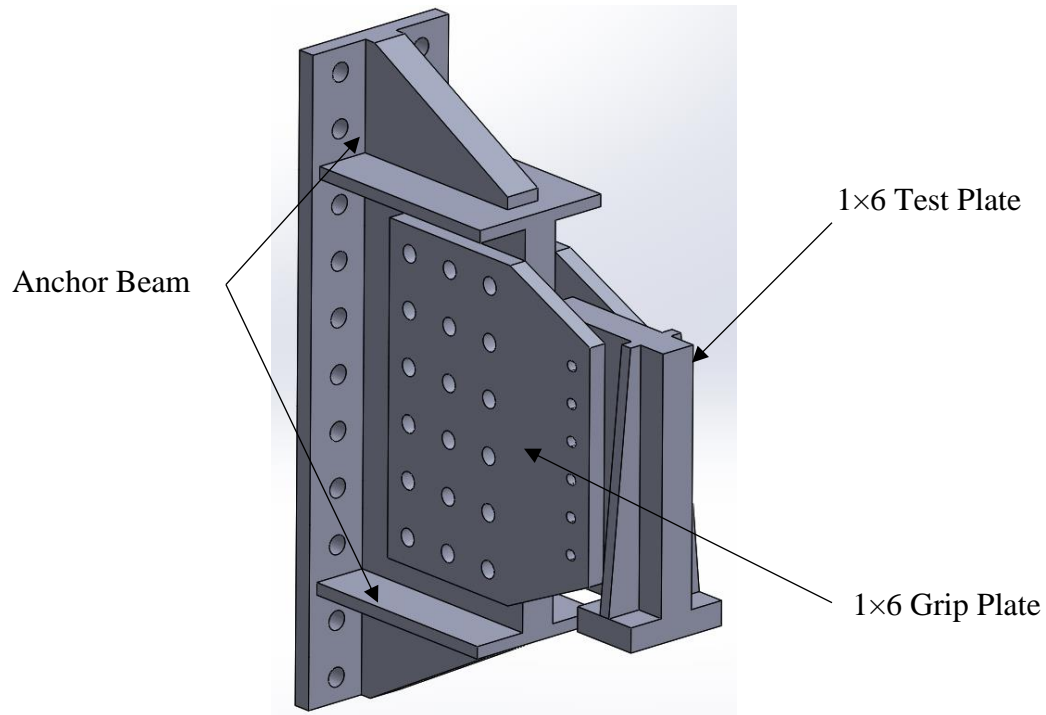
Figure 5.1: Typical 1×6 Connection

5.1.1   Test Matrix for Eccentrically Loaded Connections

The test matrix developed for this phase of testing was created to investigate several parameters that may have influence on the ultimate load and load-deformation (i.e., load-rotation) behavior of eccentrically loaded combination connections. The tested variables include bolt grade, faying surface class, bolt configuration, and weld/bolt strength ratio. For each test series, the labeling

scheme used in concentric testing is also followed for the eccentric testing (i.e., Tests 31A and 31B refer to the two tests conducted under Test 31). Table 5.1 shows the test matrix for the eccentric testing.

Table 5.1: Test matrix of eccentrically loaded connections

	Test No.	Bolt Pattern	Bolt Type	Bolt Pretensioning Method	Faying Surface Class	Weld Geometry (Size × length) [†]	R_{n_W}/R_{n_B}	No. of Samples
AISC Phase II Experimental Test Matrix								
Bolted-Only	31	2×3	A325	ToN	A	-	-	2
	33	2×3	A490	ToN	A	-	-	2
	34	2×3	A325	ToN	B	-	-	2
Welded-Only	36	-	-	-		5/16 × 4.5	-	3
Bolted & Welded	37	2×3	A325	ToN	A	5/16 × 2.25	0.25	2
	38	2×3	A325	ToN	A	5/16 × 4.5	1.0	2
	39	2×3	A325	ToN	A	5/16 × 5.5	1.5	2
	40	2×3	A325	ToN	A	5/16 × 6.5	2.0	2
	42	2×3	A490	ToN	A	5/16 × 4.5	0.82*	2
	43	2×3	A325	ToN	B	5/16 × 2.75	0.25	2
	44	2×3	A325	ToN	B	5/16 × 6	1.0	2
	45	2×3	A325	ToN	B	5/16 × 7.5	1.5	2
	46	2×3	A325	ToN	B	5/16 × 9	2.0	2
Bolted-Only	49	1×6	A325	ToN	A	-	-	2
Welded-Only	50	-	-	-	-	5/16 × 9.75	-	1
Bolted & Welded	51	1×6	A325	ToN	A	5/16 × 3	0.25	1
	52	1×6	A325	ToN	A	5/16 × 6.25	1.0	2
	53	1×6	A325	ToN	A	5/16 × 8	1.5	2
	54	1×6	A325	ToN	A	5/16 × 9.75	2.0	1

Note: All bolts are 3/4-in (short-slotted holes) unless noted otherwise

2×3 bolt eccentricity = 6.5-in; 1×6 bolt eccentricity = 5-in; All weld eccentricity = 3-in

ToN: Turn of nut method

R_{n_W} = Nominal capacity of welds; R_{n_B} = Nominal capacity of bolts

[†] Two fillet weld lines of the specified geometry per connection. Dimensions in inches

* Ratio is reported for A490 bolts.

During the testing program, several tests were dropped from the initially proposed test matrix for various reasons. For instance, the bolt tightening method (TC vs ToN) was initially included as an input parameter in the matrix (e.g., missing Test 32) but was later omitted since TC bolts with the required length were not available in the market. Tests 35 and 47 aimed at investigating the effect of 1-in. diameter bolts on the behavior of these connections but were later omitted since the delivered plates were slotted for the 3/4-in bolts due to a fabrication error.

5.1.2 Details of Eccentric Specimens

The specimens for this phase of the testing program were designed as eccentrically loaded slip-critical bolted-only, welded-only, and combination connections. Each double-shear specimen

includes one test plate and two grip plates. Figure 5.2 depicts the details of the grip plate and test plate to be assembled on the load frame attachment point. The test plate attaches to the two grip plates and the joint between them is the tested connection. The placement of the test plate in between the two grip plates provides two friction planes. This test connection region represents where the slip-critical bolts and welds will be placed together to create a specific test sample. The grip plates were attached to the test frame using 18 A490 1-3/8-in bolts designed to resist the largest predicted loads. Additionally, both the test and the grip plates were designed sufficiently thick to minimize out-of-plane distortion during eccentric load application. The test plate and grip plates are designed to reach full bolt slip and weld fracture before plate yielding or bearing failure at bolt holes.
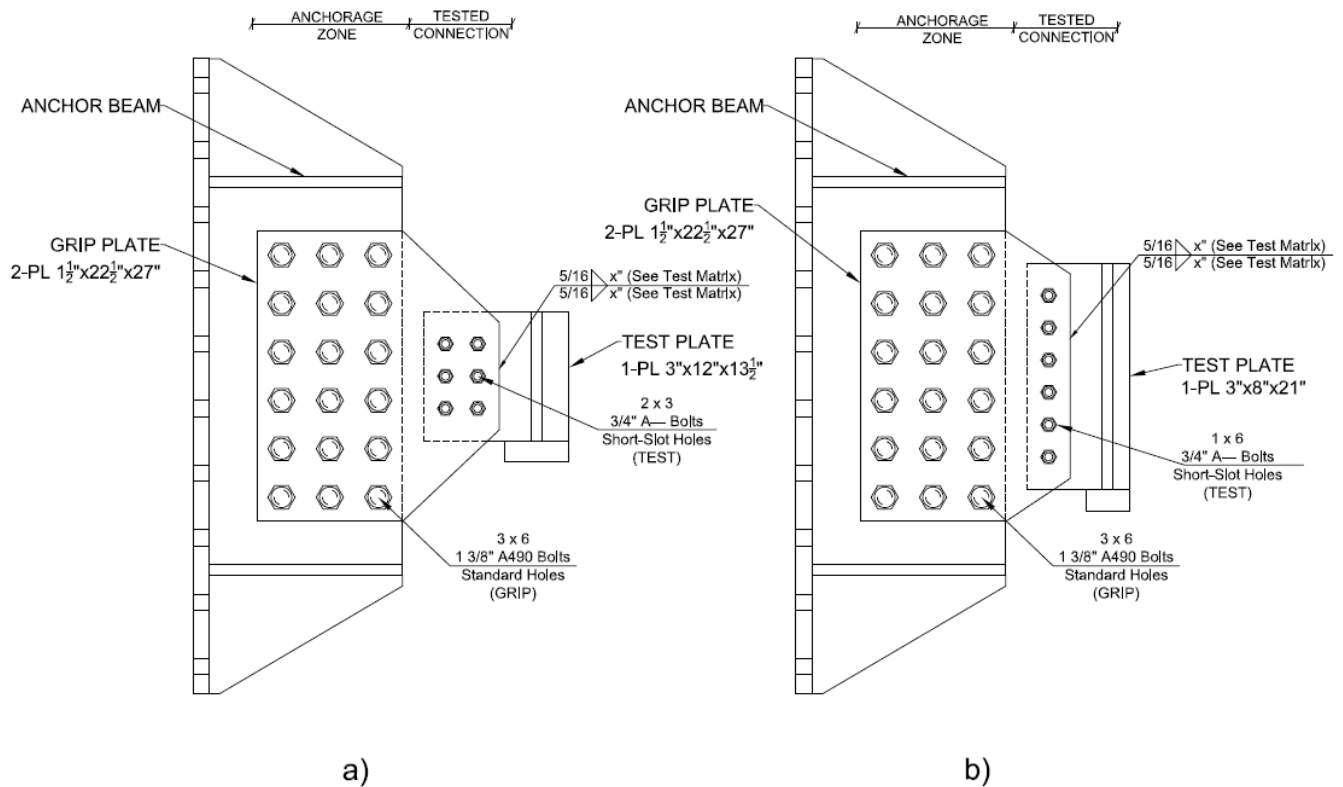
Figure 5.2: Specimen Configuration; a) 2×3 Connection Configuration, b) 1×6 Connection Configuration

The tested connection is assembled per the test matrix for each test sample. There are two fillet welds oriented longitudinally compared to the direction of the load applied at an eccentricity of 3-in (from welds) for all test specimens. The bolted connection utilized, horizontal short-slot holes for 3/4-in diameter bolts to allow studying the rotational displacement. The bolt eccentricity of the 2×3 connection is 6.5-in. and 5.0-in. for the 1×6 connection. The 3×6 bolted connection between the grip plates and the anchor beam was designed to be a bearing-type connection. The anchor beam is affixed to the test frame with a fully restrained moment

79

connection designed to resist 2,400 kip-ft of applied moment. This moment corresponds to a maximum applied actuator load of 800 kips.

5.2   TEST FRAME AND SETUP

The test frame and setup were developed specifically for testing the eccentric connections. Efforts were completed in-house at the BCEL to design and assemble the test frame, hydraulic testing system, and data acquisition setup to ensure that the specific needs of this testing were addressed. Figure 5.3 shows the 3-D view of the assembled test frame with a specimen and the hydraulic actuator.
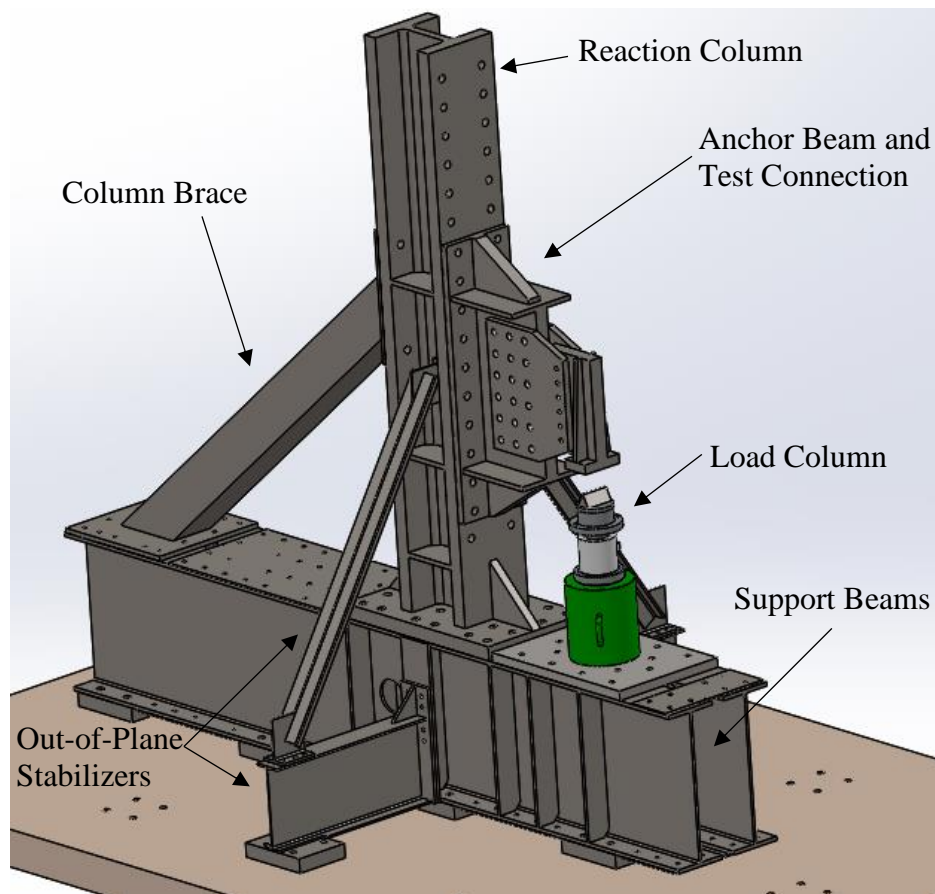
Figure 5.3: Eccentric Frame 3-D Model

The test frame consists of the following five main components: the anchor beam, reaction column, support beams, column brace, and out-of-plane stabilizers. In total, the frame is designed to withstand 800-kip load applied by the actuator. The reaction column is a single W14×455 section connected to the support beams via a fully restrained moment connection. The column flange is drilled along its length to allow the anchor beam to be moved vertically to accommodate the different heights of the 2×3 and 1×6 specimens. The column brace is an HSS 10×10×3/8 section used to distribute the applied load from the column and reduce overall section

sizes of the frame. Two W33×130 sections make up the base of the frame and provide sufficient stiffness to resist deformations experienced during testing. The out-of-plane stabilizing system consists of transverse W18×35 sections and double angle 2Ls 4×3×3/8 on both sides of the column. Figure 5.4 shows a photograph of the test setup with the specimen connected.

Figure 5.4: Eccentric Frame with 1×6 Test Specimen

The hydraulic system uses the same type of actuator employed in the concentric testing, a 565-ton Simplex hydraulic cylinder. A 10,000 psi Enerpac pump along with a manual valve was used to apply the load. An HBM C6A/5MN (1,125 kips) load cell was used to record the load acting on the specimen during the test. The load cell consists of a load button and a thrust head that improves the accuracy of registered load reading. Furthermore, a cast iron wedge is used to apply the concentrated force. Figure 5.5 shows the load application setup.

Figure 5.5: Load column: actuator, load cell, and load application wedge

The instrumentation system used to record test data for the eccentric testing is similar to the setup used in the concentric testing with an updated version of the software LabVIEW NXG 3.0 (NI, 2018). The National Instruments equipment was used for this phase of testing including the cDAQ and input cards. Recorded test data include applied load, specimen rotation and vertical translation collected at a frequency of 5.0 Hz. Rotation and vertical translation of the connection were captured by four high accuracy AC-LVDTs with a stroke of 0.2 in. Two LVDTs were used for measuring the rotation by computing the difference in horizontal displacement of two pre-identified points on the specimen, and two other LVDTs recorded the vertical displacement. The LVDTs recorded the relative displacement between the test plate and the grip plates to isolate the connection displacement from global movement of the whole test frame. Figure 5.6 shows a picture of the experimental setup with the LVDTs installed.
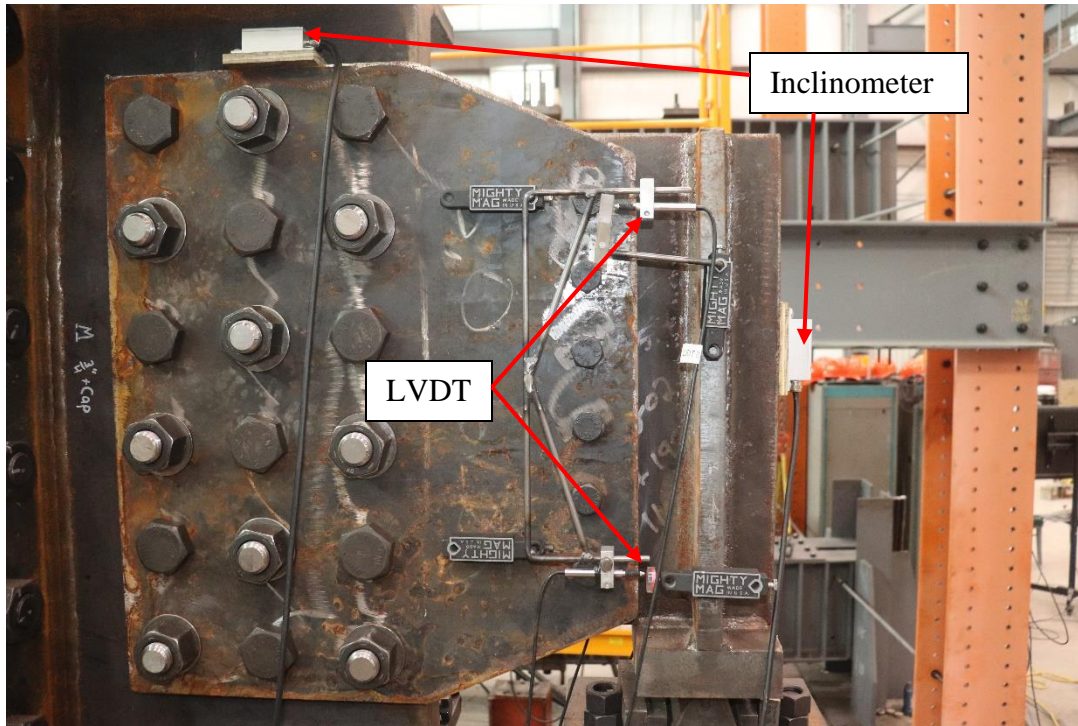
Figure 5.6: 1×6 Specimen with Instrumentation Installed

As indicated above, rotational displacement was captured by orienting two LVDTs horizontally in opposite directions to capture the horizontal displacement of the test plate relative to the grip plates. This displacement was used to calculate the rotation for every test. The values of this rotation were corroborated by two inclinometers, one on the test plate and one on the grip plate. Rotation experienced by the tested connection is computed as the difference between the readings of the two inclinometers. The reported rotation represents data obtained by the rotational LVDTs. The AC-LVDTs have an accuracy of 0.0001-in. and thus are highly accurate in calculating the rotational increments during testing. The inclinometers had an accuracy of 0.1˚ (0.002 radian) and their signal was noisy compared to LVDT signal. Nevertheless, after filtering, rotations measured by the inclinometers were in-line with those recorded by LVDTs. Vertical displacements were computed as the average reading of the two vertical LVDTs. However, since the load-rotation is the governing parameter for determining the behavior of eccentric connections, vertical translation data recorded during testing will not be included in this report.

5.3   ECCENTRIC CONNECTIONS TESTING PROCEDURE

The testing procedure for this phase is as follows:

1. Clean the faying surface of the connection area of the test and grip plates depending on the type of faying surface: degreaser for Class A and compressed air for Class B.
2. Lift both grip plates and install on testing frame using overhead crane. Rotate grip plates counterclockwise until the 3×6 grip bolts go into a bearing state. Tighten two bolts to

83

ensure they stay in place. This process reduces the global rotation of the grip zone during testing.

3. Using the overhead crane, lift the test plate into place. Move the test plate into a position that allows for maximum rotation before achieving a bearing state in the tested connection (i.e., 2×3 or 1×6 bolts). Snug tight test connection bolt group and 3×6 bolt group in the anchorage zone.

4. Complete three Skidmore tests for three bolts of the same grade used in the test. Record each bolt pretension value for the tests. Pretension the test bolts immediately after concluding the Skidmore tests according to RCSC specification (i.e., Table J3.1 AISC (2016)).

5. Complete the weld according to the test matrix. Wait 30 minutes for the weld to cool down and take as-built measurements of the weld.

6. Attach instrumentation and cameras according to the instrumentation plan.

7. Run the test.

6 TESTING RESULTS: ECCENTRICALLY LOADED CONNECTIONS

A total of 36 individual connections were tested in the eccentric configuration to assess the capacity of bolted-welded connections made of slip-critical bolts and fillet welds. Specimens were tested up to a rotation level of 0.03 radians and a load-rotation profile was generated for each connection.

6.1 CONNECTION CAPACITY CRITERIA

The nominal capacity calculation for eccentric connections will use the AISC strength equations in a manner similar to that adopted for the concentric connections. The capacity here will be noted as Table R_n. The Table R_n is related to the nominal strength of the bolted and/or welded connection under eccentric loading. This capacity corresponds to the strength a design engineer would calculate using the eccentric design tables in the AISC Steel Construction Manual (AISC 2017). The bolted connections were designed by using Tables 7-6 & 7-7 (AISC 2017) and the welded connections were designed by using Table 8-4 (AISC 2017). Capacities of the connections are determined by geometry of the bolt group and the applied load. The capacity of the bolted connections is determined as

$$R_n = C * r_n \qquad\qquad \text{Eq. 27}$$

where r_n is the strength of one bolt, C is a geometry coefficient, and R_n is the nominal connection strength. The strength of one bolt fastener is calculated by Eq. 16 discussed above. The nominal capacity of welded connections is calculated as

$$R_n = C * C_1 * D * l \qquad\qquad \text{Eq. 28}$$

in which C is the geometry coefficient, C_1 is the weld electrode coefficient, D is fillet weld size in sixteenths-of-an-inch, and l is the weld length. This report lists the capacity of the combination connection (i.e., Table R_n) computed as the sum of the nominal capacities of the bolts and welds.

6.2 DETERMINATION OF CONNECTION CAPACITY FROM TEST DATA

The rotational behavior is a key aspect that should be considered for connections under eccentric loading. The AISC (2017) discusses the criteria for identifying the maximum strength M_n and ultimate rotation θ_u of connections. Figure 6.1 shows a typical moment-rotation profile of a partially restrained connection. In summary, the maximum strength M_n is defined as the maximum moment that the connection can carry. If the moment-rotation behavior does not exhibit a peak, the strength of the connection can be taken as the moment at a rotation of 0.02 radians (AISC 2017, Hsieh and Deierlein 1991, and Leon et al. 1996). The maximum rotation θ_u that can be considered within the design of a moment resisting connection is defined by AISC (2017) as the rotation when the applied moment drops to a value equal to 0.8 M_n but not higher than 0.03 radians. Accordingly, in this report, the connection capacity is defined as the highest

load achieved at rotations equal or less than 0.02 radians. All tests conducted under the eccentric testing program of this research exceeded this limit of 0.02 radians and several connections exceeded a rotation of 0.03 radians.
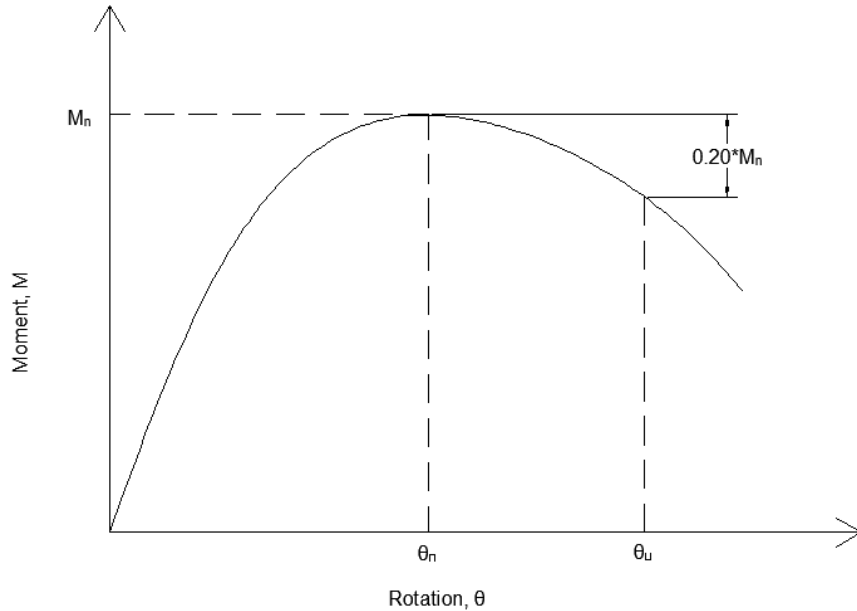
Figure 6.1: Typical moment-rotation profile of partially restrained connection (AISC 2017)

6.3   BOLTED-ONLY TESTS

Three tests of the 2×3 configuration and one test with the 1×6 configuration were conducted on bolted-only samples. These tests assess the effect of bolt grade, faying surface class, and bolt configuration on the load-rotation behavior of the connection. Table 6.1 shows the test parameters for the bolted-only specimens.

Table 6.1: Bolted-only connection characteristics

	Test No.	Bolt Pattern	Bolt Type	Bolt Pretensioning Method	Faying Surface Class	Weld Geometry	$R_{n\_W}/$ R_{n_B}	No. of Samples
Bolted-Only	31	2×3	A325	ToN	A	-	-	2
	33	2×3	A490	ToN	A	-	-	2
	34	2×3	A325	ToN	B	-	-	2
	49	1×6	A325	ToN	A	-	-	3
NOTE: All bolts are 3/4-in diameter (short- slotted holes) unless otherwise specified								
ToN = Turn of Nut Method								
R_{n_W} = nominal capacity of welds; R_{n_B} = nominal capacity of slip-critical bolts								

6.3.1 2×3 Class A Connections

The connections discussed in this section have a Class A faying surface with a 2×3 bolt pattern and an eccentricity of 6.5-in measured from the line of action of the applied load to the centroid of the bolt group. These connections include Tests 31 and 33 with two samples in each test covering A325 and A490 bolt grades, respectively. All tests were assembled and instrumented according to the testing procedure discussed in Section 5.3. All specimens were tested to identify the nominal strength up to a rotation of at least 0.02 radians. Figure 6.2 and Figure 6.3 show the load-rotation behavior of Tests 31 and 33, respectively. All connections exhibit high stiffness at low rotation and then begin to soften considerably at rotations between 0.0005-0.002 radians. After softening, the capacity continues to increase until the test is ended. Note that these tests were stopped before the bolts in the test connection would reach the bearing condition. Test 31B was stopped at a rotation 0.026 radians due to the LVDTs measuring rotational movement reaching the limit of their stroke. Table 6.2 shows the reported test capacity, Test R_n, and the Table R_n, of each sample in Tests 31 and 33. The Test R_n of each test corresponds to the highest load achieved before a rotation of 0.02 radians. The table also shows the factor of safety of each connection calculated as Test R_n / Table R_n. As seen in Table 6.2, all 2×3 Class A bolted-only connections provide a capacity (i.e., Test R_n) that is at least 49% higher than the nominal AISC capacity (i.e., Table R_n).

Table 6.2: 2×3 Bolted-only- Class A Faying Surface

	Specimen	Table R_n (kips)	Test R_n (kips)	Test R_n/ Table R_n
Test 31	A	40.3	104.3	2.59
	B	40.2	76.3	1.90
Test 33	A	50.3	74.9	1.49
	B	50.3	87.2	1.73
NOTE: Test R_n is the maximum load applied at $\theta \leq 0.02$ radian AVG = Average value; SD = Standard Deviation; CV = Coefficient of variation				**AVG = 1.887** **SD = 0.473** **CV = 25.07%**
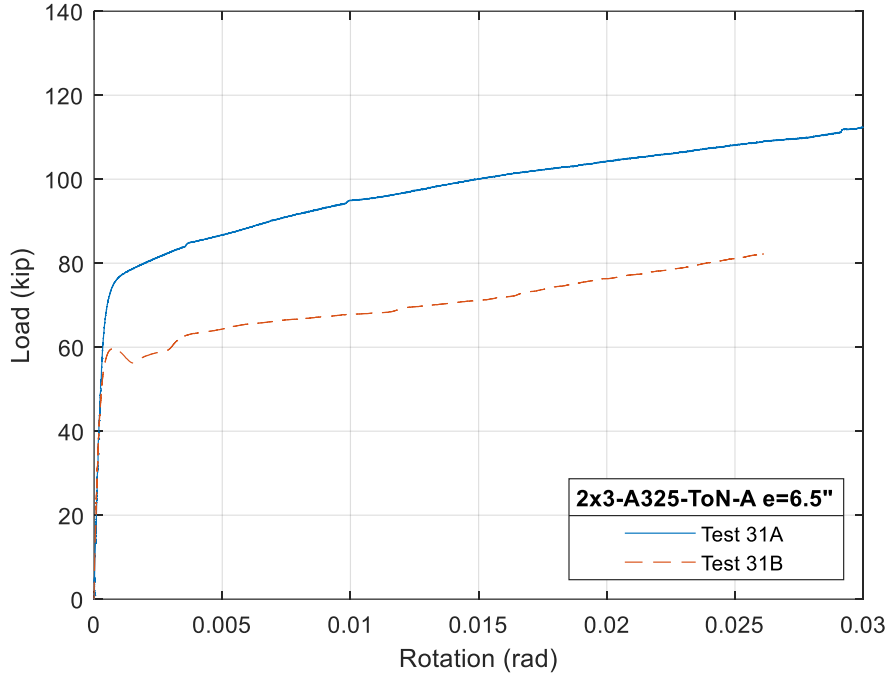
Figure 6.2: Load-rotation curves of Test 31
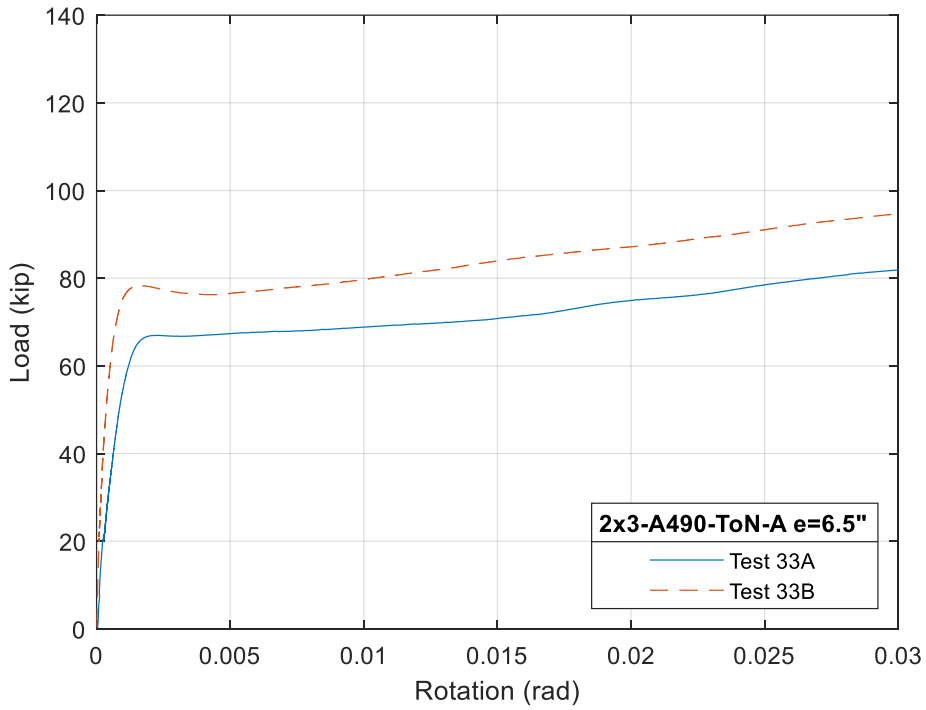
Figure 6.3: Load-rotation curves of Test 33

6.3.2 2×3 Class B Connections

The connections shown in this section have Class B faying surface with a 2×3 bolt pattern and an eccentricity of 6.5-in measured from the line of action of the applied load to the center of the bolt group. These connections include Test 34 with two samples. All tests were constructed according to the testing procedure discussed above. Figure 6.4 shows the load-rotation behavior of the tests. All connections exhibit high stiffness at low rotation and then begin to soften at rotations around 0.0005 radians. After softening begins, the capacity stays moderately constant across large rotational deformations. This behavior differs from that of concentrically loaded bolted-only Class B connection which experienced a sudden slip event after reaching the ultimate force. This is believed to be due to the unidirectional translation of the concentric connection that flattens all the faying surface peaks simultaneously as it displaces. Whereas the eccentric connections continually rotate giving a chance for the damaged areas of the faying surface to interlock and maintain capacity at higher levels of deformation. Table 6.3 displays the Test R_n, Table R_n, and the factor of safety for each sample. For samples in Test 34, the tested capacities exceed that of the nominal capacity by at least 65%.

Table 6.3: 2×3 Bolted-only- Class B Faying Surface

	Specimen	Table R_n (kips)	Test R_n (kips)	Test R_n/ Table Rn
Test 34	A	67.1	133.2	1.99
	B	67.1	110.7	1.65
NOTE: Test R_n is the maximum load applied at $\theta \leq 0.02$ radian AVG = Average value; SD = Standard Deviation; CV = Coefficient of variation				AVG = 1.818 SD = 0.237 CV = 13.05%

6.3.3 1×6 Class A Connections

The connections discussed in this section have a Class A faying surface with a 1×6 bolt pattern and an eccentricity of 5.0-in measured from the line of action of the applied load to the center of the bolt group. These connections include only Test 49 with three samples tested in this series. This specimen was assembled according to the testing procedure and was tested past a rotation of 0.02 radians. Figure 6.5 shows the load-rotation curve of the sample. During Test 49A, at approximately 115 kips, the grip plates slipped and moved suddenly causing a drop in the connection force. At the same time during the test, it is believed that some bolts went into bearing conditions leading to a continual increase in load which led to a significantly different behavior compared to the other two tests. The jumps in all tests represent sudden slip events experienced by specimens. The LVDTs measuring rotation provided rotational readings consistent with the inclinometers after each slip events. Given the different behavior of Test 49A due to the bearing state reached, the results of this specimen will not be used for capacity prediction. Table 6.4 presents the Test R_n, Table R_n, and the factor of safety for this test series.
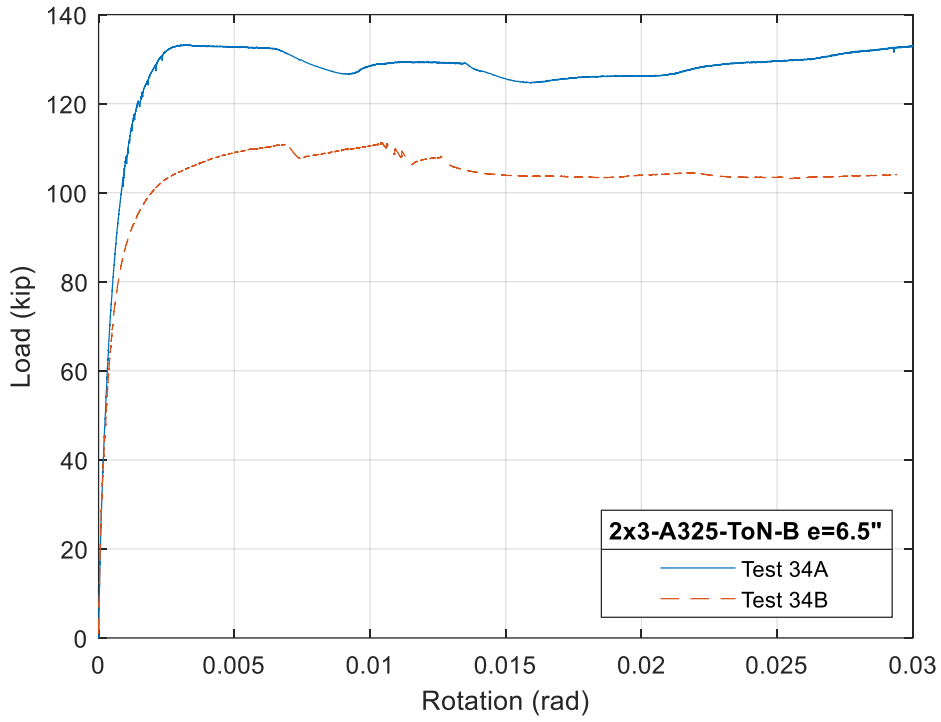
Figure 6.4: Load-rotation curves of Test 34
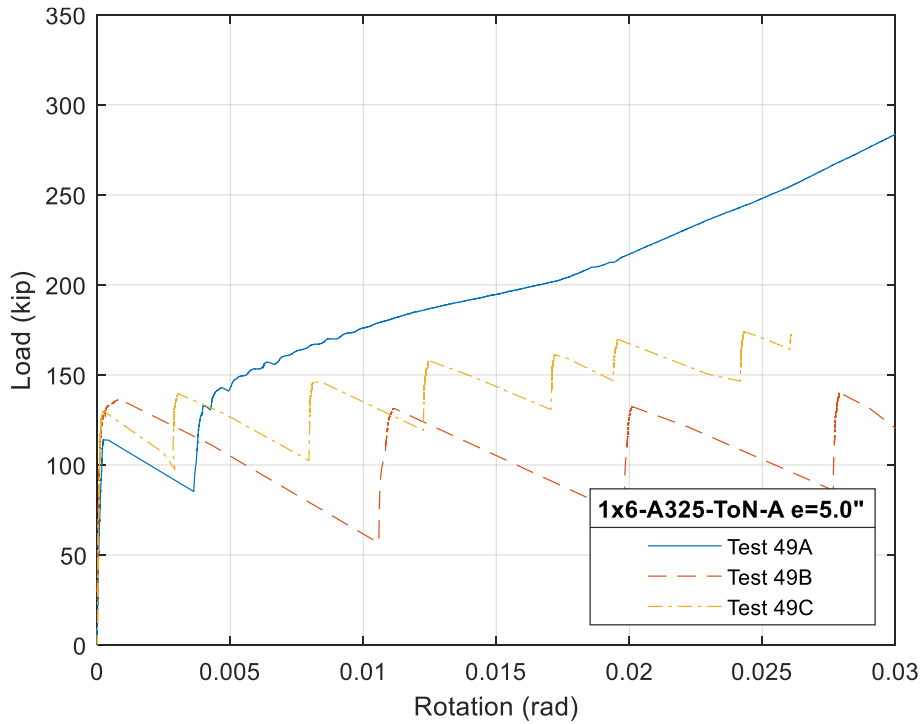
Figure 6.5: Load-rotations curves of Test 49

Table 6.4: 1×6 Bolted-only- Class A Faying Surface

	Specimen	Table R_n (kips)	Test R_n (kips)	Test R_n/ Table Rn
	A*	75.56	217.1	2.87
Test 49	B	75.56	136.2	1.80
	C	75.56	169.8	2.25
NOTE: The Test R_n is the load at rotational of 0.02 radians AVG = Average value; SD = Standard Deviation; CV = Coefficient of variation *- Not included in statistical analysis				**AVG = 2.013** **SD = 0.314** **CV = 15.61%**

6.4   WELDED-ONLY TESTS

Welded-only tests were conducted to quantify the load-deformation behavior of these connections and serve as a baseline to assist in understanding the behavior of combination connections. All the welds on the eccentric connections were completed using the same lot of welding rods used for the concentric connections and completed by the lab manager in the BCEL. The welded-only tests include Test 36 (three samples) and Test 50 (two samples) which provided enough data to characterize the load-deformation behavior of welded connections. Table 6.5 shows the characteristics of the welded-only tests.

Table 6.5: Welded-only specimen characteristics

	Test No.	Bolt Pattern	Bolt Type	Bolt Pretensioning Method	Faying Surface Class	Weld Geometry (Size × length)	R_{n_W}/ R_{n_B}	No. of Samples
Welded-Only	36	-	-	-	-	5/16 × 4.5	-	3
	50	-	-	-	-	5/16 × 9.75	-	2
Two fillet welds per connection with the noted geometry; Units are inches R_{n_W} = Shear capacity of welds; R_{n_B} = Slip capacity of bolts								

Figure 6.6 and Figure 6.7 shows the load-rotation profile of the welded-only connections. As it can be seen in the figure, there is a high variability in the weld performance. The tests in Figure 6.6 were stopped when the rotational LVDTs reached the end of their stroke. At this rotation level, the welds experienced partial fractures that were visible in the tension zone of the weld line. During Test 50A, a fracture propagated suddenly through both weld lines at a rotation of 0.0165 radians. Test 50B also lost its capacity rapidly; however, this test had a more controlled decrease in the load. This likely occurred since one weld fractured before the other. Table 6.6 presents the Test R_n, Table R_n, and the factor of safety. It seems that the AISC model is highly conservative in quantifying the capacity of these eccentric connections.
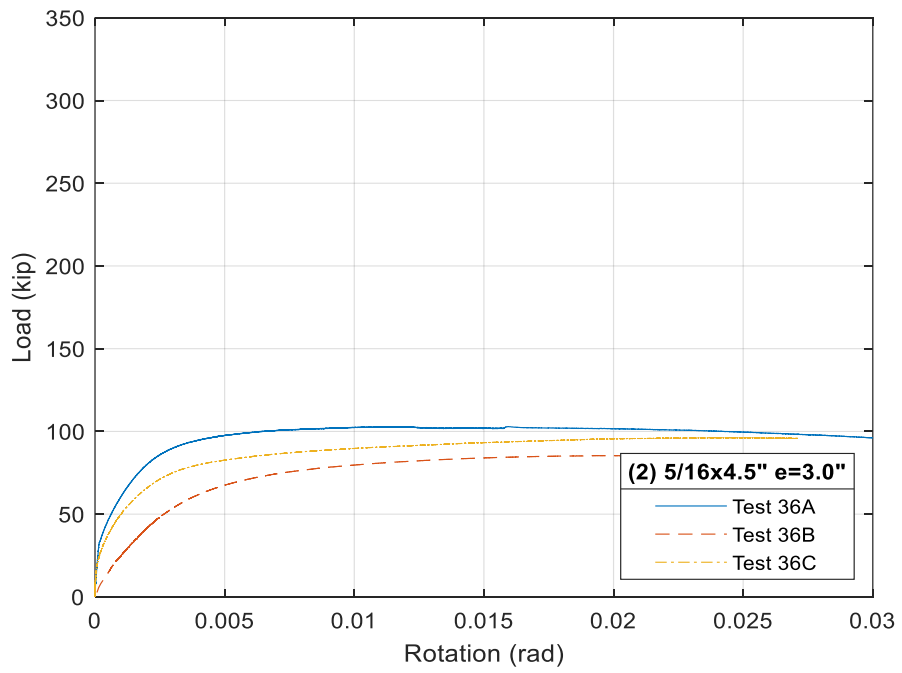
Figure 6.6: Load-rotation curves of Test 36
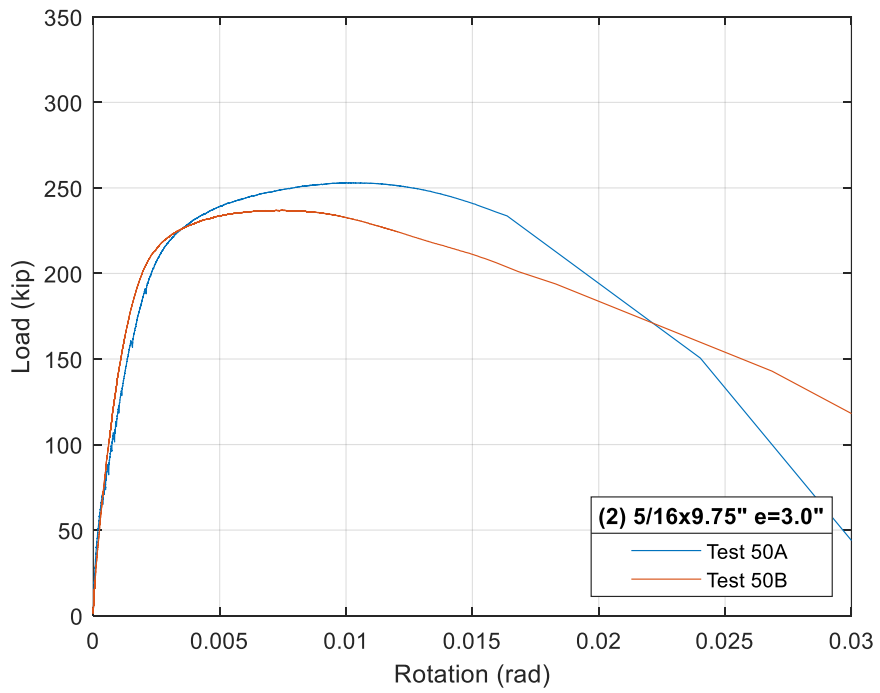
Figure 6.7: Load-rotation curves of Test 50

92

Table 6.6: Welded-only results

Test No.	Specimen	Table R_n (kips)	Test R_n (kips)	Test R_n/ Table Rn
Test 36 (5/16-in × 4.5-in)	A	41.4	103.0	2.49
	B	41.4	85.4	2.06
	C	41.1	95.6	2.33
Test 50 (5/16-in × 9.75-in)	A	149.0	253.1	1.70
	B	149.0	237.0	1.59
NOTE: Test R_n is the maximum load applied at $\theta \leq 0.02$ radian AVG = Average value; SD = Standard Deviation; CV = Coefficient of variation				AVG =2.033 SD = 0.388 CV = 19.08%

6.5   COMBINATION TESTS

This section discusses all combination connections completed within the test matrix. The tests vary bolt grad (i.e., A325 or A490), faying surface condition (Class A or B), bolt configuration, and weld/bolt strength ratios. The test matrix in Table 5.1 shows the characteristics of all the combination tests.

6.5.1   2×3 Class A Connections

A total of ten 2×3 Class A specimens were tested. These tests include Tests 37, 38, 39, 40, and Test 42. All specimens use 3/4-in diameter bolts with a bolt eccentricity of 6.5-in, have a faying surface of Class A, and Turn-of-Nut method for pretensioning. Weld eccentricity for all tests is 3-in. Test 42 investigates the difference that the bolt grade can induce in combination connections by utilizing A490 bolts. Tests 37-40 show the influence of weld/bolt strength ratio on the performance of the combination connections by varying weld length from 2.25-in to 6.5-in (i.e., weld/bolt strength ratio of 0.25 – 2.00). Table 6.7 shows the characteristics of these tests.

Table 6.7: Combination connection test characteristics – 2×3 Class A

	Test No.	Bolt Pattern	Bolt Type	Bolt Pretensioning Method	Faying Surface Class	Weld Geometry	R_{n_W}/ R_{n_B}	No. of Samples
Bolted & Welded	37	2×3	A325	ToN	A	5/16 × 2.25	0.25	2
	38	2×3	A325	ToN	A	5/16 × 4.5	1.0	2
	39	2×3	A325	ToN	A	5/16 × 5.5	1.5	2
	40	2×3	A325	ToN	A	5/16 × 6.5	2.0	2
	42	2×3	A490	ToN	A	5/16 × 4.5	0.82*	2
NOTE: All bolts are 3/4-in. diameter (short-slotted holes). ToN = Turn of Nut method; Two fillet welds per connection with the noted geometry. Units are inches. R_{n_W} = Shear capacity of welds; R_{n_B} = Slip capacity of bolts * Ratio adjusted for A490 bolts								

The load-rotation curves for each test series is shown in Figure 6.8 – Figure 6.13, while Table 6.8 lists the nominal strength Table R_n, the test capacity Test R_n, and the computed factor of safety for each test. Most of the tests achieved the maximum capacity before reaching the rotational limit of 0.02 radians. Data in Table 6.8 show that the combination connections with Class A surfaces provided a higher capacity (Test R_n) than the nominal capacity (Table R_n) computed as the sum of the nominal capacities of welds and bolts.

Table 6.8: Combination connection test results- 2×3 Class A

	Specimen	Table R_n (kips)	Test R_n (kips)	Test R_n/ Table R_n
Test 37	A	51.3	118.3	2.31
	B	51.3	126.1	2.46
Test 38	A	81.7	180.7	2.21
	B	81.7	162.3	1.99
Test 39	A	99.8	201.6	2.02
	B	99.8	182.7	1.83
Test 40	A	119.5	233.9	1.96
	B	119.5	227.7	1.91
Test 42	A	91.7	193.8	2.11
	B	91.7	177.1	1.93
NOTE: Test R_n is the maximum load applied at $\theta \leq 0.02$ radian AVG = Average value; SD = Standard Deviation; CV = Coefficient of variation				AVG = 2.064 SD = 0.199 CV = 9.64%
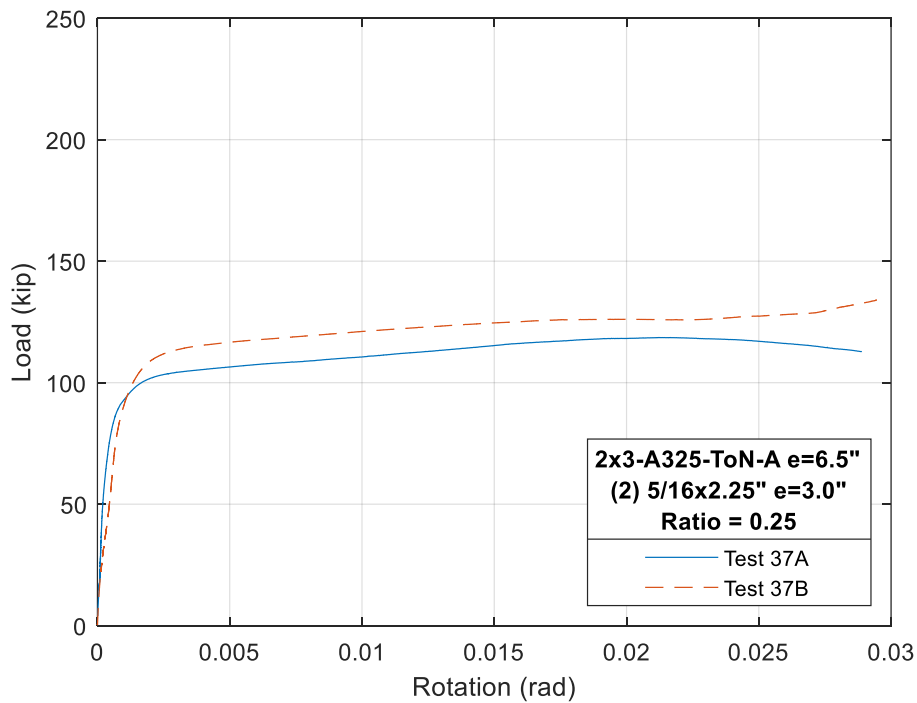
Figure 6.8: Load-rotation curves of Test 37
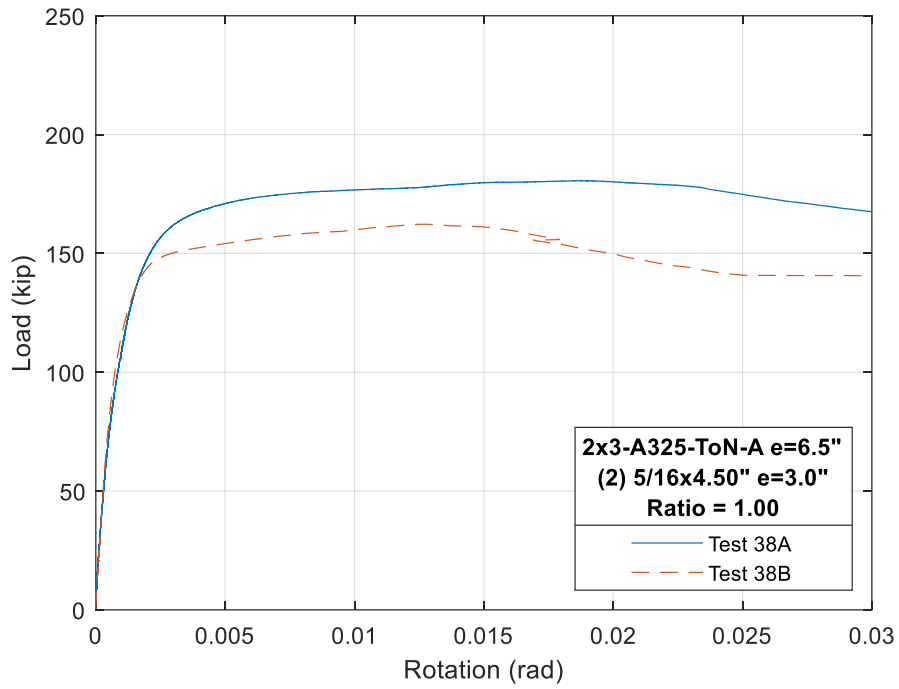
Figure 6.9: Load-rotation curves of Test 38
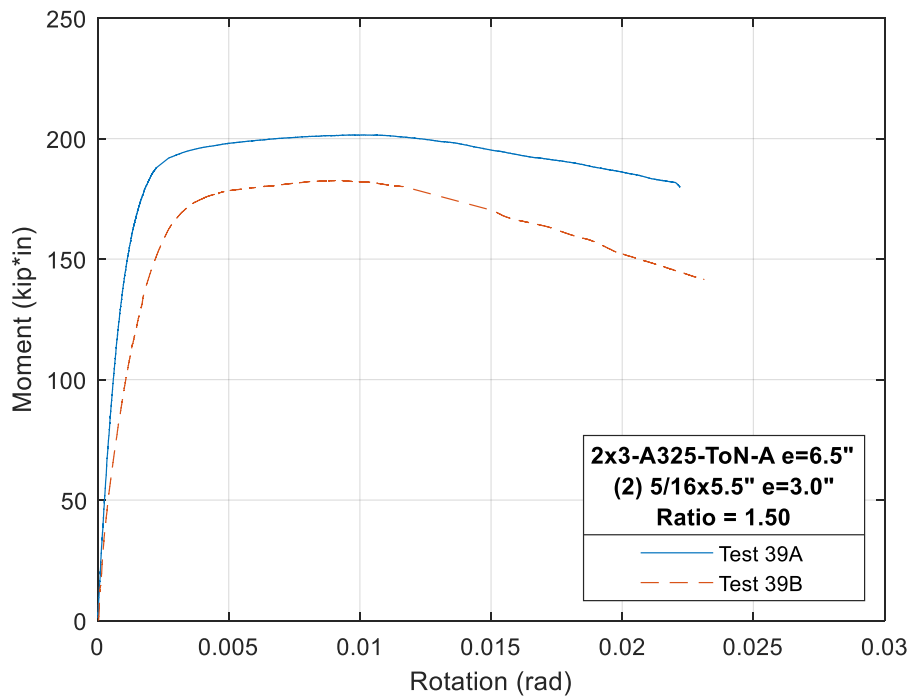
Figure 6.10: Load-rotation curves of Test 39
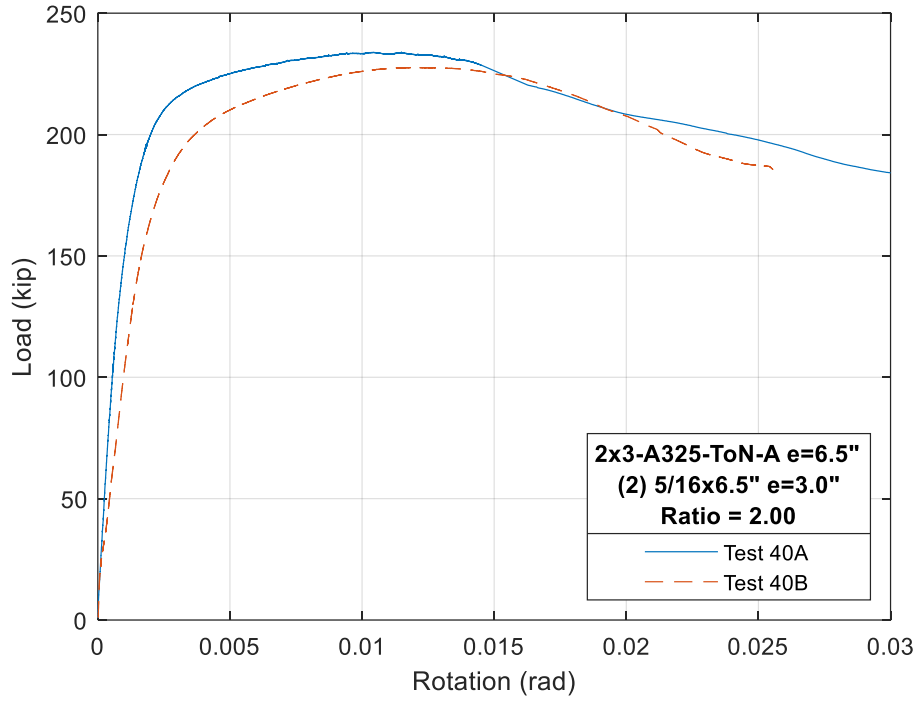
Figure 6.11: Load-rotation curves of Test 40
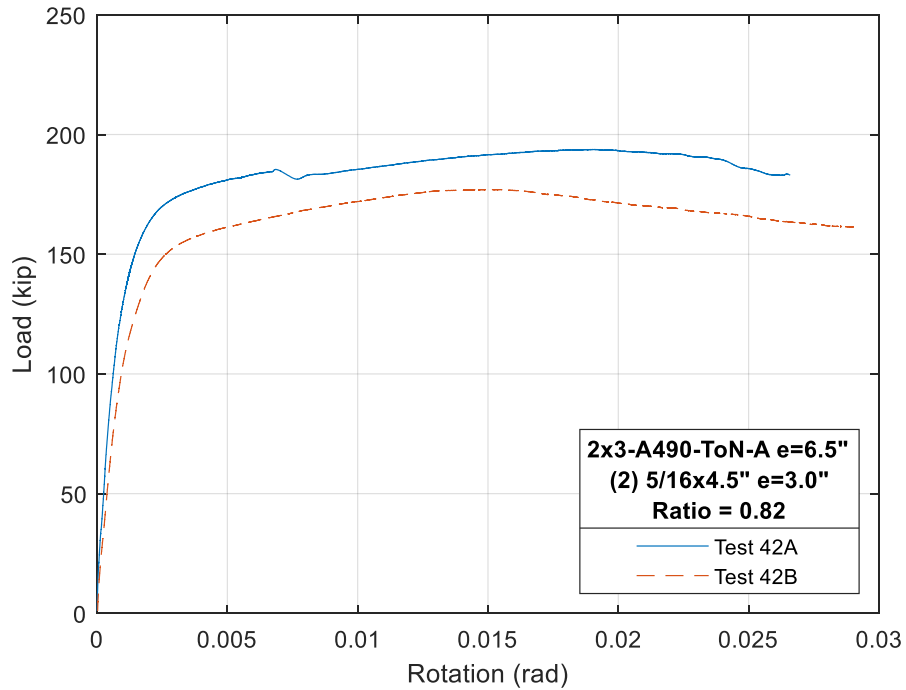
Figure 6.12: Load-rotation curves of Test 42

6.5.2 2×3 Class B Connections

Eight more 2×3 specimens were tested to evaluate the performance of combination connections with Class B faying surfaces. These include Tests 43 – 46 in which the specimen configuration followed the weld/bolt strength ratios used for Class A tests. These tests show the influence of (a) the faying surface condition and (b) weld/bolt strength ratio on the performance of the combination connections. Table 6.9 shows the test characteristics of these specimens.

Table 6.9: Combination connections Test characteristics- 2×3 Class B

	Test No.	Bolt Pattern	Bolt Type	Bolt Pretensioning Method	Faying Surface Class	Weld Geometry (Size × length)	R_{n_W}/ R_{n_B}	No. of Samples
Bolted & Welded	43	2×3	A325	ToN	B	5/16 × 2.75	0.25	2
	44	2×3	A325	ToN	B	5/16 × 6	1.0	2
	45	2×3	A325	ToN	B	5/16 × 7.5	1.5	2
	46	2×3	A325	ToN	B	5/16 × 9	2.0	2
NOTE: All bolts are 3/4-in. diameter (short-slotted holes). ToN = Turn of nut method; Two fillet welds per connection with the noted geometry. Units are inches. R_{n_W} = Shear capacity of welds; R_{n_B} = Slip capacity of bolts								

The load-rotation curves for each test series are shown in Figure 6.13 – Figure 6.16 while a comparison between the test capacity and AISC capacity is shown in Table 6.10. All tests reached a maximum rotation of approximately 0.03 radians. Tests 46 A & B would have ultimate design rotations θ_u of 0.0200 radians and 0.0235 radians, respectively, because the resisted load dropped more than 20% of the maximum load before reaching 0.03 radians, the maximum rotation allowed by the AISC (2017). Of all connections tested to 0.03 radians, Tests 46 A & B are the only ones that have an ultimate rotation less than 0.03 radians.

Table 6.10: Combination connection test results – 2×3 Class B

	Specimen	Table R_n (kips)	Test R_n (kips)	Test R_n/ Table R_n
Test 43	A	83.4	180.6	2.16
	B	83.4	143.9	1.73
Test 44	A	136.1	249.5	1.83
	B	136.1	248.8	1.83
Test 45	A	166.8	292.2	1.75
	B	166.8	279.8	1.68
Test 46	A	199.7	321.2	1.61
	B	199.7	355.3	1.78
NOTE: Test R_n is the maximum load applied at $\theta \leq 0.02$ radian AVG = Average value; SD = Standard Deviation; CV = Coefficient of variation				**AVG = 1.790** **SD = 0.170** **CV = 9.33%**
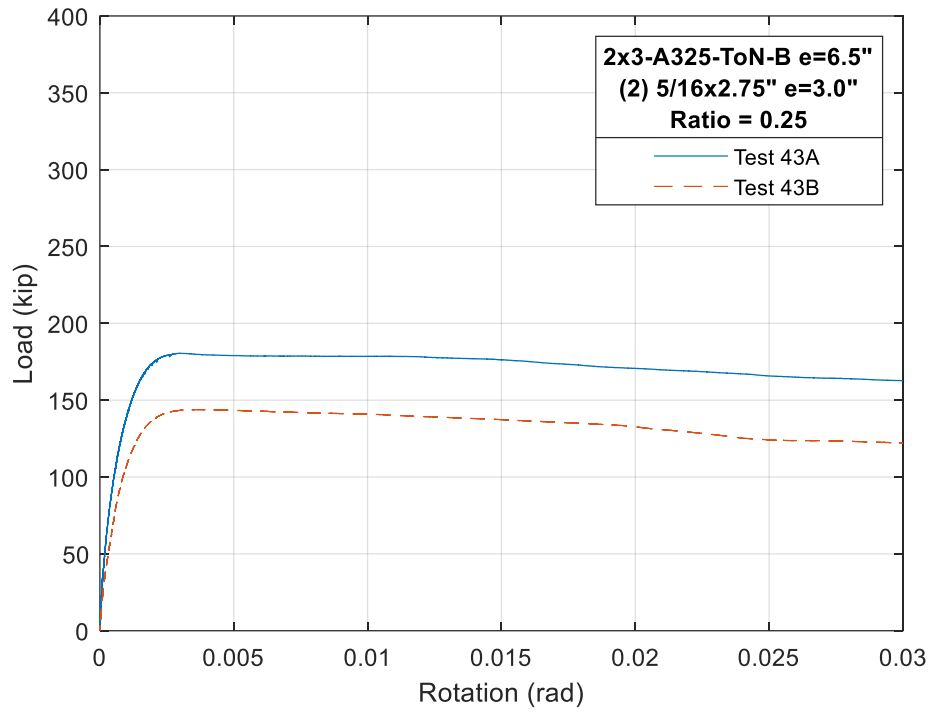
Figure 6.13: Load-rotation curves of Test 43
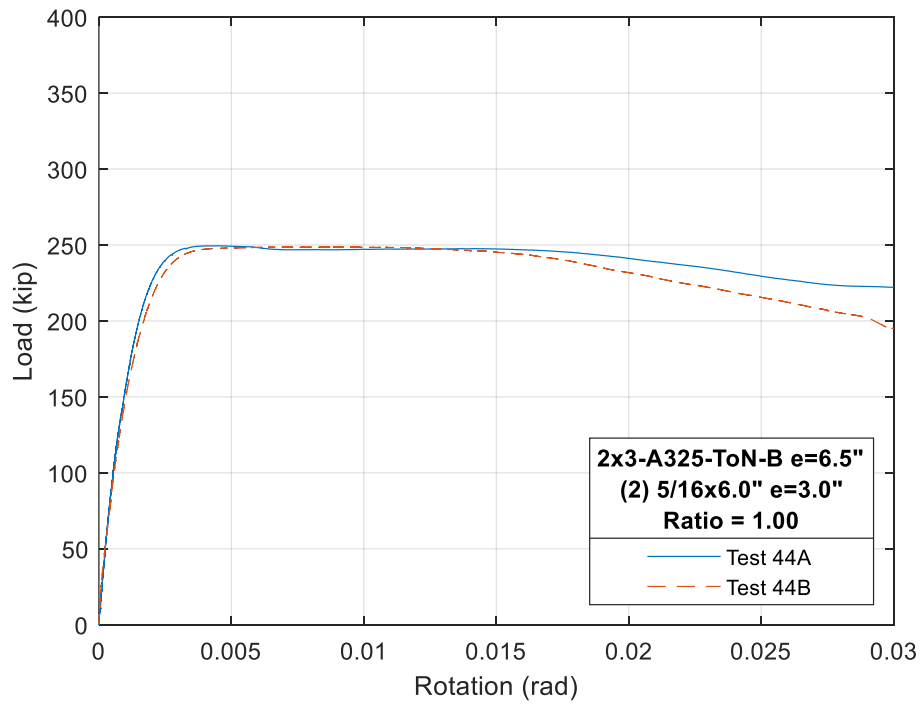
Figure 6.14: Load-rotation curves of Test 44
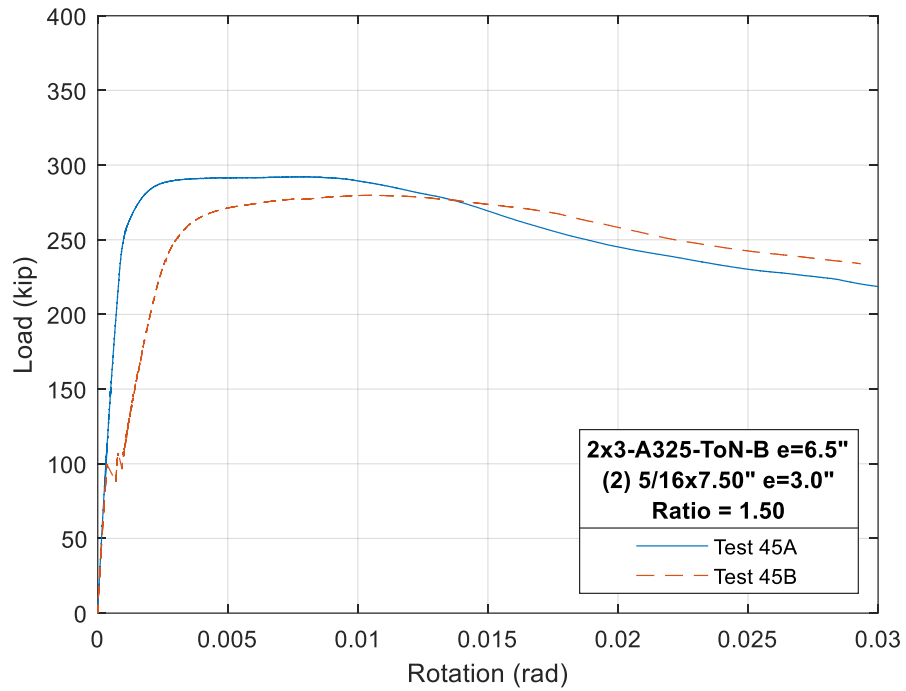
Figure 6.15: Load-rotation curves of Test 45
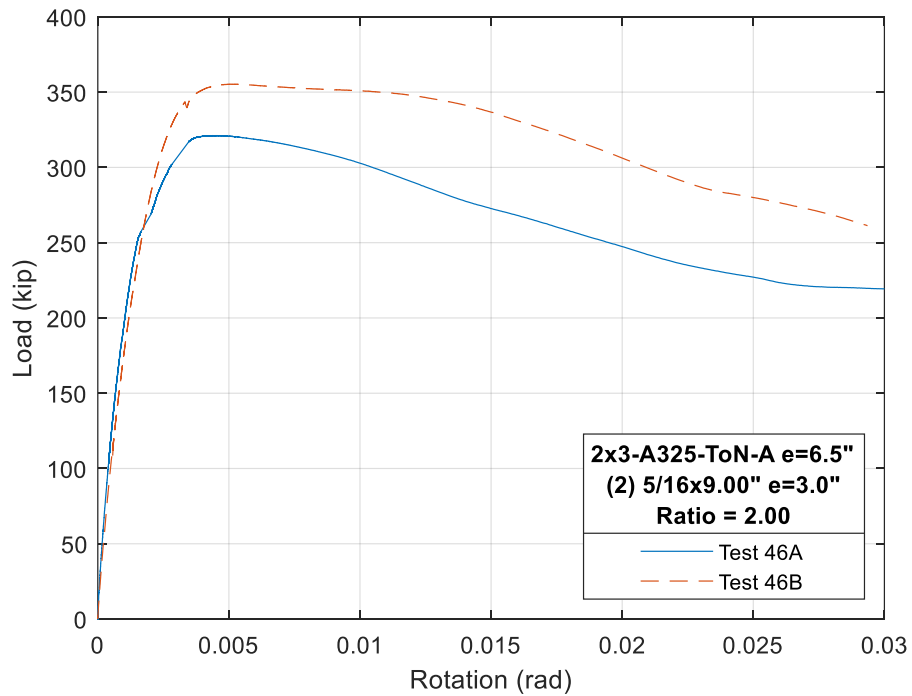
Figure 6.16: Load-rotation curves of Test 46

6.5.3 1×6 Class A Connections

Seven tests were conducted to understand the influence of the bolt configuration on the behavior of combination connections. Tests 51 – 54 each had one or two samples at varying bolt-to-weld strength ratios (0.25 – 2.00) all with Class A faying surface and A325 bolts. Table 6.11 shows the characteristics of each of those tests. All connections were assembled according to the test procedures. Load-rotation curves of these tests are shown in Figure 6.17 – Figure 6.20 and the tests capacities are reported in Table 6.12. All tests reached or exceeded a rotation of 0.02 radians. Data presented in Table 6.12 show that the combination connections test capacities exceed the AISC nominal capacity. The load-rotation profile for Test 54A in Figure 6.20 is constructed based on inclinometer data since the rotational LVDTs experienced a malfunction during the test.

Table 6.11: Combination connections test characteristics- 1×6 Class A

	Test No.	Bolt Pattern	Bolt Type	Bolt Tensioning Method	Faying Surface Class	Weld Geometry (Size × length)	R_{n_W}/R_{n_B}	No. of Samples
Bolted & Welded	51	1×6	A325	ToN	A	5/16 × 3	0.25	1
	52	1×6	A325	ToN	A	5/16 × 6.25	1.0	2
	53	1×6	A325	ToN	A	5/16 × 8	1.5	2
	54	1×6	A325	ToN	A	5/16 × 9.75	2.0	2
NOTE: All bolts are 3/4-in. diameter (short-slotted holes). ToN = Turn of Nut method; Two fillet welds per connection with the noted geometry. Units are inches. R_{n_W} = Shear capacity of welds; R_{n_B} = Slip capacity of bolts								

Table 6.12: Combination connection test results- 1×6 Class A

	Specimen	Table Rn (kips)	Test Rn (kips)	Test Rn/ Table Rn
Test 51	A	94.8	221.1	2.33
Test 52	A	149.7	256.3	1.71
	B	149.7	281.9	1.88
Test 53	A	186.3	310.6	1.67
	B	186.3	283.0	1.52
Test 54	A	224.6	348.4	1.55
	B	224.6	386.1	1.72
NOTE: Test R_n is the maximum load applied at $\theta \leq 0.02$ radian AVG = Average value; SD = Standard Deviation; CV = Coefficient of variation				**AVG = 1.753** **SD = 0.276** **CV = 15.74%**
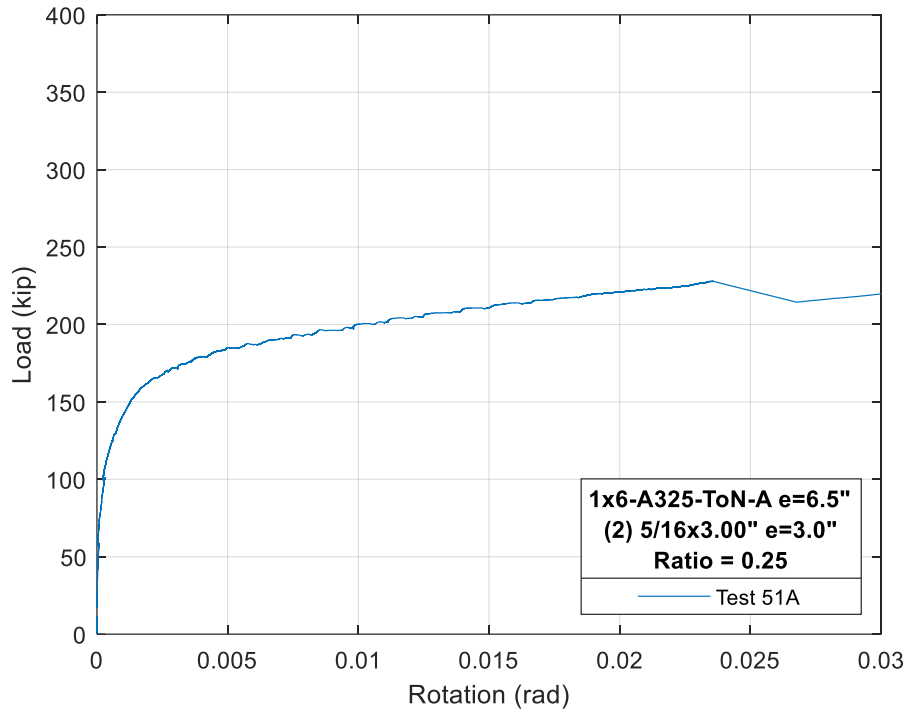
Figure 6.17: Load-rotation curves of Test 51
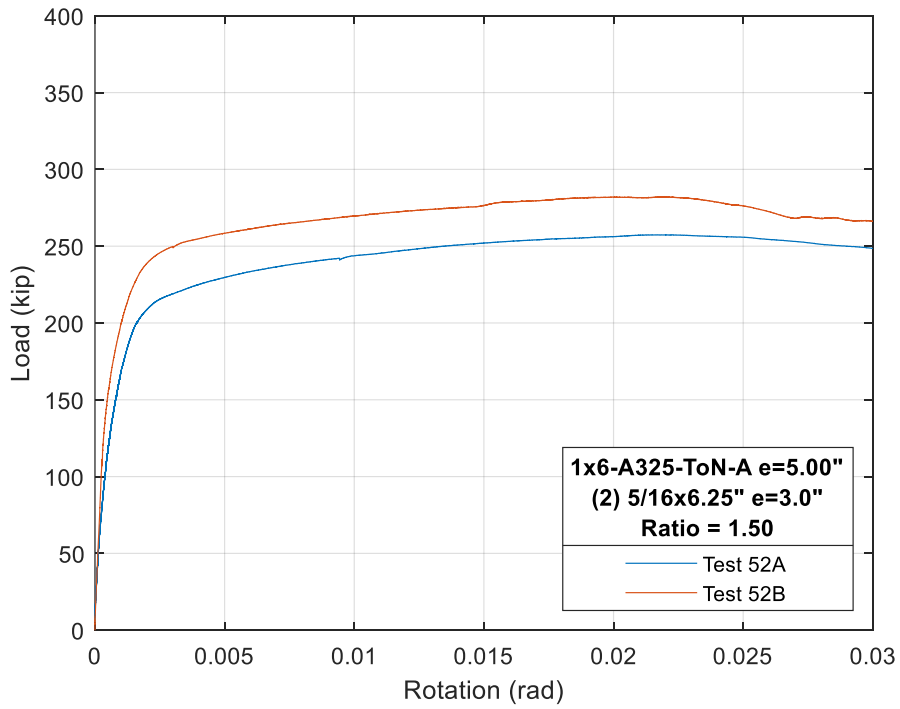
Figure 6.18: Load-rotation curves of Test 52

101
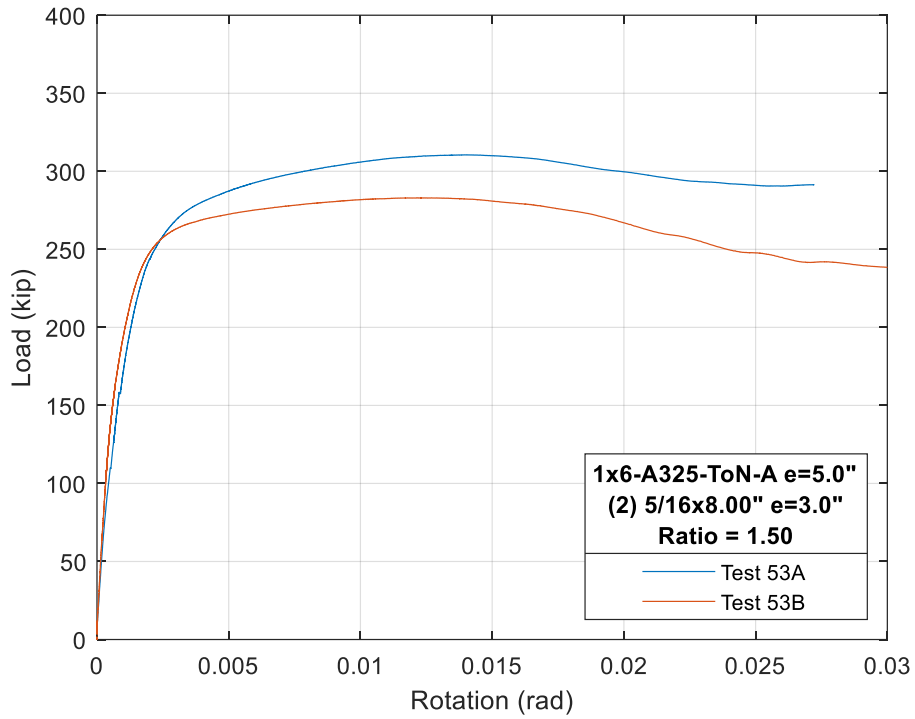
Figure 6.19: Load-rotation curves of Test 53
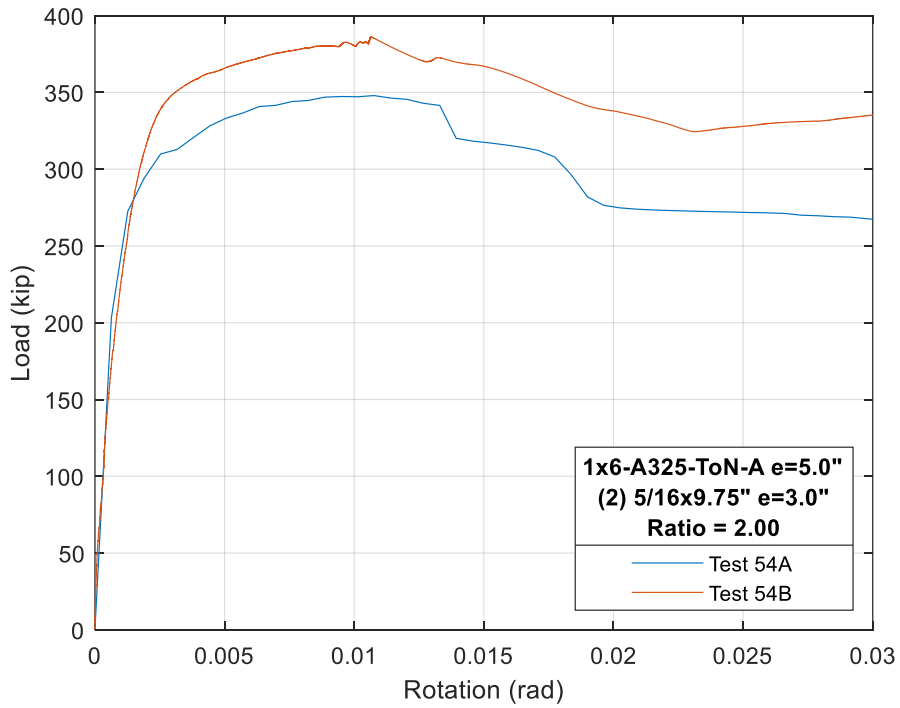
Figure 6.20: Load-rotation curves of Test 54

102

6.6 CAPACITY EVALUATION OF THE AISC MODEL

For each connection, the Table R_n is plotted against its matching Test R_n to demonstrate the safety factor of all eccentric connection tests included in this report. The Table R_n is calculated using respective design tables in the Steel Manual (Tables 7-6, 7-7, and 8-4) and nominal values for pretensioning force and weld electrode mechanical properties. Combination connection nominal strengths are obtained by summing the weld strength and the bolt strength. As seen in Figure 6.21, all connections exceeded the nominal Table R_n capacity with an average safety factor of 1.90.
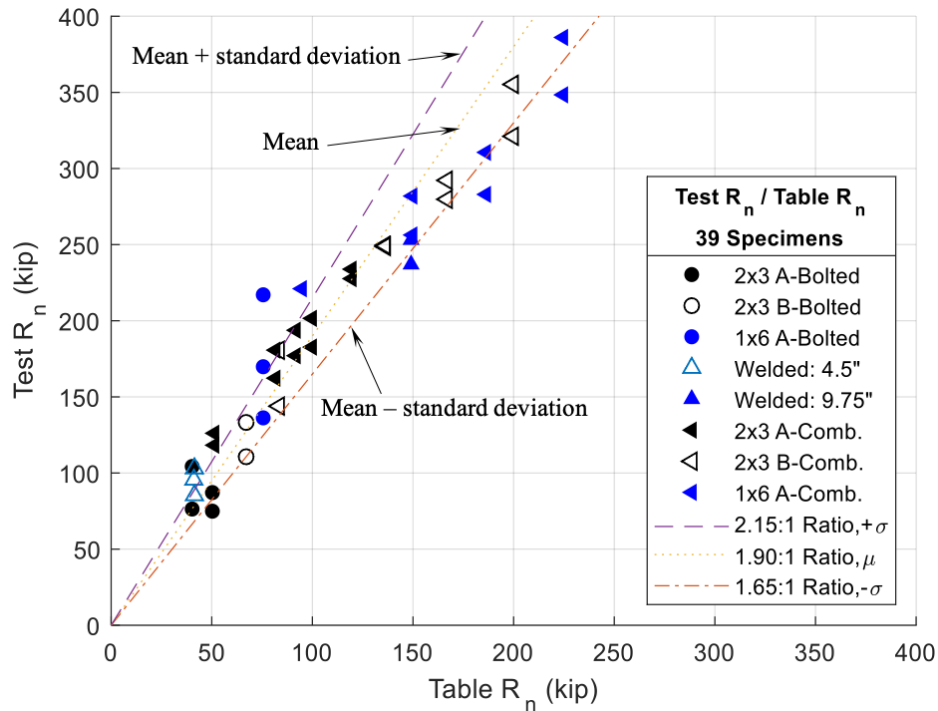
Figure 6.21: Factor of safety plot for eccentrically loaded connections based on AISC design tables

7 DISCUSSION: ECCENTRICALLY LOADED CONNECTION

This section provides an alternative capacity prediction model that (a) properly considers the load-deformation behavior of the welds and bolts within the eccentrically loaded connecting and (b) accounts for the realistic mechanical properties of welds and faying surface characteristics. This capacity prediction will rely on the instantaneous center of rotation (IC) method by employing both welds and bolts in a single load sharing system. The IC model will be used to predict the connection capacity and investigate the influence of key test variables.

7.1 BOLT PRETENSION

Similar to the concentric connections testing, Skidmore tests were conducted for all eccentric tests. Bolt load cells were not used in the eccentric tests since they were all damaged due to the repeated use during Phase I testing. All bolts had a diameter of ¾-in and were 7.5-in long with grades A325 and A490. All bolts achieved a significantly higher pretension force than the minimum values required by AISC (i.e., 28 kips for A325 and 35 kips for A490). The larger group of bolts was the A325 grade bolts and had 90 bolts tested in the Skidmore. The number of samples, mean, and standard deviation of each population is shown in Table 7.1. The mean value of the pretension force established based on the ToN method for these longer bolts (i.e., 43.8 kips) was very close to that quantified for the concentric tests (i.e., 42.73 kips). Figure 7.1 shows the pretension force histogram for the 3/4-in A325 bolts. The mean values of the pretension force shown in the table are used for the IC model prediction.

Table 7.1: Statistical descriptors of bolt pretension force

	3/4-in A325-ToN	3/4-in A490-ToN
# of Samples	90	12
Mean	43.8	47.6
Standard Deviation	1.37	2.21
Note: ToN- Turn of Nut		
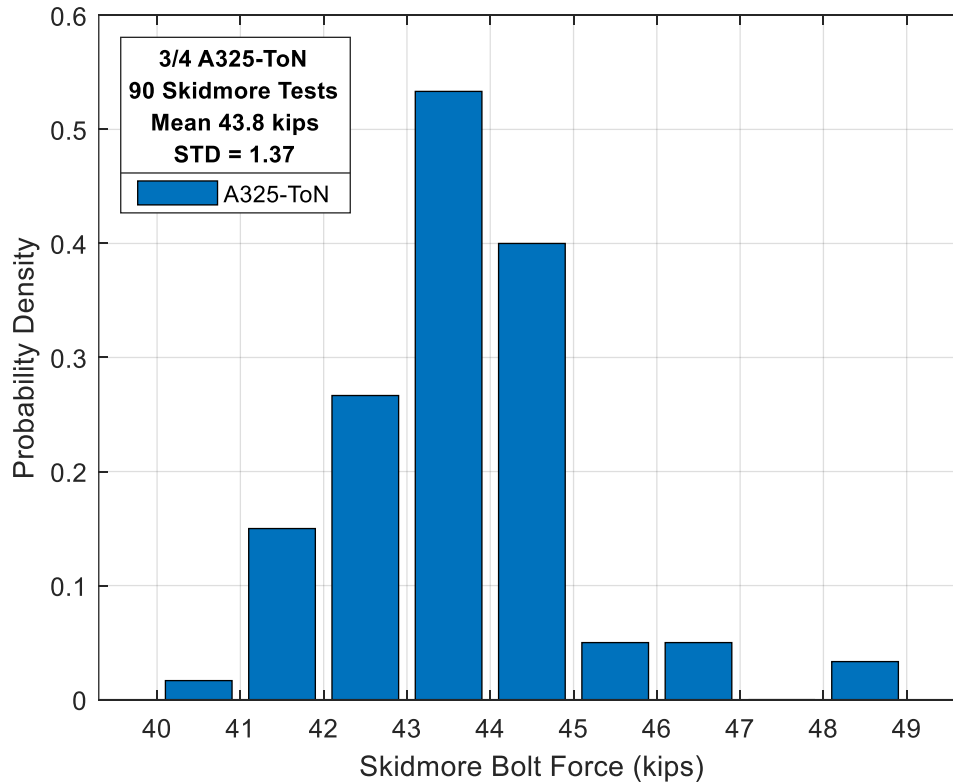
Figure 7.1: 3/4-in. bolts histogram of the pretension force measured using the Skidmore

7.2   CAPACITY PREDICTION: IC MODEL

The IC R_n represents the effort to predict the capacity of combination connections based on as-built dimensions and the measured material properties. This includes bolt pretension measured by Skidmore tests, slip coefficient from bolted-only tests, and weld shear strength measured from concentric welded-only testing.

In this section, the capacity of the connections is predicted based on the instantaneous center of rotation method considering the connecting elements (i.e., bolts and welds) to be participating in a single load sharing mechanism. The capacity of connecting elements is computed based on the load-deformation characteristics calculated using the geometric and mechanical properties measured within the testing program. The characteristics of each weld line were measured before the test to better predict the ultimate capacity. Computing the connection strength will utilize the individual fastener strength equations provided by AISC along with the necessary modifications to adopt the measured quantities.

The instantaneous center of rotation (IC) method is an equilibrium model that utilizes the load-deformation behavior of individual fasteners in a system. The method constructs the force vectors of all elements within the system that satisfy the global equilibrium as explained in Crawford and Kulak (1968). Once the load-deformation behavior is developed and geometry is selected, the IC of the whole connection is selected. The force magnitudes of all elements are

calculated while the directions of the forces are considered to be perpendicular to the line from the centroid of the individual fastener to the IC location. With all the forces calculated and assigned directions, the system equilibrium is evaluated, and the location of the IC is iterated until equilibrium is achieved. Figure 7.2 depicts the IC of a combination connection and illustrate the force resultants of each fastener and how the system reacts against the applied load.
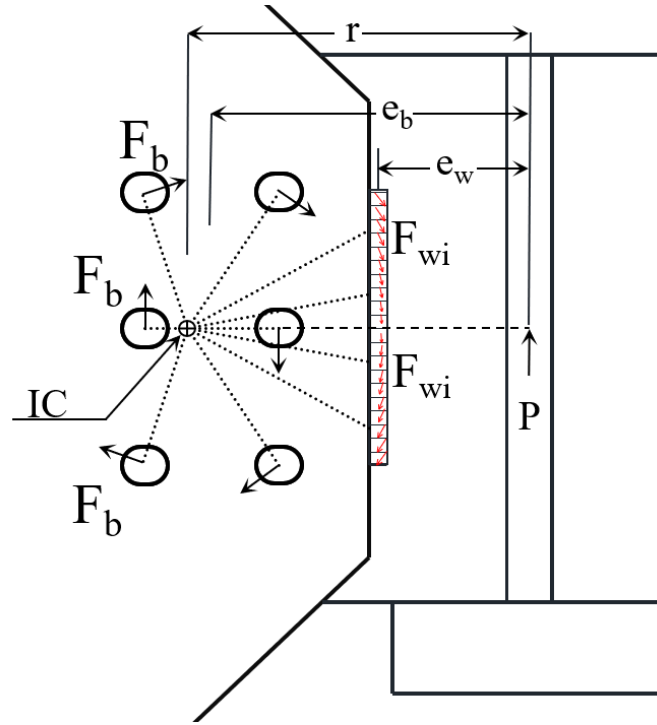
Figure 7.2: IC Force diagram for combination connections

The bolt load-deformation behavior is taken as the ultimate frictional force provided by the bolt with the measured pretension force and coefficient of friction (Kulak 1975). Each bolt will provide the same resistive force that will not depend on the IC location. Accordingly, the force resisted by each bolt in eccentrically loaded slip-critical connection is

$$F_B = T_{B,avg} * k_s * n_s \qquad \text{Eq. 29}$$

F_B is the slip capacity of a single bolt within the connection system computed using the average pretension force of the three Skidmore tests completed prior to every test. The load-deformation behavior of welds follows the AISC (2017) specification. The weld is broken up into several units, each carrying a certain level of stress. The unit weld force is calculated as (AISC 2017):

$$F_{wi} = F_{nwi} * A_{wei} \qquad \text{Eq. 30}$$

$$F_{nwi} = \tau * (1.0 + 0.5 * sin^{1.5}(\theta_i)) * (p_i * (1.9 - 0.9 * p_i))^{0.3} \qquad \text{Eq. 31}$$

$$p_i = \frac{\Delta_i}{\Delta_{mi}} \qquad \text{Eq. 32}$$

$$\Delta_i = \Delta_{cr} * \frac{r_i}{r_{cr}} \qquad \text{Eq. 33}$$

$$\Delta_{ui} = 1.087 * (\theta_i + 6)^{-0.65} * d \leq 0.17 * d \qquad \text{Eq. 34}$$

F_{wi} = force in ith weld, kips

A_{wei} = effective weld area taken at the theoretical throat

d = leg size of the ith weld, in.

F_{nwi} = nominal stress in the ith weld element, ksi

τ = shear stress of the weld, ksi

θ_i = angle between the longitudinal axis of ith weld element and the direction of the resultant force acting on the element, degrees

p_i = ratio of element i deformation to its deformation at maximum stress

r_{cr} = distance from instantaneous center of rotation to weld element with minimum $\frac{\Delta_{ui}}{r_i}$ ratio, in.

Δ_i = deformation of the ith weld element at an intermediate stress level, linearly proportioned to the critical deformation based on the distance from the instantaneous center of rotation, r_i, in.

Δ_{cr} = deformation of the weld element with minimum ratio $\frac{\Delta_{ui}}{r_i}$ at ultimate stress (rupture), in.

Δ_{ui} = deformation of the ith weld element at ult-imate stress (rupture), in.

Once the forces in the weld elements are calculated, the force vectors are added into the system and iterations are performed over the location of the IC until system equilibrium is reached.

7.2.1 Bolted-Only Connections

Tests 31-34 and 49 cover the bolted-only specimens in the eccentric testing. The specifics of each test series can be found in the test matrix Table 5.1. The friction factors used for the analysis are 0.339 for Class A and 0.535 for Class B similar to the ones obtained from the axial lap tests. The Class A surfaces did not have the rust patina that induced higher friction coefficient for the 2×2 axial lap connection plates. Since the blasted surfaces are manufactured by the same facility, it also seemed appropriate to use the mean friction coefficient from Class B double shear concentric connections. Test 31A is not considered in the prediction effort of Tests 31 & 33 because after testing, mechanical damage to the faying surface was observed on the test plate with matching grooving on the corresponding grip plate. The high capacity of the test is attributed to the mechanical interlock due to the test plate mechanical damage and thus it is excluded from the statistical analysis. Table 7.2 shows the IC R_n, the Test R_n, and the factor of safety for each bolted-only test and the statistical data for each group of testing.

7.2.2 Welded-Only Connections

Test 36 and Test 50 are the welded-only tests conducted for the eccentric testing. Each sample was constructed as specified by the test matrix in Table 5.1. The ultimate weld shear stress is assumed as 69.53 ksi for all connections. Table 7.3 shows the IC R_n, the Test R_n, and the factor of safety for the welded-only tests as well as the statistical data.

Table 7.2: IC model prediction results: bolted-only tests

	Specimen	Bolt Pattern	Bolt Type	Faying Surface Class	IC R_n (kips)	Test R_n (kips)	Test R_n/ IC Rn
Test 31	A*	2×3	A325	A	52.5	104.3	1.99
	B	2×3	A325	A	58.7	76.3	1.30
Test 33	A	2×3	A490	A	63.3	74.9	1.18
	B	2×3	A490	A	62.8	87.2	1.39
NOTE: Test R_n is the maximum load applied at $\theta \leq 0.02$ radian *-Test 31A is not included in the statistical data analysis due to mechanical deformations on the faying surface							**AVG = 1.288** **SD = 0.103** **CV = 7.96%**
Test 34	A	2×3	A325	B	88.6	133.2	1.50
	B	2×3	A325	B	85.2	110.7	1.30
NOTE: Test R_n is the maximum load applied at $\theta \leq 0.02$ radian							**AVG = 1.402** **SD = 0.144** **CV = 10.30%**
Test 49	A*	1×6	A325	A	104.6	217.1	2.08
	B	1×6	A325	A	100.8	136.2	1.35
	C	1×6	A325	A	101.7	169.8	1.67
NOTE: Test R_n is the maximum load applied at $\theta \leq 0.02$ radian *- Test 49A is not included in the statistical data analysis since bolts are expected to have reached the bearing condition							**AVG = 1.510** **SD = 0.225** **CV = 14.87%**

Table 7.3: IC model prediction results: welded-only tests

	Specimen	Weld Geometry (Size × length)	IC R_n (kips)	Test R_n (kips)	Test R_n/ IC Rn
Test 36	A	5/16 × 4.5	55.4	103.0	1.86
	B	5/16 × 4.5	60.7	85.4	1.41
	C	5/16 × 4.5	48.4	95.6	1.97
NOTE: The Test R_n is the rotational limit of 0.02 radians					**AVG = 1.746** **SD = 0.300** **CV = 17.20%**
Test 50	A	5/16 × 9.75	222.3	253.1	1.14
	B	5/16 × 9.75	195.9	237.0	1.21
NOTE: Test R_n is the maximum load applied at $\theta \leq 0.02$ radian AVG = Average value; SD = Standard Deviation; CV = Coefficient of variation Two fillet welds per connection with the noted geometry. Units are inches.					**AVG = 1.174** **SD = 0.051** **CV = 4.30%**

7.2.3 Combination Connections

Table 7.4 shows the IC R_n, Test R_n, and the factor of safety (Test R_n / As-Built R_n) for all combination tests broken up by faying surface class and bolt configuration. The IC R_n represents the predicted capacity using the IC method which includes measured material properties, pretension force, and weld geometry. Figure 7.3 plots the IC R_n against the Test R_n.

Table 7.4: As-Built prediction test results for combination connections

	Test No.	R_{n_w}/ R_{n_B}	AVG IC Rn (kips)	AVG Test Rn (kips)	AVG Test Rn / IC Rn	SD Test Rn / IC Rn	Group Test Rn / IC Rn
2×3 Class A	37	0.25	91.8	122.1	1.330	0.014	**AVG = 1.278** **SD = 0.083** **CV = 6.50%**
	38	1.00	130.8	171.2	1.309	0.165	
	39	1.50	163.4	191.9	1.174	0.054	
	40	2.00	191.3	230.7	1.206	0.036	
	42	0.82	135.4	185.2	1.368	0.104	
2×3 Class B	43	0.25	124.6	161.2	1.294	0.195	**AVG = 1.323** **SD = 0.019** **CV = 1.47%**
	44	1.00	187.6	249.2	1.328	0.096	
	45	1.50	214.5	286.0	1.333	0.045	
	46	2.00	252.8	337.8	1.336	0.051	
1×6 Class A	51	0.25	173.4	221.1	1.275	-	**AVG = 1.270** **SD = 0.057** **CV = 4.48%**
	52	1.00	200.5	268.8	1.341	0.139	
	53	1.50	246.8	296.5	1.201	0.061	
	54	2.00	289.8	367.2	1.267	0.148	
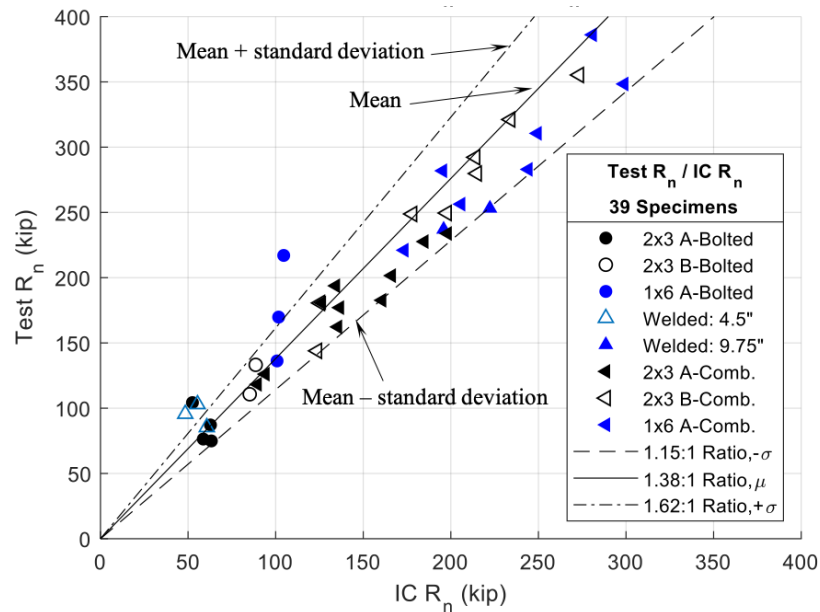
Figure 7.3: Factor of safety plot for eccentrically loaded connections based on the IC method

109

7.3   INFLUENCE OF INVESTIGATED CONNECTION VARIABLES

7.3.1   Weld/Bolt Strength Ratio

The increase in the weld/bolt strength ratio is expected to lead to an increase in the capacity of the connection. Phase II investigated weld/bolt strength ratios of 0.25, 1.00, 1.50, and 2.00 in both Class A and Class B faying surfaces for different bolt configurations. The testing results of different weld/bolt strength ratio are shown in Figure 7.4 and Figure 7.5, for the 2×3 connections with Class A and B surfaces, respectively. The corresponding results for the 1×6 bolt configuration are shown in Figure 7.6. This ratio does have a significant influence on the behavior of the connection. As seen in the figures, the higher the weld/bolt strength ratio, the more the load-deformation behavior resembles that of the welded-only connections. This happens because the extreme weld fibers for longer welds are subjected to higher displacement demand. The longer the weld is, the smaller the rotation would be before the weld extreme fibers reach their ultimate deformation. Thus, the weld portion of the connection begins to fracture and its contribution to the capacity decreases as the fracture propagate with additional rotation. The bolts, however, may continue carrying higher loads (i.e., Class A) or reach a maximum and maintain capacity (i.e., Class B) at large rotations.

Class A connections at low ratios tend to show a behavior resembling the bolted-only behavior (see. Figure 6.2) by exhibiting a slip-hardening behavior. The higher the ratio, the more the load-rotation curve resembles the welded-only behavior by having a defined ultimate peak and a steeper downward slope in the post-ultimate portion of the curve. A similar trend can also be noticed in Class B connections where the peak and post-ultimate loss in capacity depends on the length of the weld. The ultimate capacity of connections with Class B surfaces tends to occur around a rotation of 0.0025-0.0045 radians.
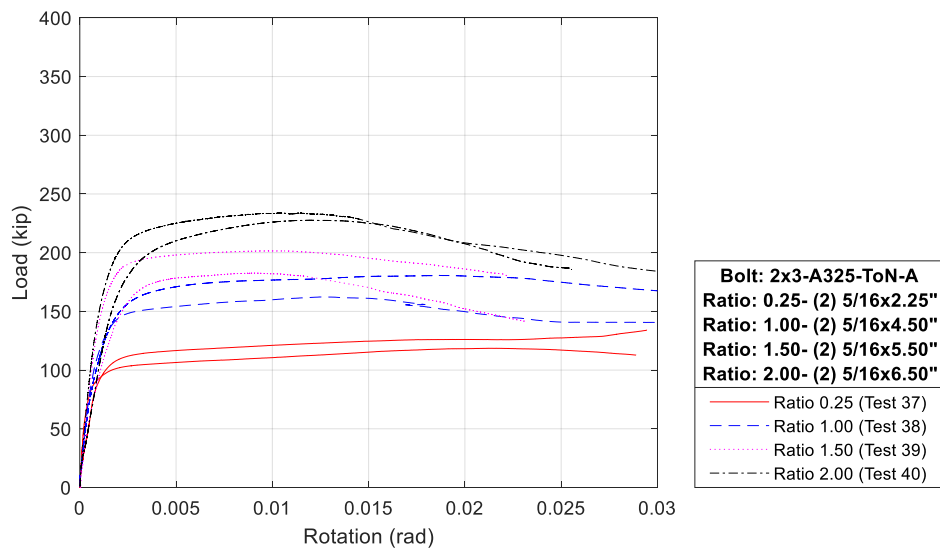
Figure 7.4: Load-rotation for different weld/bolt strength ratios: 2×3-Class A
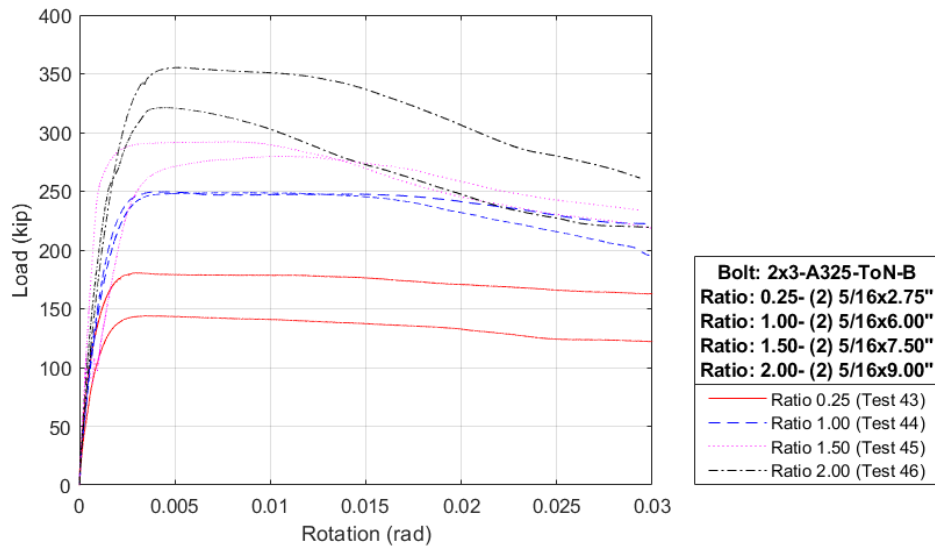
Figure 7.5: Load-rotation for different weld/bolt strength ratios: 2×3-Class B
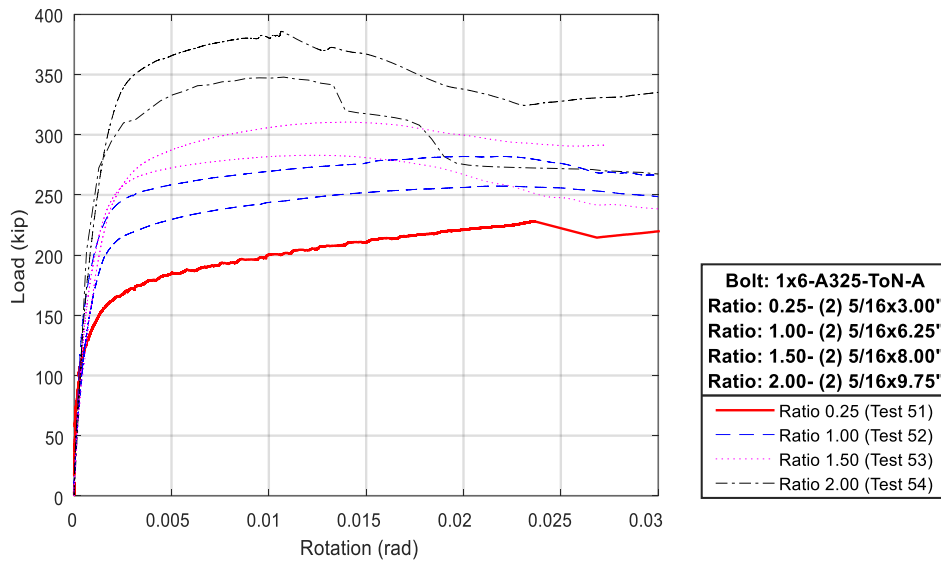
Figure 7.6: Load-rotation for different weld/bolt strength ratios: 1×6-Class A

7.3.2   Faying Surface Class

This section presents four comparisons that will highlight how the faying surface class affects the capacity and behavior of combination connections. As expected, Class B connections display a higher strength that is attributed to the higher friction coefficient. At low rotations (i.e., 0.0025-0.004 radians), all connections show a stiff elastic region. The Class B combination connections are on average 60% stiffer than the Class A connections as shown in Figure 7.7. This can be attributed to the weld contribution to the connection as the Class B connection has a longer weld than its Class A counterpart. This is confirmed by comparing the stiffness of the bolted-only tests

with different faying surfaces. Figure 7.8 shows that the initial stiffness of bolted-only connections is similar for both faying surface types. Figure 7.9 – Figure 7.12 depict the combination tests with matching weld/bolt strength ratios. For these connections, the IC prediction of Class B connections provides on average 4.5% higher safety factor compared to Class A connections with similar strength ratio.
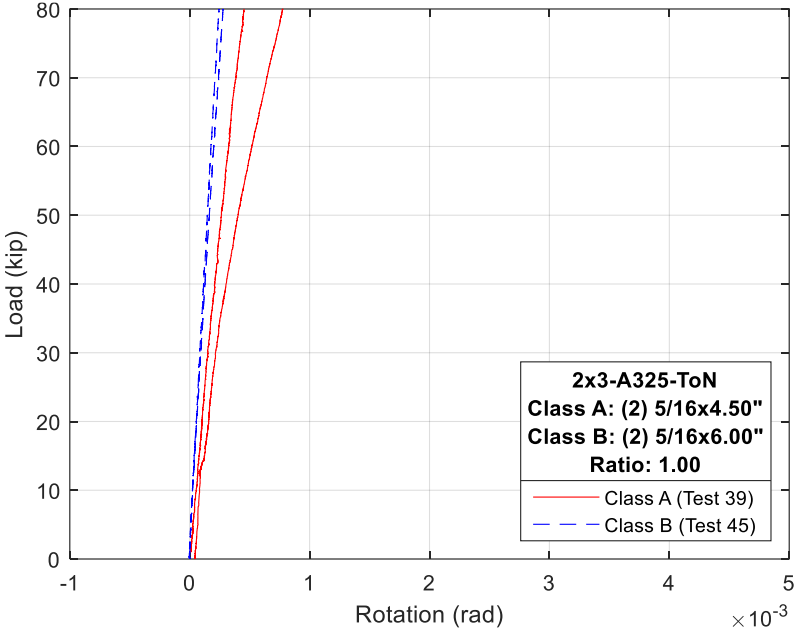
Figure 7.7: Initial rotational stiffness of combination connections utilizing Class A and Class B faying surfaces
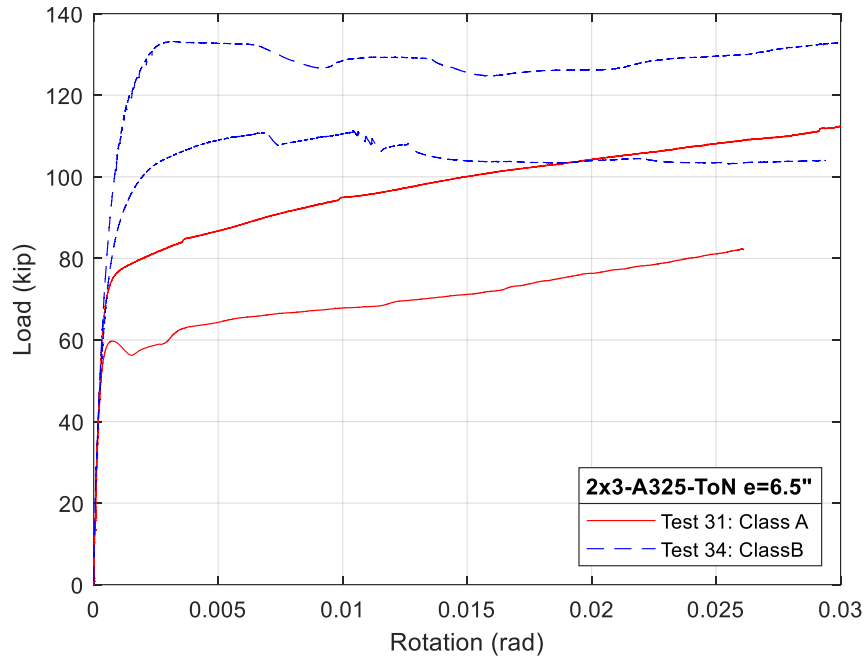
Figure 7.8: Load-rotation behavior of bolted-only connections with Class A and B faying surfaces
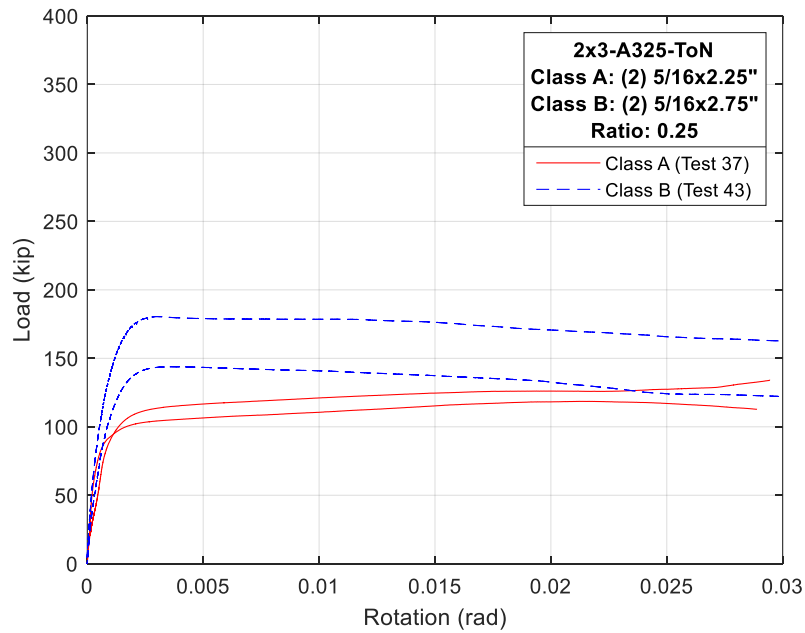
Figure 7.9: Load-rotation behavior of combination connections with Class A and B faying surfaces (2×3 – weld/bolt strength ratio: 0.25)
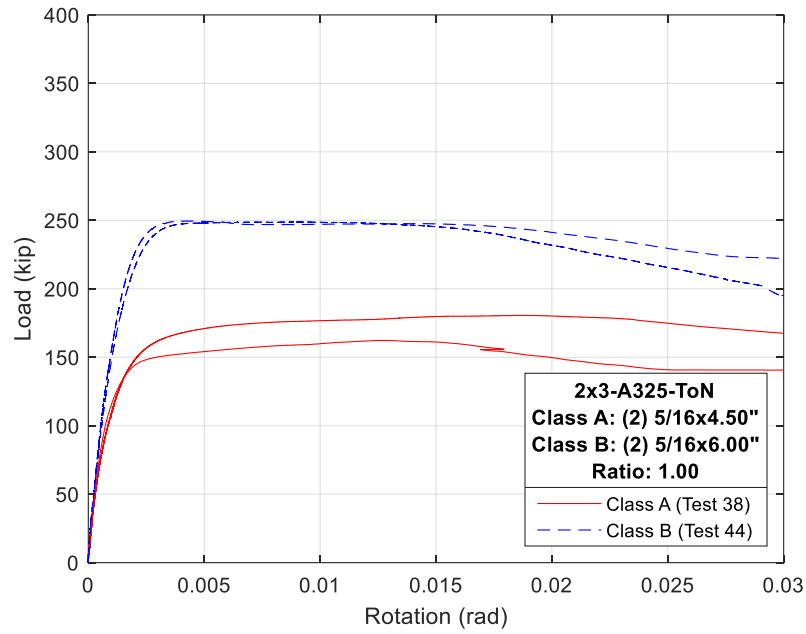
Figure 7.10: Load-rotation behavior of combination connections with Class A and B faying surfaces (2×3 – weld/bolt strength ratio: 1.00)
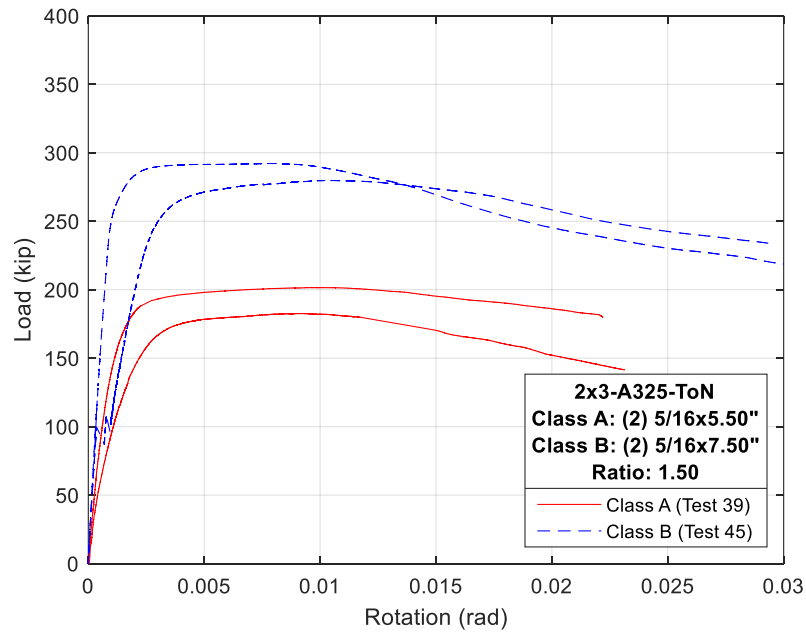
Figure 7.11: Load-rotation behavior of combination connections with Class A and B faying surfaces (2×3 – weld/bolt strength ratio: 1.50)
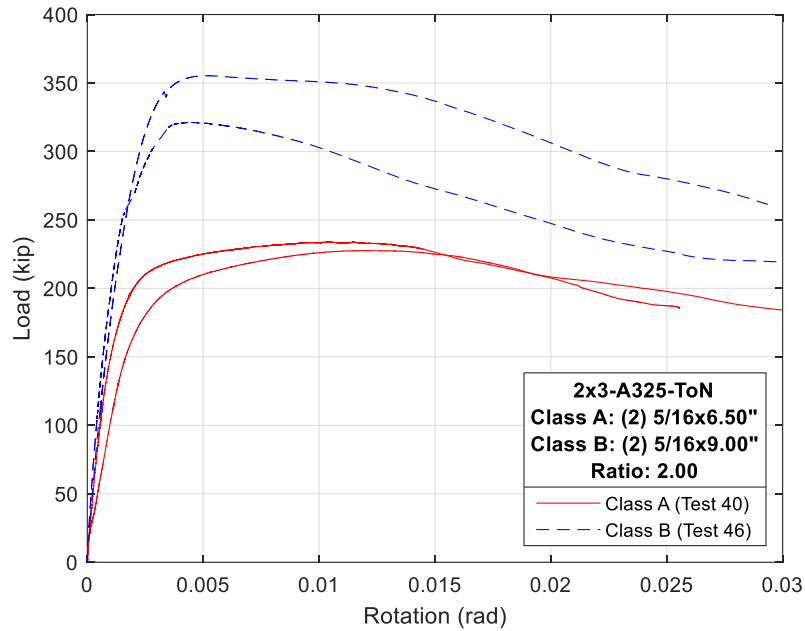
Figure 7.12: Load-rotation behavior of combination connections with Class A and B faying surfaces (2×3 – weld/bolt strength ratio: 2.00)

7.3.3 Bolt Configuration

Bolt configuration was investigated by comparing Tests 37-40 and 51-54 which cover the 2×3 and 1×6 configurations. The tests will be compared by pairing the weld-to-bolt strength ratio (0.25-2.00). Further parameters of each test can be found in the test matrix (Table 5.1). Across all these tests, good ductility is seen even at high rotations. Figure 7.13 – Figure 7.16 show the load-rotation curves of these comparisons for ratios 0.25, 1.00, 1.50, and 2.00 respectively. As seen in the figures, the 1×6 connections are stiffer than the 2×3 ones; this could be attributed to both the longer weld of Tests 51-54 compared to 37-40 and that the 1×6 connection bolted-only connection being stiffer than the 2×3 bolted-only. The factor of safety with respect to IC prediction for the 2×3 seems to be on average 0.8% higher than that of the 1×6 connections.
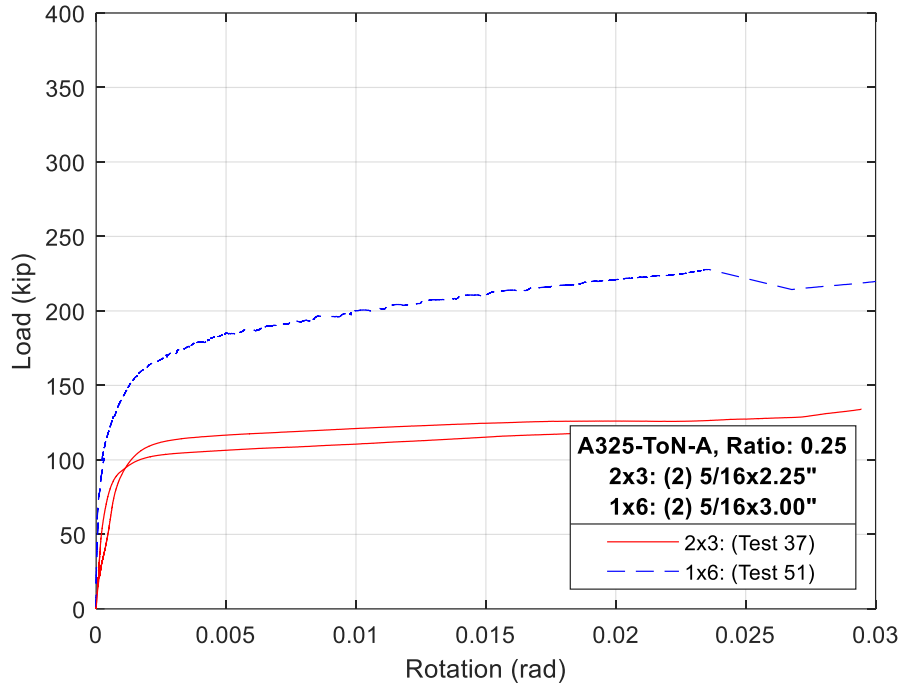
Figure 7.13: Load-rotation behavior of combination connections with 2×3 and 1×6 bolts (Class A, weld/bolt strength ratio of 0.25)
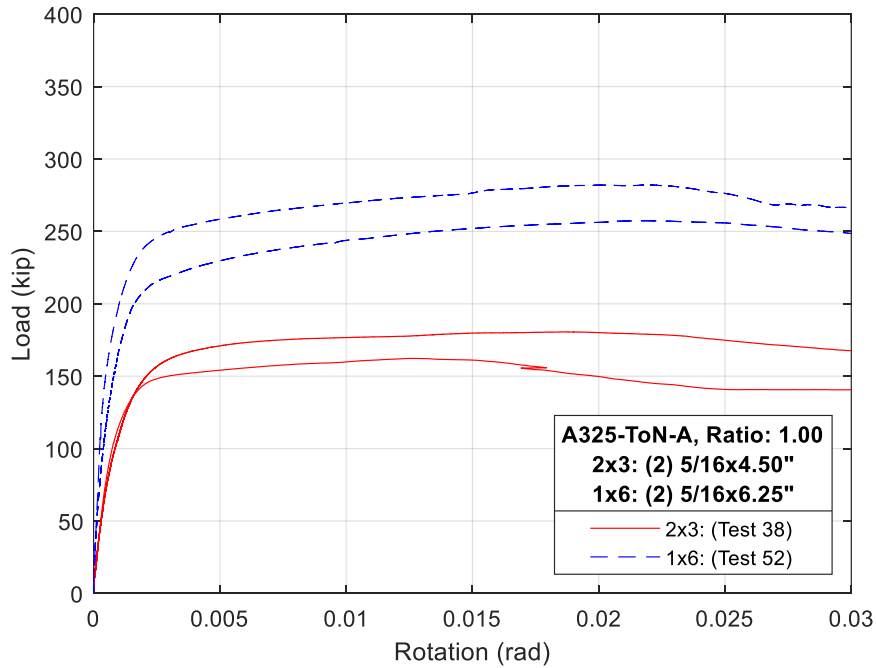
Figure 7.14: Load-rotation behavior of combination connections with 2×3 and 1×6 bolts (Class A, weld/bolt strength ratio of 1.00)
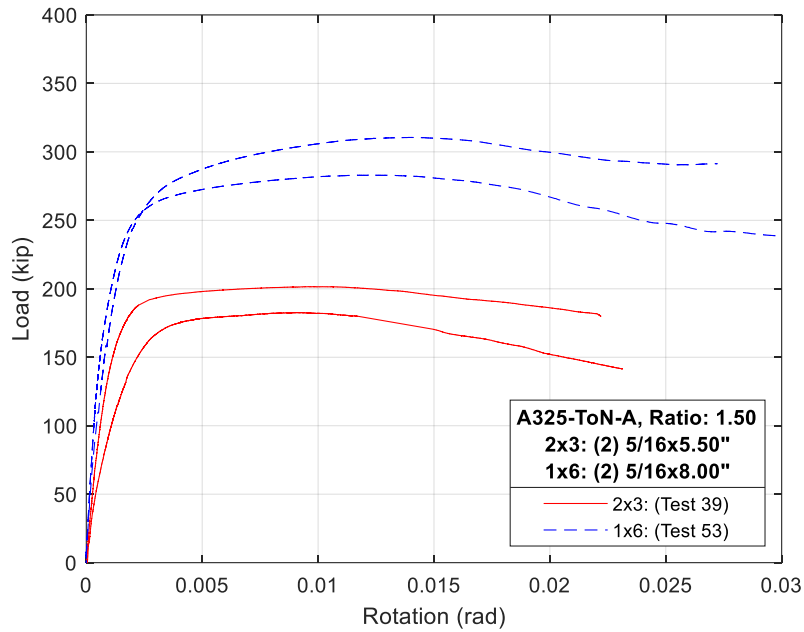
Figure 7.15: Load-rotation behavior of combination connections with 2×3 and 1×6 bolts (Class A, weld/bolt strength ratio of 1.50)
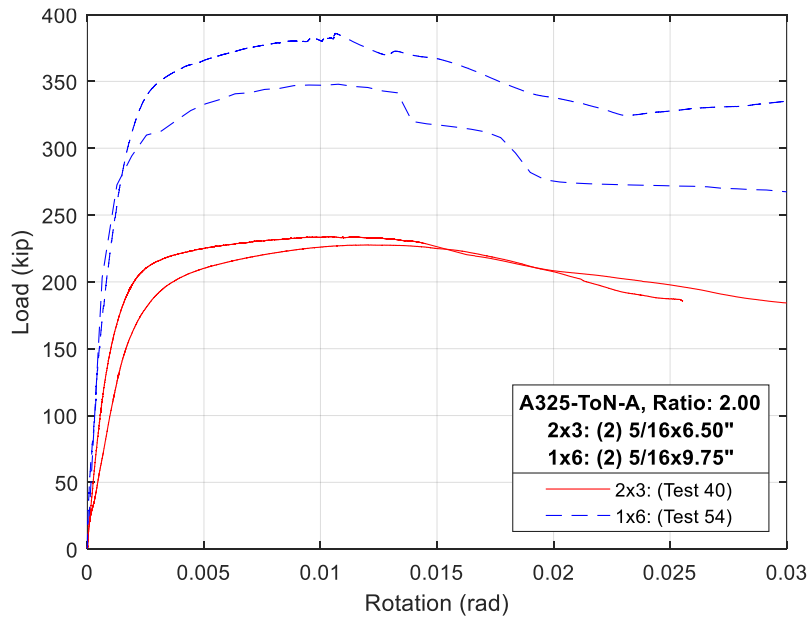
Figure 7.16: Load-rotation behavior of combination connections with 2×3 and 1×6 bolts (Class A, weld/bolt strength ratio of 2.00)

7.3.4 Bolt Grade

Most tests in this phase utilized A325 bolts except Test 42, which is a combination test that used A490 bolts to investigate the differences a higher-grade bolt can impart on a combination

connection. Test 42 is compared to Test 38, both use Class A faying surface and have the same weld geometry and pretensioning method. This allows for easier comparison of the effect of bolt grade; accordingly, Test 42 has a lower bolt-to-weld strength ratio than Test 38 given the same weld length. Figure 7.17 shows the load-rotation curves for both tests. The tests using A490 bolts seem to have 5.9% higher experimental capacity than those utilizing A325 bolts. This percentage slightly lower than 8.6% increase in the pretension force of the A490 bolts compared to A325 as reported in Table 7.1. The bolts grade seems to have a quantifiable influence on the performance. The stiffness, softening, and ductility plateau are all within some levels of similarity. The higher capacity of the A490 bolt test stems from the increase in pretension force and the slightly larger measured weld dimensions attributed to weld variability.
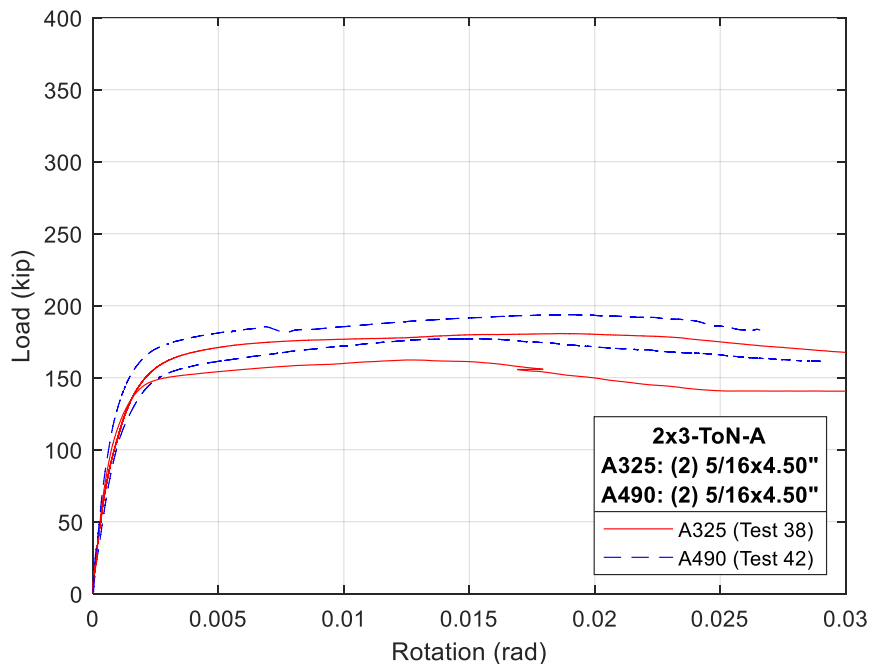
Figure 7.17: Bolt Grade Comparison: A325 vs. A490

7.4   SUMMARY: ECCENTRICALLY LOADED CONNECTIONS

Based on the experimental results presented above, it is apparent that the connections combining slip-critical bolts and fillet welds that are loaded eccentrically will exhibit an increase in the capacity compared to that of the individual fasteners. Figure 7.18 shows the load-rotation curves of the bolted-only, welded-only, and combination connection to describe the combined behavior of the connection. The initial stiffness of the combination connection is comparable to that of the bolted-only tests. As indicated previously, it also apparent that the behavior after softening follows that of the fastener that contributes more strength to the combination connection.
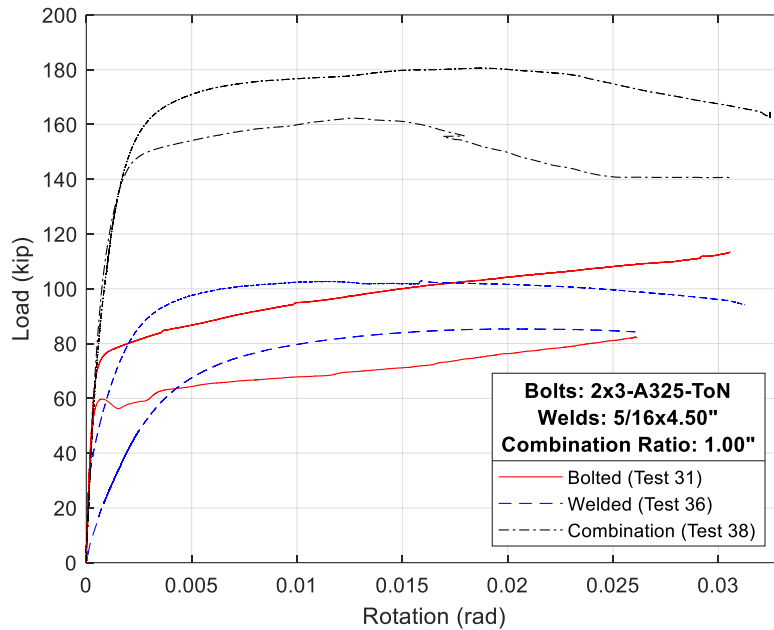
Figure 7.18: Load-rotation of bolted-only, welded-only, and a combination connection with the same attributes (2×3-Class A-Ratio 1.00)

It was also found that adding the capacity of individual faster types to establish the capacity of the eccentrically loaded combination connection provides mixed estimates of the failure load. To highlight this point, load-rotation curves are plotted for (a) bolted-only, (b) welded-only, (c) summations of bolted-only and welded-only, and finally (d) the test combination with same characteristics of bolted and welded connections. Figure 7.19 depicts Test 31B (i.e., 2×3 bolted-only, Class A surface utilizing A325-ToN), welded-only behavior (two fillet welds 5/16×4.5-in), summation of bolted-only and welded-only, and Test 38 which has the combined characteristics of the welded and bolted connections. As shown in the figure, the addition model underpredicts the capacity at low rotations and overpredicts it at higher rotations.

However, for other configurations, it is believed that the direct summation may yield unconservative estimates of the capacity of the connection. Figure 7.20 shows the same comparison for Test 52 (strength ratio 1.50) with 1×6 bolts, Class A faying surface, and 5/16×6.25-in welds. Since no tests have been conducted with this weld lengths, finite element modeling was used to generate the welded-only load-rotation profile for welded connection with 5/16×6.25-in welds. As shown, the summation may significantly overpredict the actual capacity of the connection. Accordingly, it is believed that the IC method provides a more rational and accurate estimation of the capacity of combination connections under eccentric loading. However, more research is needed to assess its accuracy for connections with larger weld sizes.
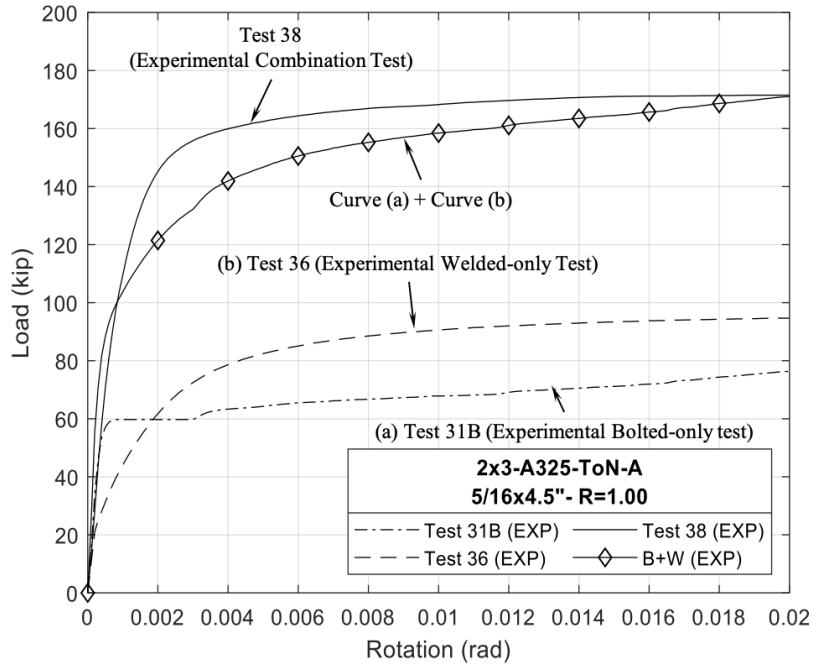
Figure 7.19: Test 38 Fastener contribution comparison
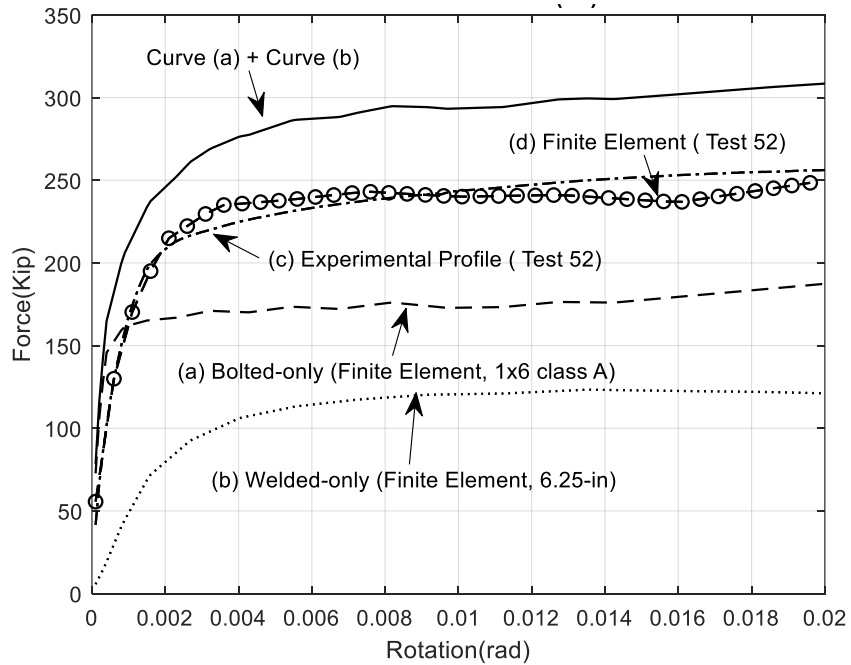
Figure 7.20: Test 52 fastener contribution comparison

120

8 SUMMARY, CONCLUSIONS, AND RECOMMENDATIONS

This report presented the results of an experimental investigation aiming at understanding the behavior of steel connections employing both slip-critical bolts and fillet welds in a single load sharing system. The study presented and analyzed the results of experimental testing of several connections under concentric and eccentric loading conditions. These specimens covered a wide range of critical connection variables including the effect of bolt grade, condition of faying surfaces, bolt tightening technique, load eccentricity, and connection size, among others. Concentrically loaded specimens were double shear tension splices with four or six bolts in a 2×2 or 2×3 configurations and faying surface Class A and B. These connections included four fillet welds lines with different lengths to represent different weld/bolt strength ratios. Eccentrically loaded connections were in double shear configuration that covered 2×3 or 1×6 bolt patterns along with two fillet weld lines between the eccentrically loaded center plate and the two external plates. An analytical investigation was carried out to establish the prediction model that provides the best fit to the test data. Based on the results of this investigation, the following conclusions can be drawn:

1. The combination of longitudinal fillet welds to a concentrically loaded slip-critical bolted connection leads to an increase in the carrying capacity of the connection and improves the stiffness and ductility of the connection.

2. Bolted-only slip-critical connections utilizing Class A faying surface show a ductile slip-hardening behavior while those with Class B condition exhibited sudden slip. However, combined connections for both Class A and Class B surfaces show a ductile behavior which implies that bolt and welds in combination can lead to improved connection characteristics.

3. Combination connections with Class A faying surface seem to reach their ultimate capacity at a slip displacement ranging from 0.05-in to 0.14-in. However, depending on the faying surface characteristics, the force in the connection at 0.02-in of slip can be as high as 96% of the ultimate capacity of the connection. Accordingly, it is recommended to use 0.02-in as the slip limit for predicting the capacity of combination connections utilizing Class A faying surfaces.

4. Combination connections with Class B faying surface reach their ultimate capacity at or below a slip level of 0.02-in. It is recommended to predict the capacity of the connection at a slip limit that does not exceed 0.02-in.

5. The capacity of concentrically loaded bolted and welded combination connection for Class A faying surface can be computed as the summation of the separate capacities of bolted-only and welded-only connections while maintaining the load-slip compatibility. It is recommended to compute the capacity of the connection by adding the slip-capacity of bolts and the weld force at 0.02-in of slip.

6. For combination connections with Class B faying surface, the summation of the slip-load of bolts and weld force at 0.02-in of slip provides a lower-bound conservative estimate for the experimental combined capacity.

7. A proposed capacity equation, which considers weld shear stress at the onset of bolt slip, can predict the combined connection capacity accurately. This model is expressed as

$$R_n = R_b + C_w R_w$$

where C_w reflects the ratio between the weld shear stress at 0.02-in of slip to its ultimate shear strength. A C_w value of 0.92 value was obtained from the results of the welded-only tests conducted on 5/16-in fillet welds in this test program. A lower ratio of 0.86 can be found for fillet welds with 5/16-in size based on the load-deformation fillet weld model reported in Lesik and Kennedy (1990). Based on this load-deformation model, it is recommended to use the following equation to compute C_w for design purposes:

$$C_w = \left(\frac{0.227w - 0.013}{w^2} \right)^{0.3}$$

8. The weld-to-bolt strength ratio, bolt pattern, bolt tension method and bolt grade show a negligible effect on the general behavior of the concentrically loaded combination connections and on the accuracy of the proposed prediction model.
9. The bolt and hole size (i.e., oversized vs. standard) could affect the safety factor associated with capacity prediction of the combined connection.

With respect to the combination connections loaded eccentrically in the plane of the faying surface, the following conclusions can be drawn:
10. Using the instantaneous center of rotation method with the appropriate load-deformation models of the fasteners can provide an accurate prediction of the capacity of eccentrically loaded combination connections.
11. The weld/bolt strength ratio can impact the behavior of the combination connection. The higher the ratio, the stiffer the connection becomes due to the longer weld. Additionally, with higher ratios, the load-rotation curve trends to the welded-only behavior with higher peak and steeper descent in the post-ultimate behavior.
12. The bolt grade, faying surface, and bolt configuration contribute to the load-deformation behavior of the connection. However, the ability to accurately predict the capacity of the connection is not significantly affected by these factors.

9 REFERENCES

AISC, 2016. *Specification for Structural Steel Buildings*, ANSI/AISC 360-16. Chicago, IL: American Institute of Steel Construction.

AISC, 2017. *Steel Construction Manual, 15th Edition*. Chicago, IL: American Institute of Steel Construction.

Allan, R.N. and Fisher, J.W., 1968. Bolted joints with oversize or slotted holes. *Journal of the Structural Division*, ASCE, 94(9):2061–2080

AWS B4.0:2016, 2016. *Standard Method for Mechanical Testing of Welds*. Miami, FL: American Welding Society.

Bowman, M.D., and Quinn, B.P., 1994. Examination of fillet weld strength. *Engineering Journal,* AISC*,* 31(3), 98-108.

Butler, L.J., and Kulak, G.L., 1971. Strength of fillet welds as a function of direction of load. *Welding Journal*, 50(5), 231s-234s.

Butler, L.J., Pal, S., and Kulak, G.L., 1972. Eccentrically Loaded Welded Connections. *Journal of the Structural Division,* 98(5), 989-1005.

CISC, 2006. *Handbook of Steel Construction*, 9th Edition. Toronto, Ont.: Canadian Institute of Steel Construction.

Crawford, S. F., and Kulak, G. L., 1968. *Behavior of Eccentrically Loaded Bolted Connections, Studies in Structural Engineering*, *No. 4*. Department of Civil Engineering, Nova Scotia Technical College, Halifax, Nova Scotia.

Deng, K., Grondin, G.Y., and Driver, R.G., 2003. *Effect of loading angle on the behavior of fillet welds, Structural Engineering Report 251*, Department of Civil and Environmental Engineering, University of Alberta, Edmonton, Alta.

Fisher, J.W., 1964. *On the Behavior of Fasteners and Plates with Holes (No. 288-18).* Fritz Engineering Laboratory, Department of Civil Engineering, Lehigh University.

Fisher, J.W., and Struik, J. H. A., 1973. *Guide to Design Criteria for Bolted and Riveted Joints*. New York, NY: John Willey and Sons. Inc.

Fisher, J.W., Ravindra, M.K., Kulak, G.L., and Galambos, T.V., 1978. Load and resistance factor design criteria for connectors. *Journal of the Structural Division*, 104(9), 1427-1441.

Godfrey, H.J., and Mount, E.H., 1940. Pilot tests on covered electrode welds, *Welding Journal*, 19, Reprint No. 48 (40-2).

Grondin, G., Jin, M., and Josi, G., 2007. Slip critical bolted connections— A reliability analysis for design at the ultimate limit state. Rep. No. *Structural Engineering Rep. 274*, Univ. of Alberta, Edmonton, AB, Canada.

Heistermann, C., Veljkovic, M., Simões, R., Rebelo, C., and Da Silva, L. S., 2013. Design of slip resistant lap joints with long open slotted holes. *Journal of Constructional Steel Research*, 82, 223-233.

Higgins, T.R, 1971. Treatment of Eccentrically-loaded Connections in the AISC Manual, *Engineering Journal*, AISC, 8, 52-54.

Higgins, T.R and Preece, F.R., 1969. Proposed working stresses for fillet welds in building Construction. *Engineering Journal*, AISC, 6(1), 16-20.

Holtz, N.M. and Kulak, G.L., 1970. *High-strength bolts and welds in load-sharing systems, Structural Engineering Report No. 8*. Department of Civil Engineering, Nova Scotia Technical College, Halifax, Nova Scotia.

Hsieh, S.H. and Deierlein, G.G., 1991. Nonlinear analysis of three-dimensional steel frames with semi-rigid connections. *Computers & structures*, 41(5), 995-1009.

Jarosch, K.H. and Bowman, M.D., 1986. Tension butt joints with bolts and welds. *Engineering Journal*, AISC, 23(1), 25-35.

Kato, B., and Morita, K., 1969. The strength of fillet welded joints. *International Institute of Welding*, Doc. XV-267-69.

Kim, D.K. and Lee, C.H., 2020. Experimental and analytical study of combined bolted-welded lap joints including high-strength steel. *Journal of Constructional Steel Research*, 168, p.105995.

Kulak, G. L., 1975. Eccentrically loaded slip-resistant connections. *Engineering Journal*, AISC, 12(2), 52-55.

Kulak, G.L., and Grondin, G.Y., 2003. Strength of joints that combine bolts and welds. *Engineering Journal*, AISC, 40(2), 89-98.

Kwan, Y.K., and Grondin, G.Y., 2008. *Strength of welded joints under combined shear and out-of-plane-bending, Structural Engineering Report 280*, Department of Civil and Environmental Engineering, University of Alberta, Edmonton, Alta.

Leon, R.R., Hoffman, J. and Staeger, T., 1996. *Design of Partially Restrained Composite Connections*, Design Guide 8, ASIC, Chicago, IL.

Lesik, D. F., and Kennedy, D. L., 1990. Ultimate strength of fillet welded connections loaded in plane. *Canadian Journal of Civil Engineering*, 17(1), 55-67.

Manuel, T.J., 1996. *Strength of joints that combine bolts and welds*, M.Sc. Thesis. Department of Civil Engineering, University of Alberta, Edmonton, Alberta.

Manuel, T.J., and Kulak, G.L., 2000. Strength of joints that combine bolts and welds. *Journal of Structural Engineering*, 126(3), 279-287.

Miazga, G. S., and Kennedy, D. L., 1989. Behavior of fillet welds as a function of the angle of loading. *Canadian Journal of Civil Engineering*, 16(4), 583-599.

NI, 2018. *LabVIEW NXG 3.0 User Manual,* National Instruments, Austin, TX, https://www.ni.com/documentation/en/labview/3.0/manual/manual-overview/. Accessed 10 Dec. 2018.

Quinn, B.P., 1991. *The effect of profile and root geometry on the strength of fillet welds*, M.Sc. Thesis. Department of Civil Engineering, Purdue University, West Lafayette, IN.

RCSC, 2014. *Specification for Structural Joints Using High-Strength Bolts*, Research Council on Structural Connections, Chicago, IL: American Institute of Steel Construction.

Salmon, C.G., Johnson, J.E., and Malhas, F.A., 2009. *Steel Structures: Design and Behavior: Emphasizing Load and Resistance Factor Design*. Upper Saddle River, NJ: Person Education.

Shi, Y., Wang, L., Wang, Y., Ma, J., and Bai, R., 2011a. Finite element analysis of the combined connection with bolts and welds. *Applied Mechanics and Materials*, 94, 316-321.

Shi, Y., Wang, L., Wang, Y., Ma, J., and Bai, R., 2011b. Proposed design method of combined connections with bolts and longitudinal welds. *Applied Mechanics and Materials*, 94, 923-928.

Shoukry, Z., and Haisch, W. T., 1970. Bolted connections with varied hole diameters. *Journal of the Structural Division*, 96(6), 1105-1118.

Steinhardt, O., Möhler, K., and Valtinat, G., 1969. *Versuche zur anwendung vorgespannter schrauben im stahlbau*. IV. Teil. Berichte des deutschen Ausschusses für Stahlbau, 25.

Ugural, A.C., and Fenster, S.K., 2011. *Advanced mechanics of materials and applied elasticity*. Upper Saddle River, NJ: Person Education.